astro8405

An Introduction to the

Cosmic Microwave Background

Kaustuv Basu

kbasu@uni-bonn.de

eCampus | Lernplattform der Universität Bonn

astro8405: The Cosmic Microwave Background

Aktionen

This course intends to give you a modern and up-to-date introduction to the science and experimental techniques relating to the Cosmic Microwave Background. No prior knowledge of cosmology is necessary, your prerequisite are a basic understanding of electrodynamics and thermal physics and some familiarity with Python programming.

Lecture 10:

Part 1: CMB Anomalies

Part 2: Detectors and Experiments

CMB is Gaussian random field

The CMB data is perfectly described as a Gaussian random field, originating from stochastic density fluctuations created by inflation and enhanced by baryonic interactions.

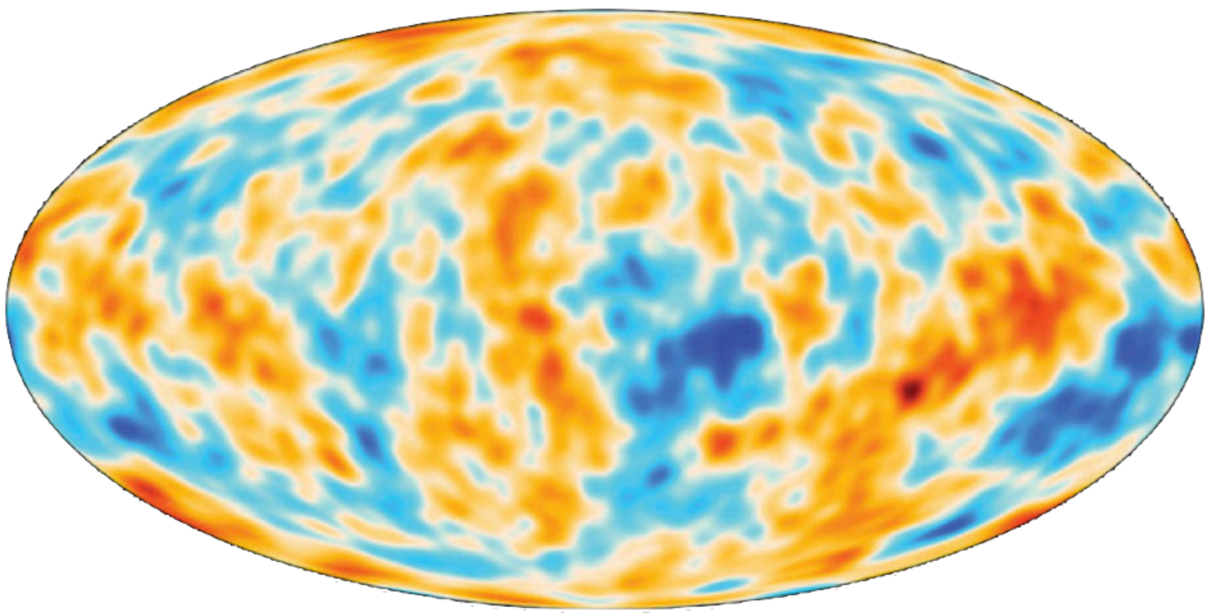

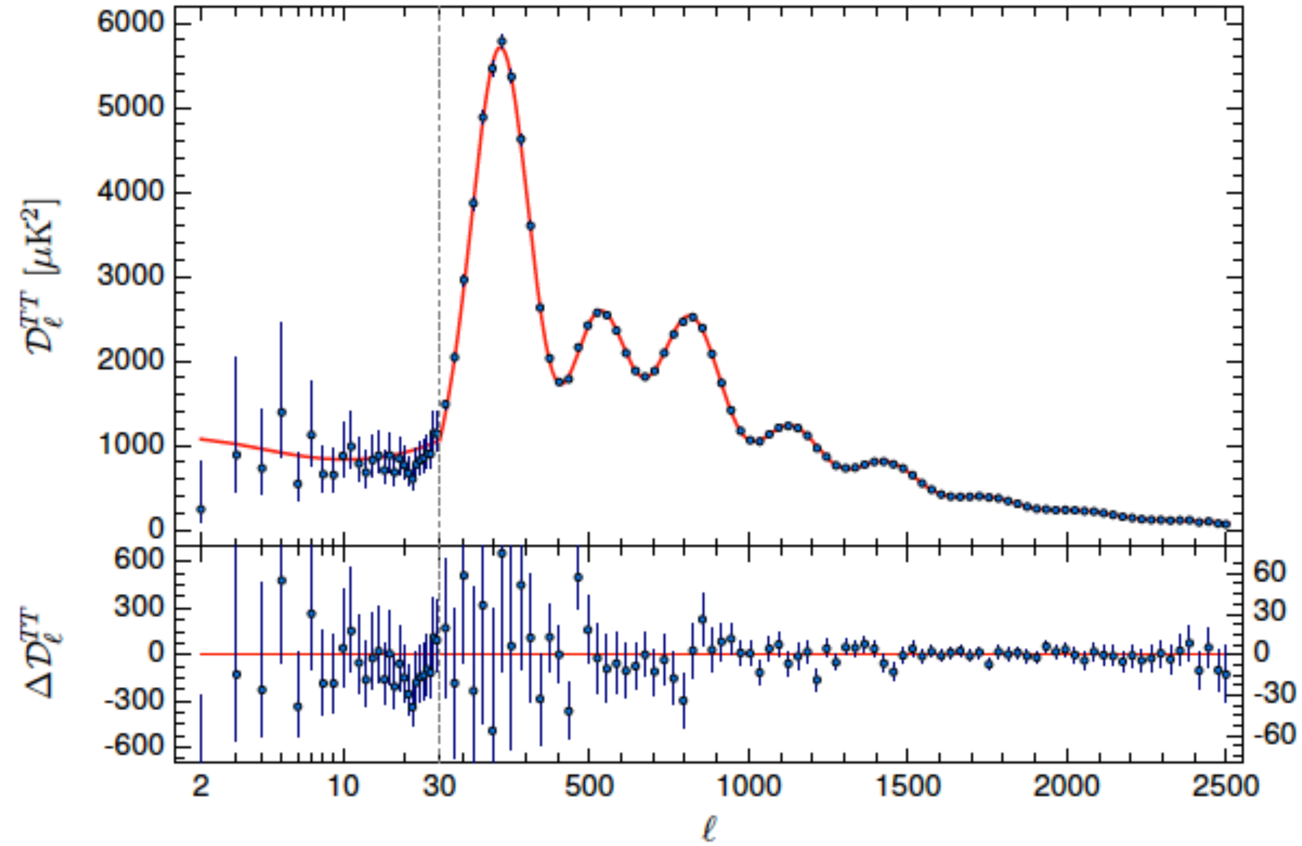

Smoothed CMB map (above), TT (right above), TE (right), and EE (far right) angular power spectrum measurements from *Planck* satellite data, fitted with a 6-parameter ΛCDM cosmology model.

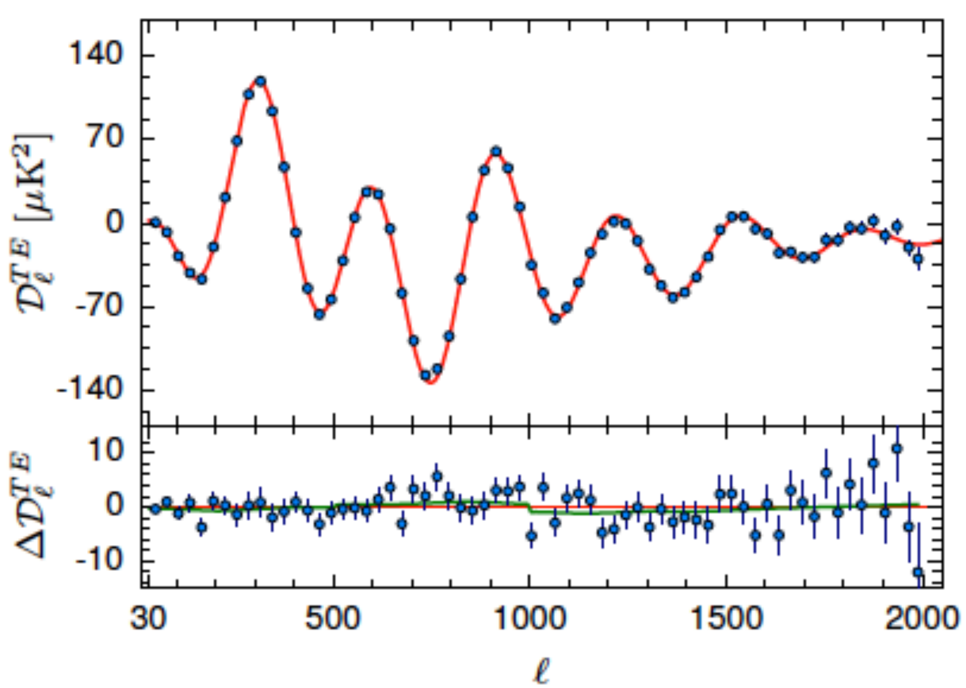

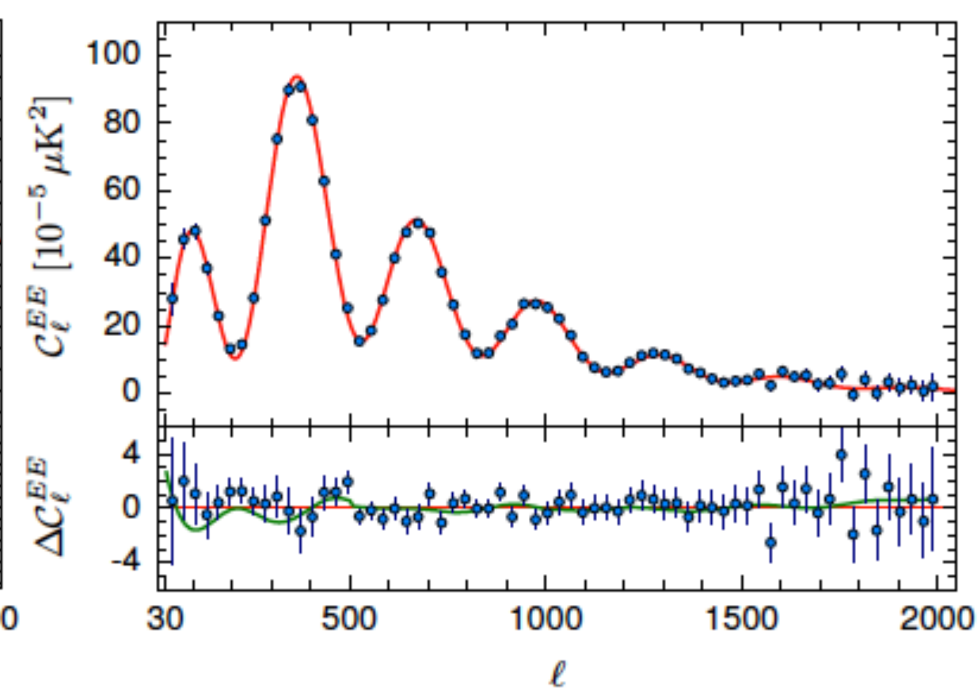

Low multipole "anomaly"

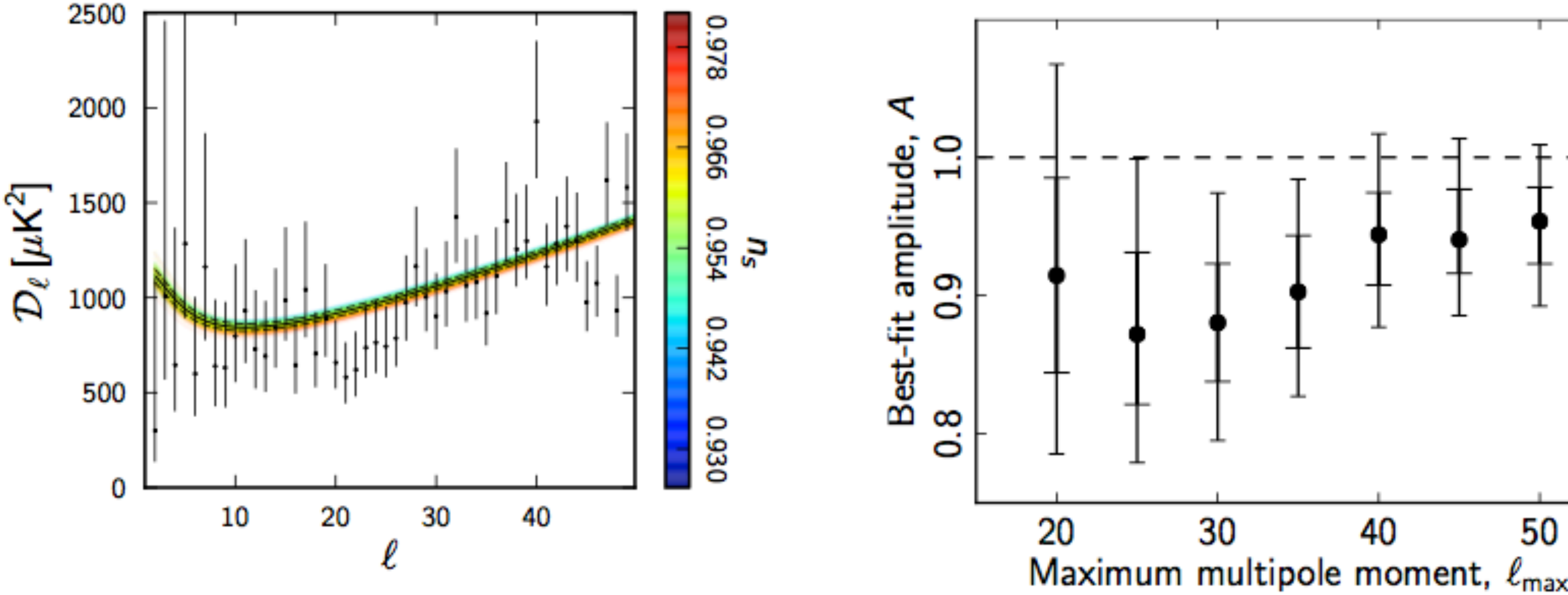

Fig. 39. *Left*: *Planck TT* spectrum at low multipoles with 68% ranges on the posteriors. The "rainbow" band show the best fits to the entire *Planck*+WP likelihood for the base ΛCDM cosmology, colour-coded according to the value of the scalar spectral index n_s. *Right*: Limits (68% and 95%) on the relative amplitude of the base ΛCDM fits to the *Planck*+WP likelihood *fitted only to the Planck TT likelihood* over the multipole range $2 \leq \ell \leq \ell_{max}$.

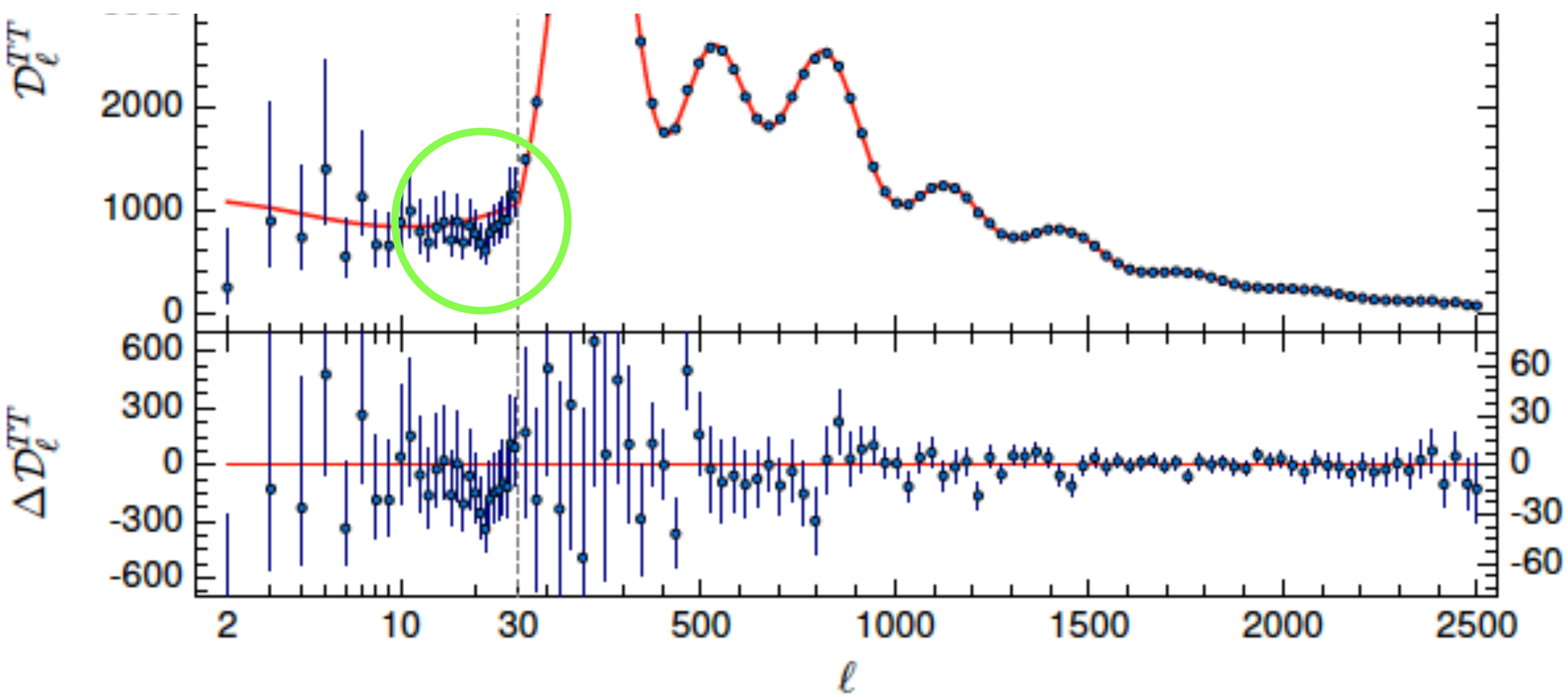

Planck collaboration (2013)

Low multipole “anomaly”

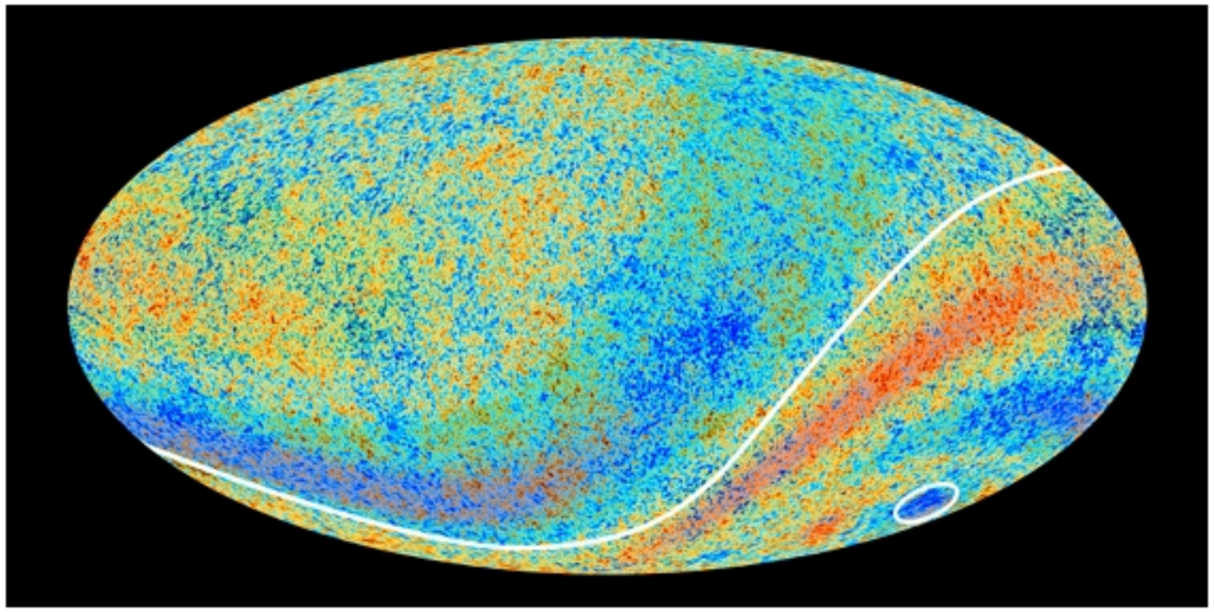

Planck’s anomalous sky: the hemispheric asymmetry and the cold spot. *Credit: ESA and the Planck Collaboration*

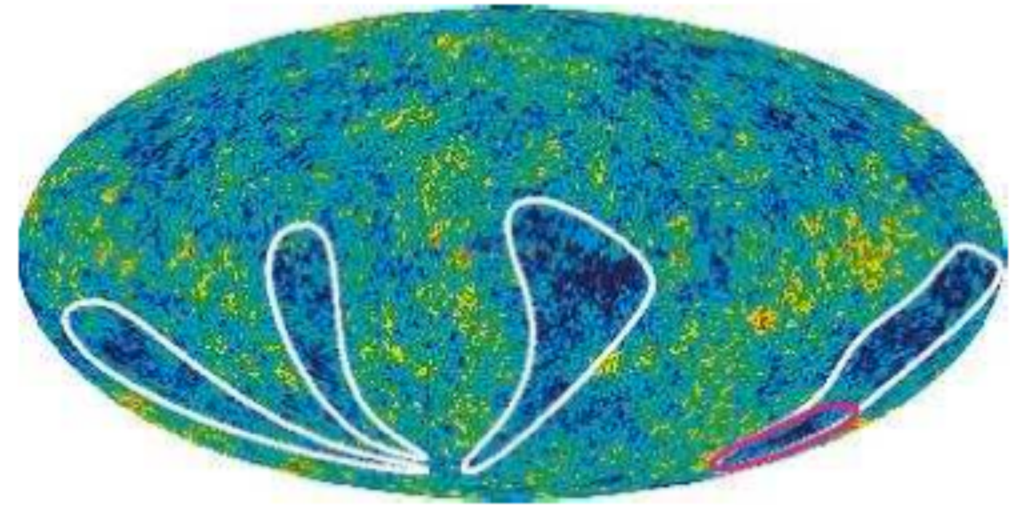

WMAP “fingers”

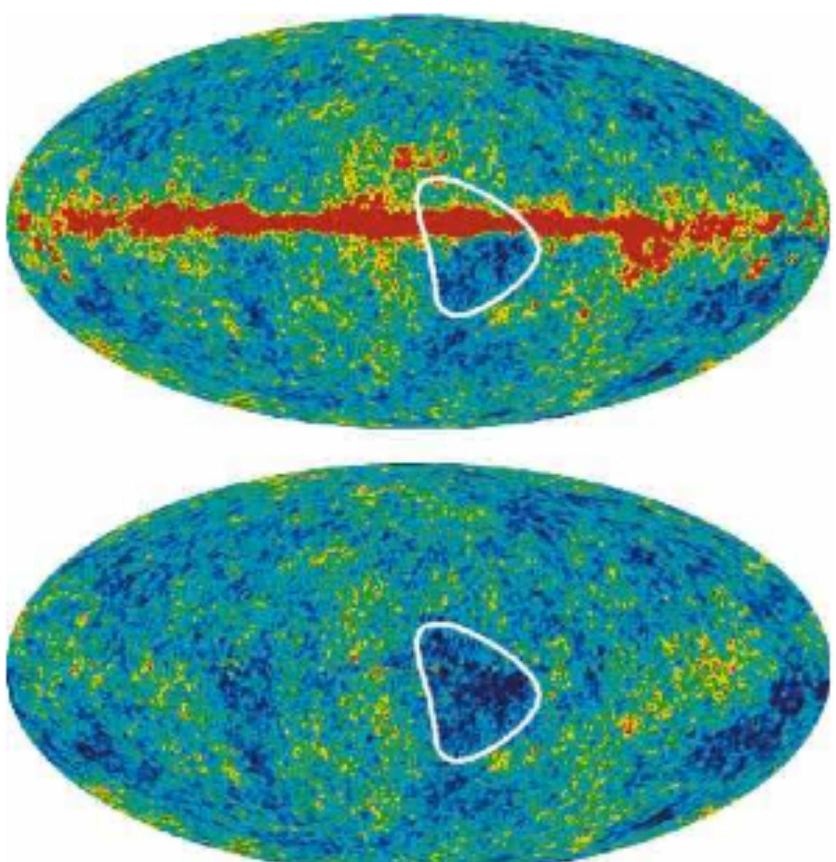

WMAP cold spot

Bennett et al. (2011)

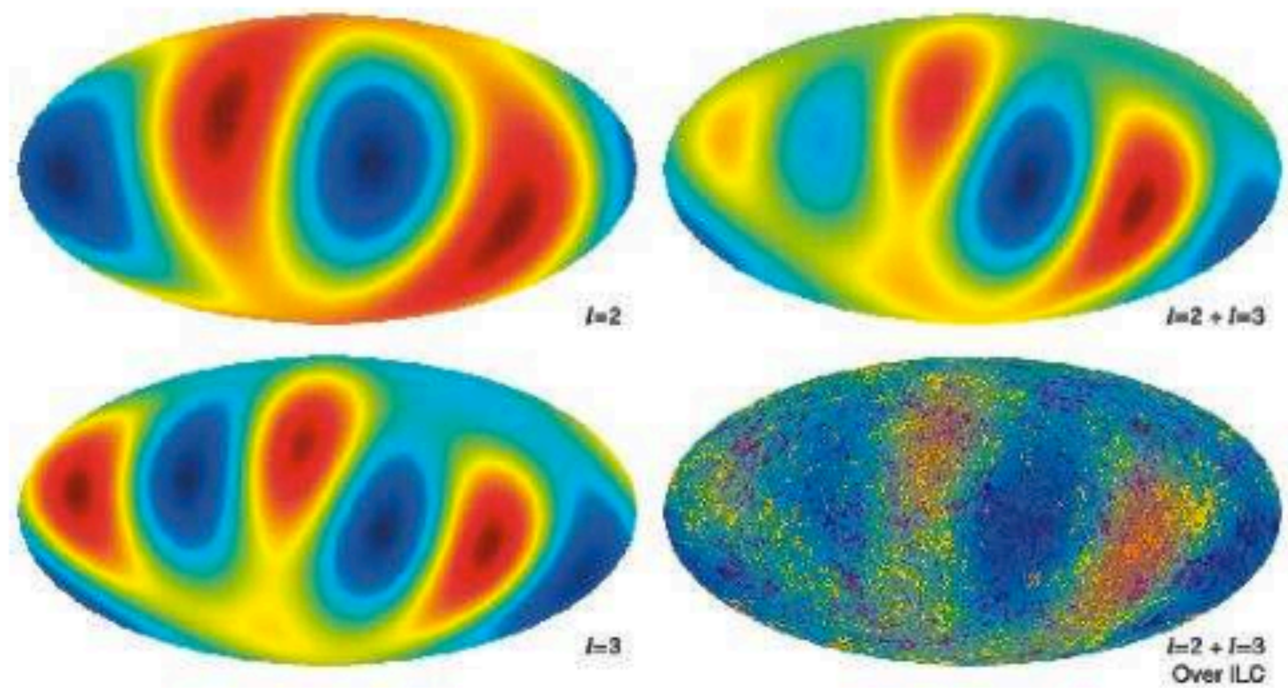

Figure 14. $l = 2$ quadrupole and $l = 3$ octupole maps are added. The combined map is then shown superposed on the ILC map from Figure 2. Note that the quadrupole and octupole components arrange themselves to match the cool fingers and the warm regions in between. The fingers and the alignment of the $l = 2$ and $l = 3$ multipoles are intimately connected.

CMB “anomalies”

WMAP 7 yr result
Bennett et al. (2011)

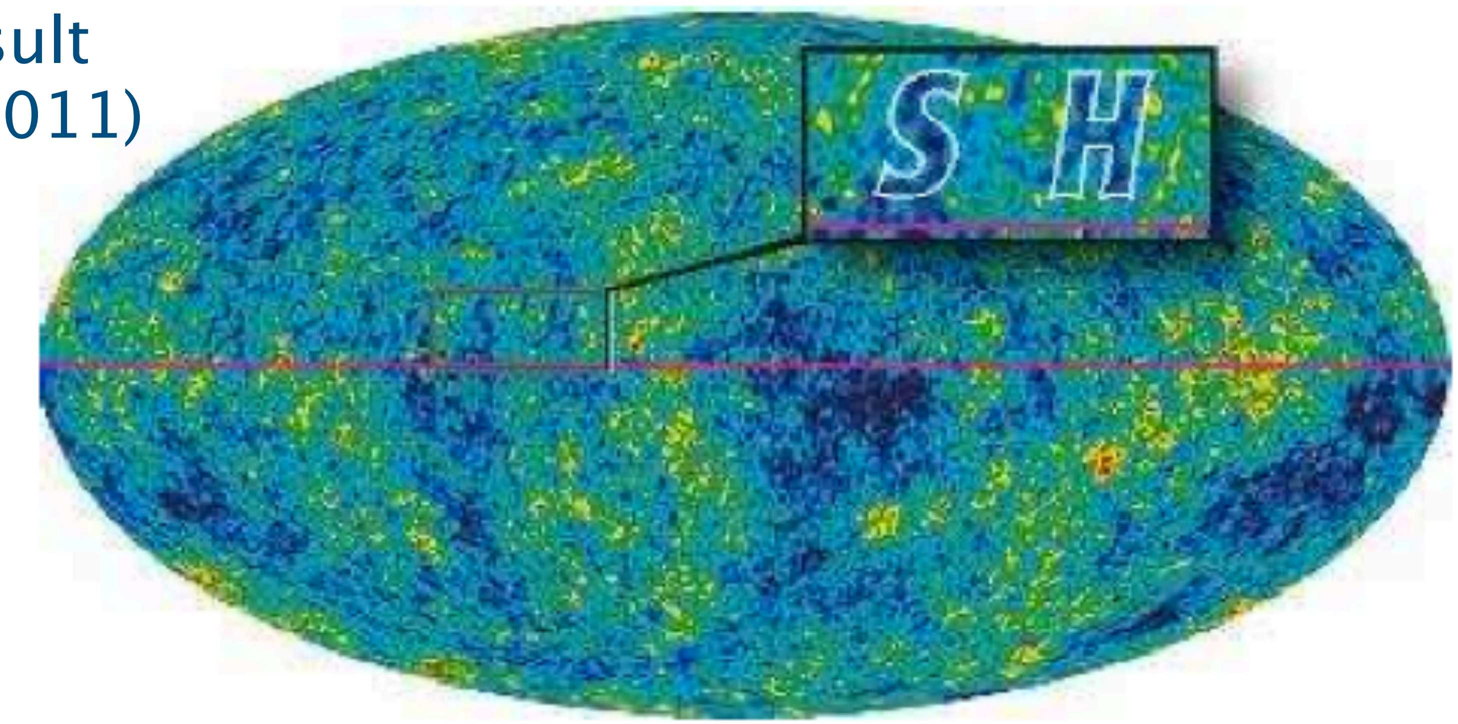

Figure 17. “SH” initials of Stephen Hawking are shown in the ILC sky map. The “S” and “H” are in roughly the same font size and style, and both letters are aligned neatly along a line of fixed Galactic latitude. A calculation would show that the probability of this particular occurrence is vanishingly small. Yet, there is no case to made for a non-standard cosmology despite this extraordinarily low probability event. It is clear that the combined selection of looking for initials, these particular initials, and their alignment and location are all *a posteriori* choices. For a rich data set, as is the case with *WMAP* , there are a lot of data and a lot of ways of analyzing the data. Low probability events are guaranteed to occur. The *a posteriori* assignment of a likelihood for a particular event detected, especially when the detection of that event is “optimized” for maximum effect by analysis choices, does not result in a fair unbiased assessment. This is a recurrent issue with CMB data analysis and is often a tricky issue and one that is difficult to overcome.

CMB “anomalies”

WMAP 7 yr result
Bennett et al. (2011)

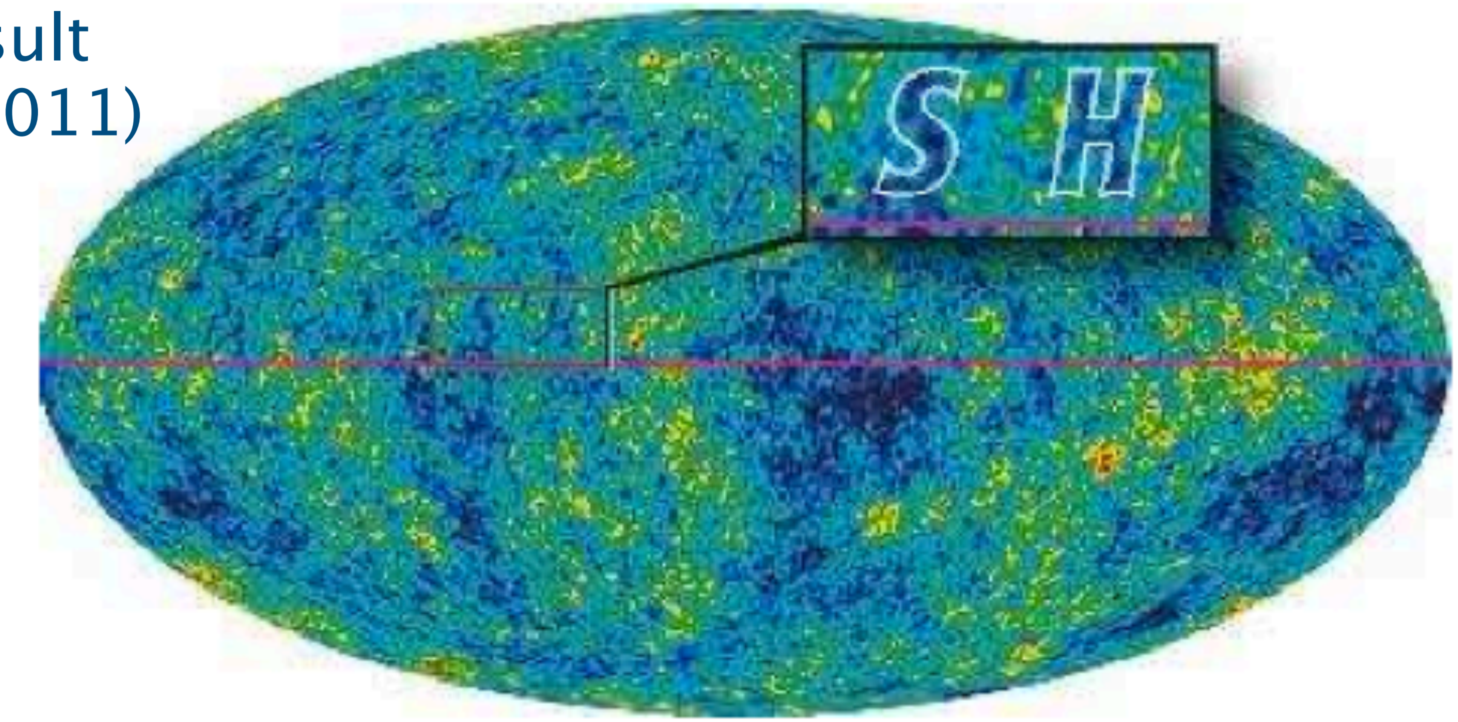

Figure 17. “SH” initials of Stephen Hawking are shown in the ILC sky map. The “S” and “H” are in roughly the same font size and style, and both letters are aligned neatly along a line of fixed

A large fraction of simulated CMB skies will have some kind of anomaly or oddity. The key is whether the oddity is specified in advance.

timized” for maximum effect by analysis choices, does not result in a fair unbiased assessment. This is a recurrent issue with CMB data analysis and is often a tricky issue and one that is difficult to overcome.

"pi" in the sky

Ali Frolop & Douglas Scott, arXiv:1603.09703

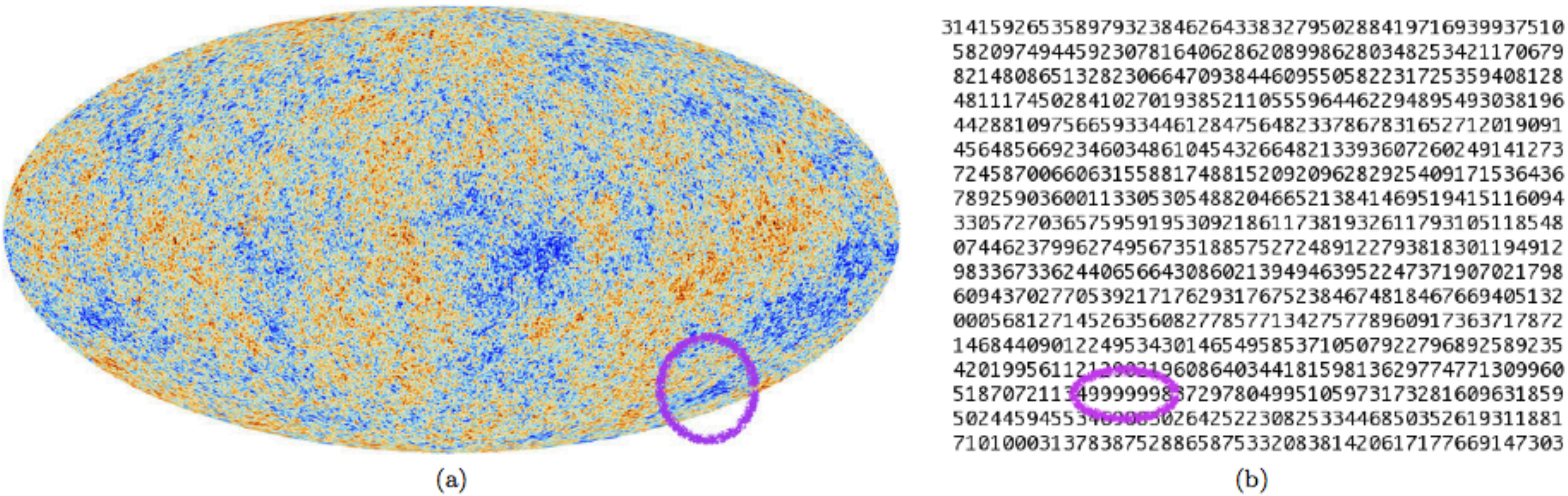

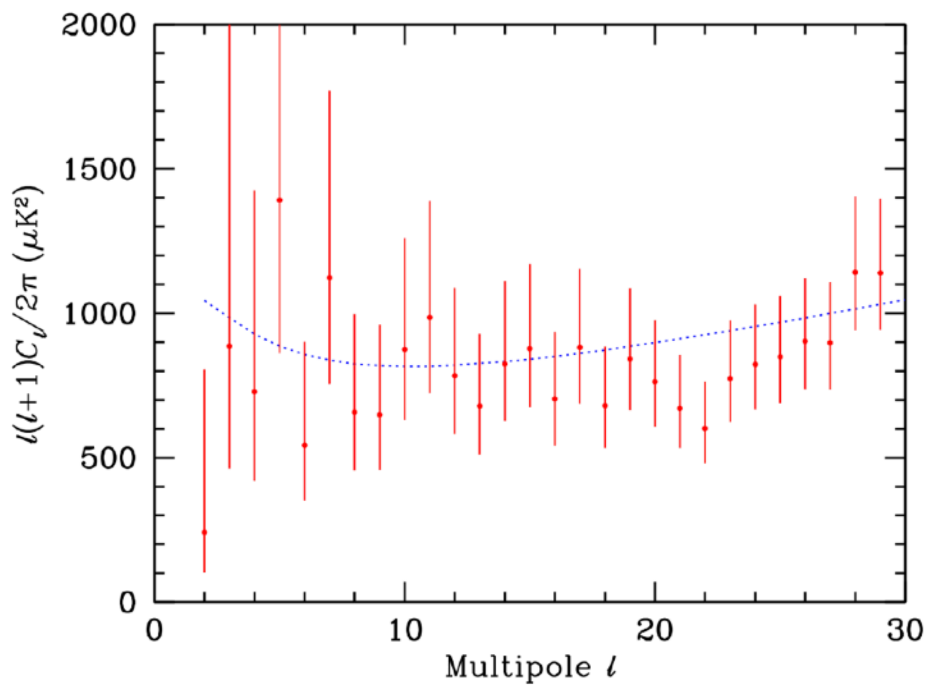

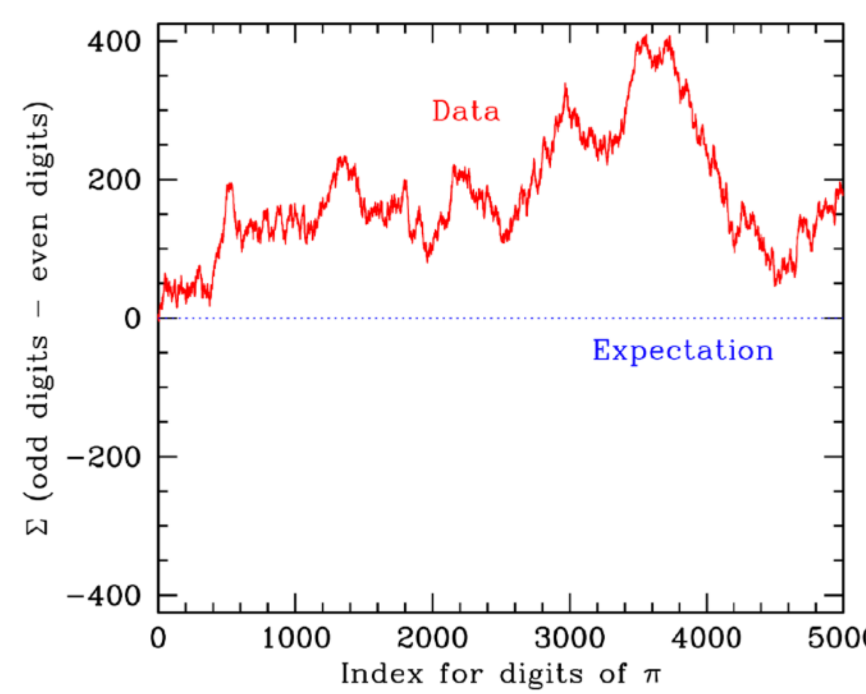

Search for anomalies: Penrose's CCC "rings" in the CMB sky

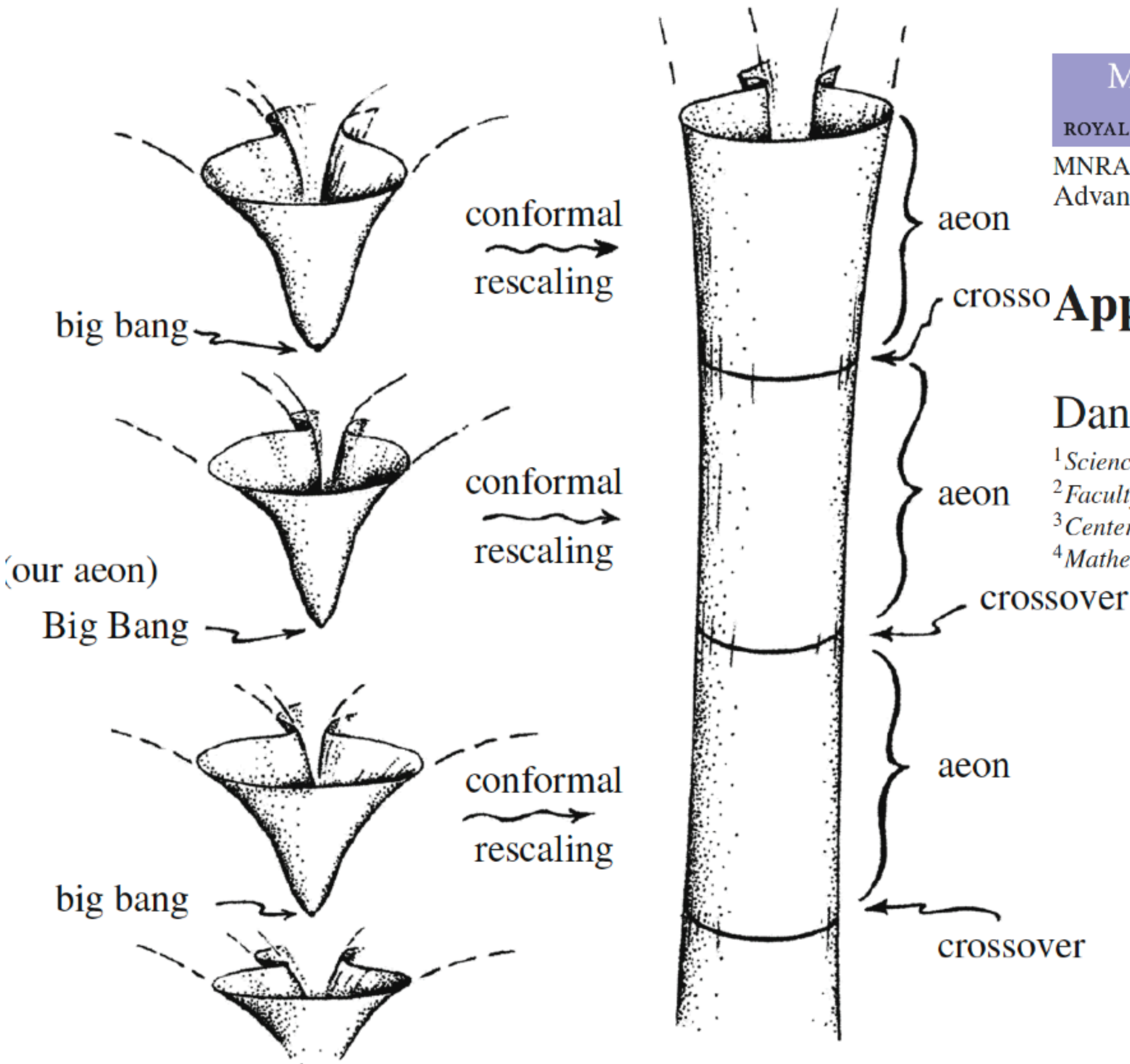

Monthly Notices of the ROYAL ASTRONOMICAL SOCIETY

MNRAS **495**, 3403–3408 (2020) doi:10.1093/mnras/staa1343
Advance Access publication 2020 May 18

Apparent evidence for Hawking points in the CMB Sky★

Daniel An,[1] Krzysztof A. Meissner,[2] Paweł Nurowski[3]† and Roger Penrose[4]

[1] *Science Department, SUNY Maritime College, 6 Pennyfield Av., Throggs Neck, NY 10465, USA*
[2] *Faculty of Physics, University of Warsaw, Pasteura 5, PL-02-093 Warsaw, Poland*
[3] *Center for Theoretical Physics of PAS, Al. Lotników 32/46, PL-02-688 Warsaw, Poland*
[4] *Mathematical Institute, Oxford University, Radcliffe Observatory Quarter, Woodstock Rd., Oxford OX2 6GG, UK*

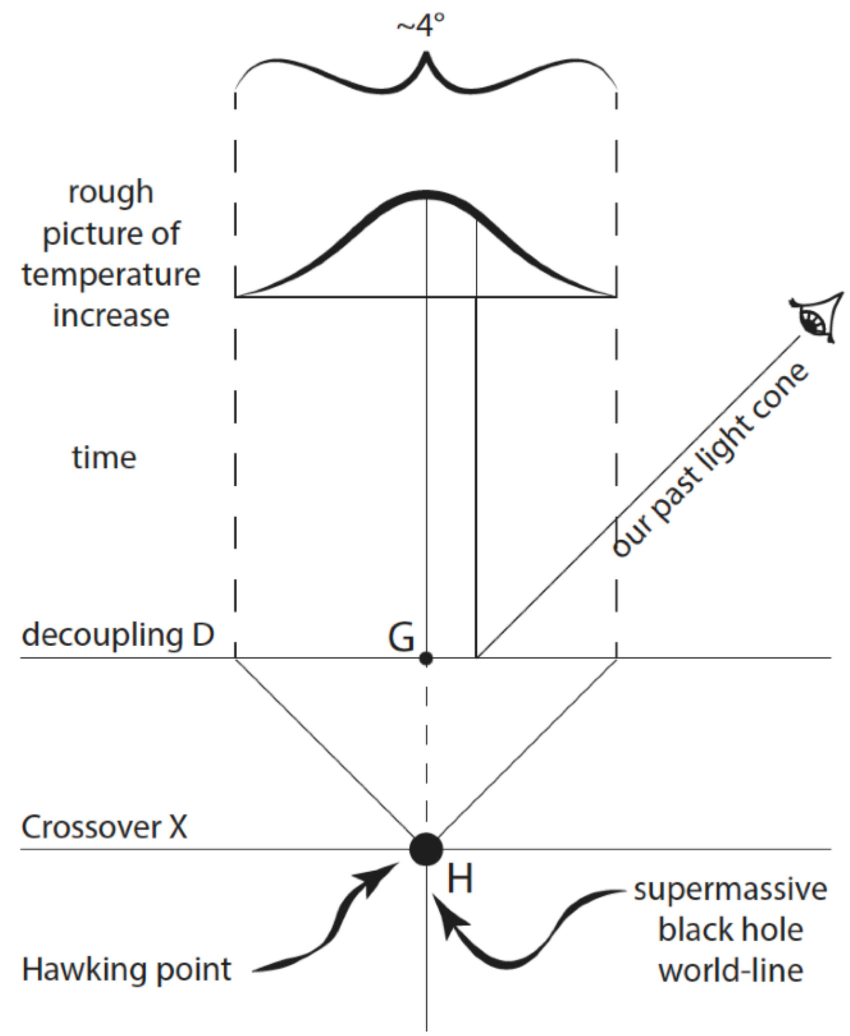

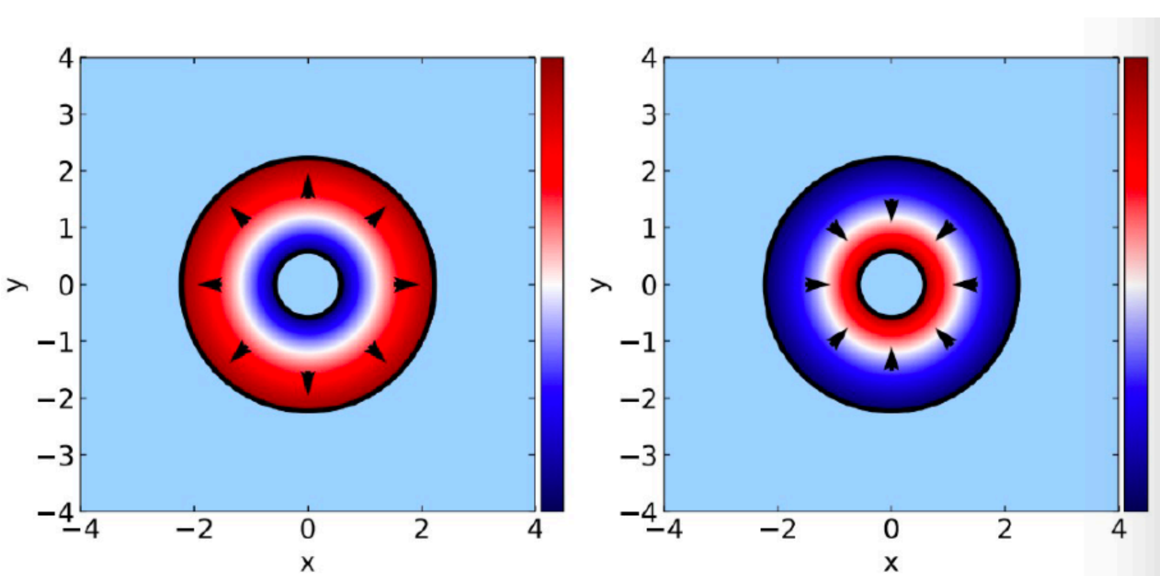

Search for anomalies: Penrose's CCC "rings" in the CMB sky

- Expect a gaussian gradient of the Temperature centred at G
- Look for annular regions in the CMB sky and check for significant drop of temperature from inner to outer boundary of annulus.
- Compare with simulations of randomly generated CMB

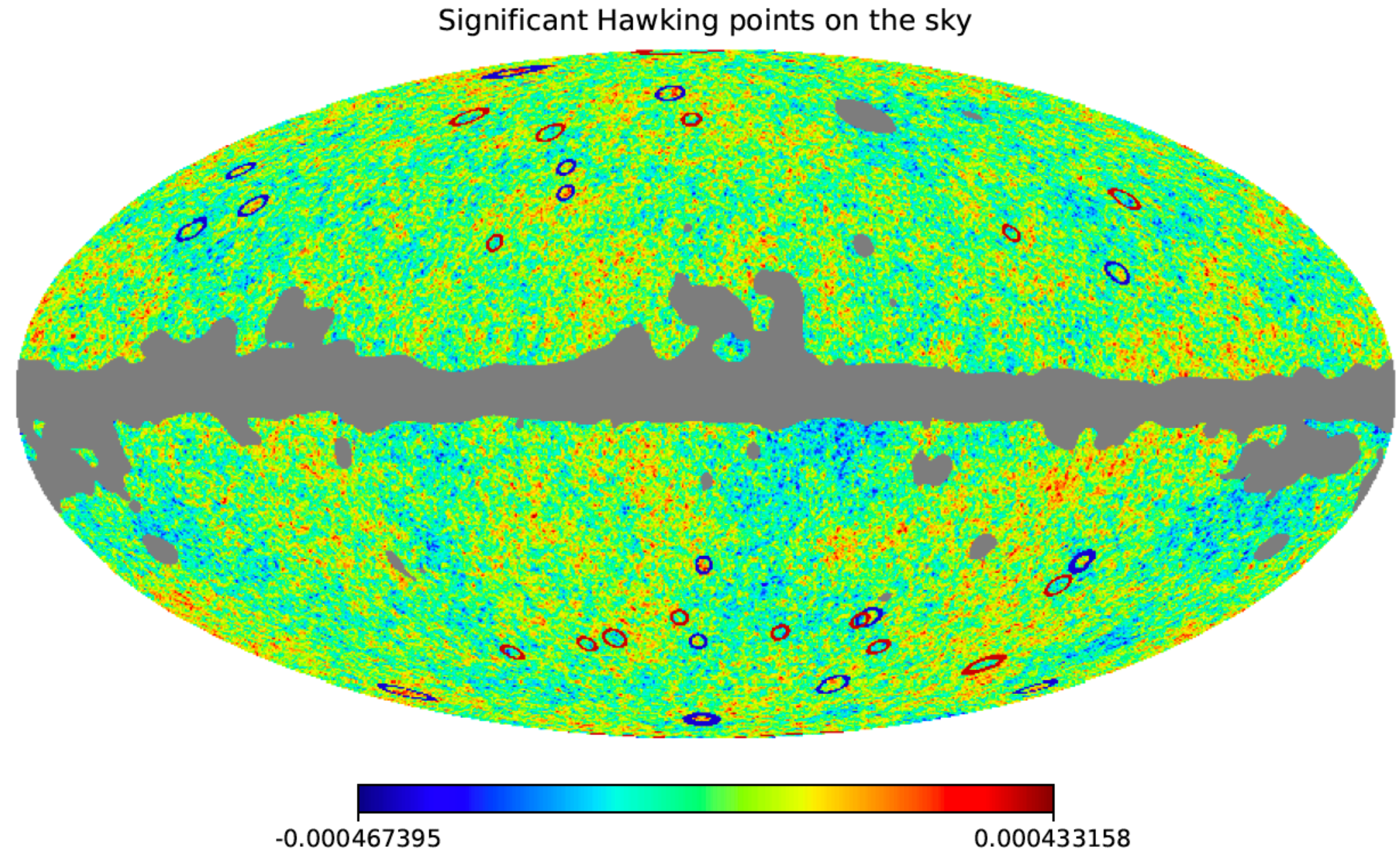

◉ If marginalized over all possible ring sizes, there is no evidence for "excess" positive-gradient rings (CCC authors do not provide an a-priori size estimate)

◉ There is no evidence of these rings in the polarization data either

arXiv.org > astro-ph > arXiv:1909.09672

Astrophysics > Cosmology and Nongalactic Astrophysics

[Submitted on 20 Sep 2019 (v1), last revised 21 Jan 2020 (this version, v2)]

Re-evaluating evidence for Hawking points in the CMB

Dylan L. Jow, Douglas Scott

Signs of non-Gaussianity

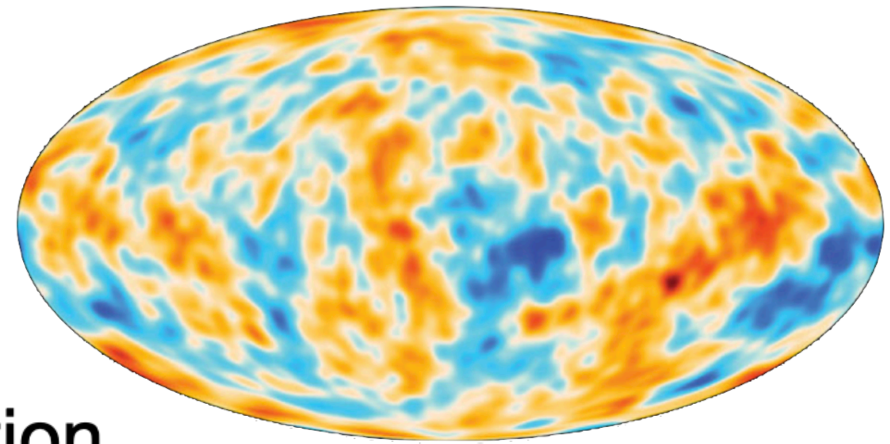

Gaussian + statistical isotropy

$$\langle \Theta(l_1)\Theta(l_2)\rangle = \delta(l_1 + l_2)C_l$$

- power spectrum encodes all the information
- modes with different wavenumber are independent

- Primordial non-Gaussianity:
  - Are the initial conditions Gaussian? What is the physics of inflation?
- Intrinsic CMB bispectrum:
  - non-Gaussianity induced by non-linear evolution of perturbations.

Quantifying non-Gaussianity

Bispectrum

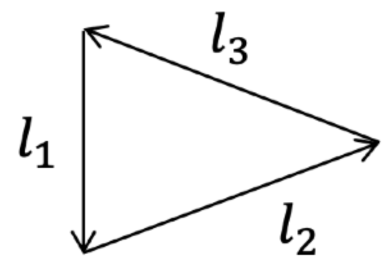

$$\boldsymbol{l_1} + \boldsymbol{l_2} + \boldsymbol{l_3} = \boldsymbol{0}$$

Flat sky approximation: $\langle \Theta(l_1)\Theta(l_2)\Theta(l_3)\rangle = \frac{1}{2\pi}\delta(l_1 + l_2 + l_3) b_{l_1 l_2 l_3}$

Trispectrum

$$\langle \Theta(\mathbf{l}_1)\Theta(\mathbf{l}_2)\Theta(\mathbf{l}_3)\Theta(\mathbf{l}_4)\rangle_C = (2\pi)^{-2}\delta(\mathbf{l}_1 + \mathbf{l}_2 + \mathbf{l}_3 + \mathbf{l}_4) T(\mathbf{l}_1, \mathbf{l}_2, \mathbf{l}_3, \mathbf{l}_4)$$

$$\langle \Theta(\mathbf{l}_1)\Theta(\mathbf{l}_2)\Theta(\mathbf{l}_3)\Theta(\mathbf{l}_4)\rangle_C = \frac{1}{2}\int \frac{d^2\mathbf{L}}{(2\pi)^2}\delta(\mathbf{l}_1 + \mathbf{l}_2 + \mathbf{L})\delta(\mathbf{l}_3 + \mathbf{l}_4 - \mathbf{L})\mathbb{T}^{(\ell_1 \ell_2)}_{(\ell_3 \ell_4)}(L) + \text{perms.}$$

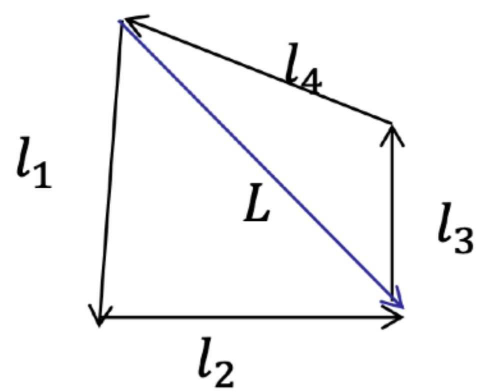

N-spectra…

- Scalar non-Gaussianity

$$\langle \delta(k_1)\delta(k_2)\delta(k_3)\rangle \propto Shape \times f_{NL}$$

f_{NL} to parametrize non-Gaussianity

Primordial non-Gaussianities are generally described by a non-zero value of the three-point correlation function of the primordial curvature function $\phi(k)$ in the Fourier space:

$$\langle \Phi(\mathbf{k_1})\Phi(\mathbf{k_2})\Phi(\mathbf{k_3})\rangle = (2\pi)^3\delta^{(3)}(\mathbf{k_1}+\mathbf{k_2}+\mathbf{k_3})F(k_1,k_2,k_3)$$

$F(k)$ is the shape function of the bispectrum. In this limit, the primordial curvature perturbations can be parametrized by the dimensionless quantity f_{NL} with respect to the linear Gaussian part *in real space*:

$$\Phi(\mathbf{x}) = \Phi_L(\mathbf{x}) + f_{\rm NL}\left(\Phi_L^2(\mathbf{x}) - \langle\Phi_L^2(\mathbf{x})\rangle\right)$$

$f_{NL} = 0$

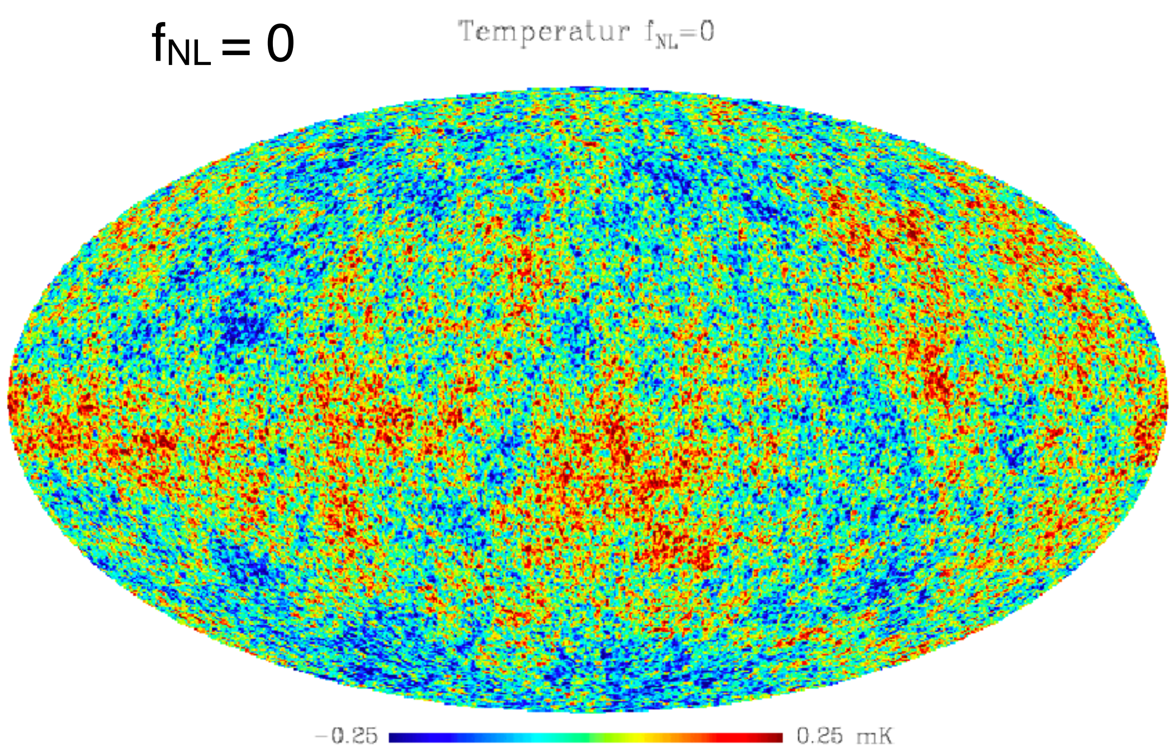

$f_{NL} = 3000$

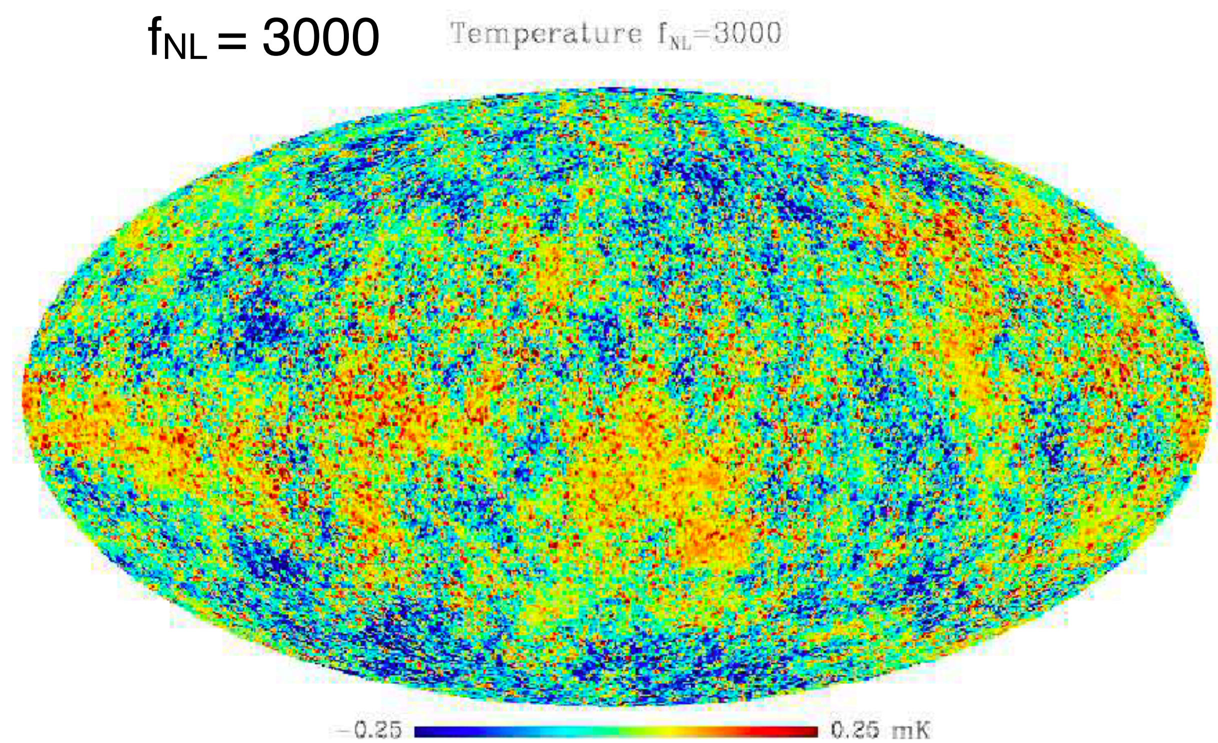

From Liguori et al. (2007)

Planck limits on non-Gaussianity

<u>There is no evidence of a non-zero f_{NL} from Planck data</u>

Planck (2018) results

Temperature bispectrum calculations from different flavors of the CMB maps.

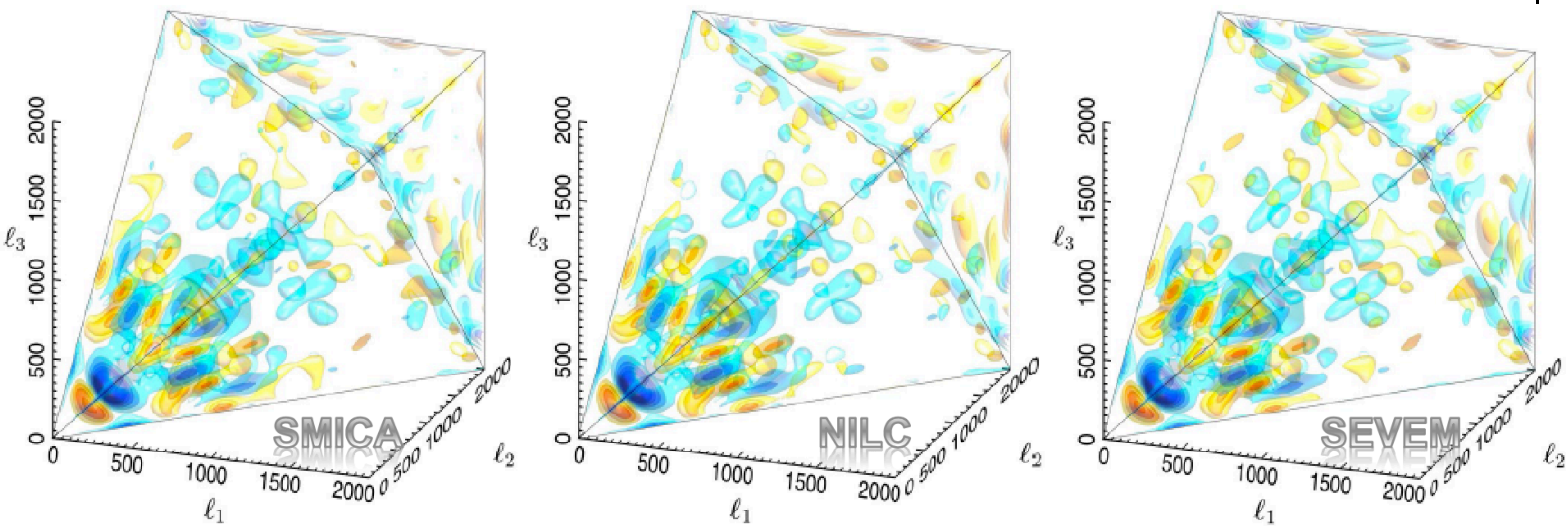

	SMICA		SEVEM		NILC		Commander	
Shape	Independent	Joint	Independent	Joint	Independent	Joint	Independent	Joint
f_{NL}^{local}	-0.1 ± 5.6	5.0 ± 8.4	0.0 ± 5.7	1.7 ± 8.7	0.0 ± 5.6	5.2 ± 8.5	-1.3 ± 5.6	3.1 ± 8.3
f_{NL}^{equil}	26 ± 69	5 ± 73	43 ± 70	30 ± 74	5 ± 69	-12 ± 73	32 ± 69	20 ± 73
f_{NL}^{ortho}	-11 ± 39	-5 ± 44	8 ± 39	13 ± 45	4 ± 39	13 ± 45	29 ± 39	35 ± 44
$b_{PS}/(10^{-29})$	6.3 ± 1.0	5.0 ± 2.7	9.7 ± 1.1	7.1 ± 2.9	5.7 ± 1.1	5.4 ± 2.7	5.4 ± 1.0	3.6 ± 2.6
$A_{CIB}/(10^{-27})$	3.0 ± 0.5	0.6 ± 1.3	4.6 ± 0.5	1.3 ± 1.4	2.6 ± 0.5	0.1 ± 1.3	2.6 ± 0.5	0.9 ± 1.3
$f_{NL}^{dust}/(10^{-2})$	6.6 ± 4.4	6.7 ± 5.9	4.8 ± 4.6	1.9 ± 6.1	4.8 ± 4.4	5.1 ± 5.9	4.4 ± 4.3	3.1 ± 5.7

CMB Experiments and Detector Types

Arno Penzias & Robert Wilson, 1965

A MEASUREMENT OF EXCESS ANTENNA TEMPERATURE
AT 4080 Mc/s

Measurements of the effective zenith noise temperature of the 20-foot horn-reflector antenna (Crawford, Hogg, and Hunt 1961) at the Crawford Hill Laboratory, Holmdel, New Jersey, at 4080 Mc/s have yielded a value about 3.5° K higher than expected. This excess temperature is, within the limits of our observations, isotropic, unpolarized, and free from seasonal variations (July, 1964–April, 1965). A possible explanation for the observed excess noise temperature is the one given by Dicke, Peebles, Roll, and Wilkinson (1965) in a companion letter in this issue.

May 13, 1965

BELL TELEPHONE LABORATORIES, INC
CRAWFORD HILL, HOLMDEL, NEW JERSEY

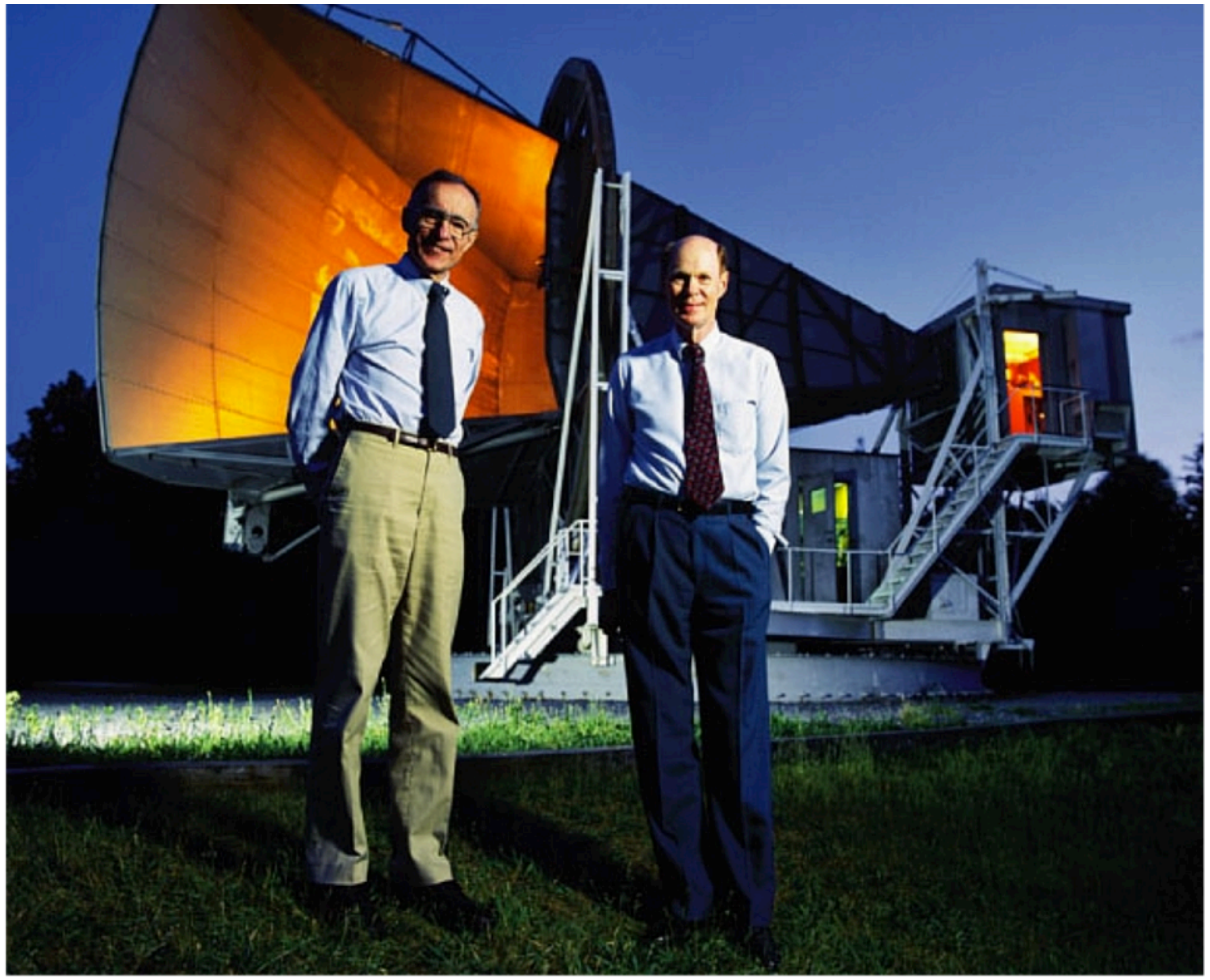

COBE satellite

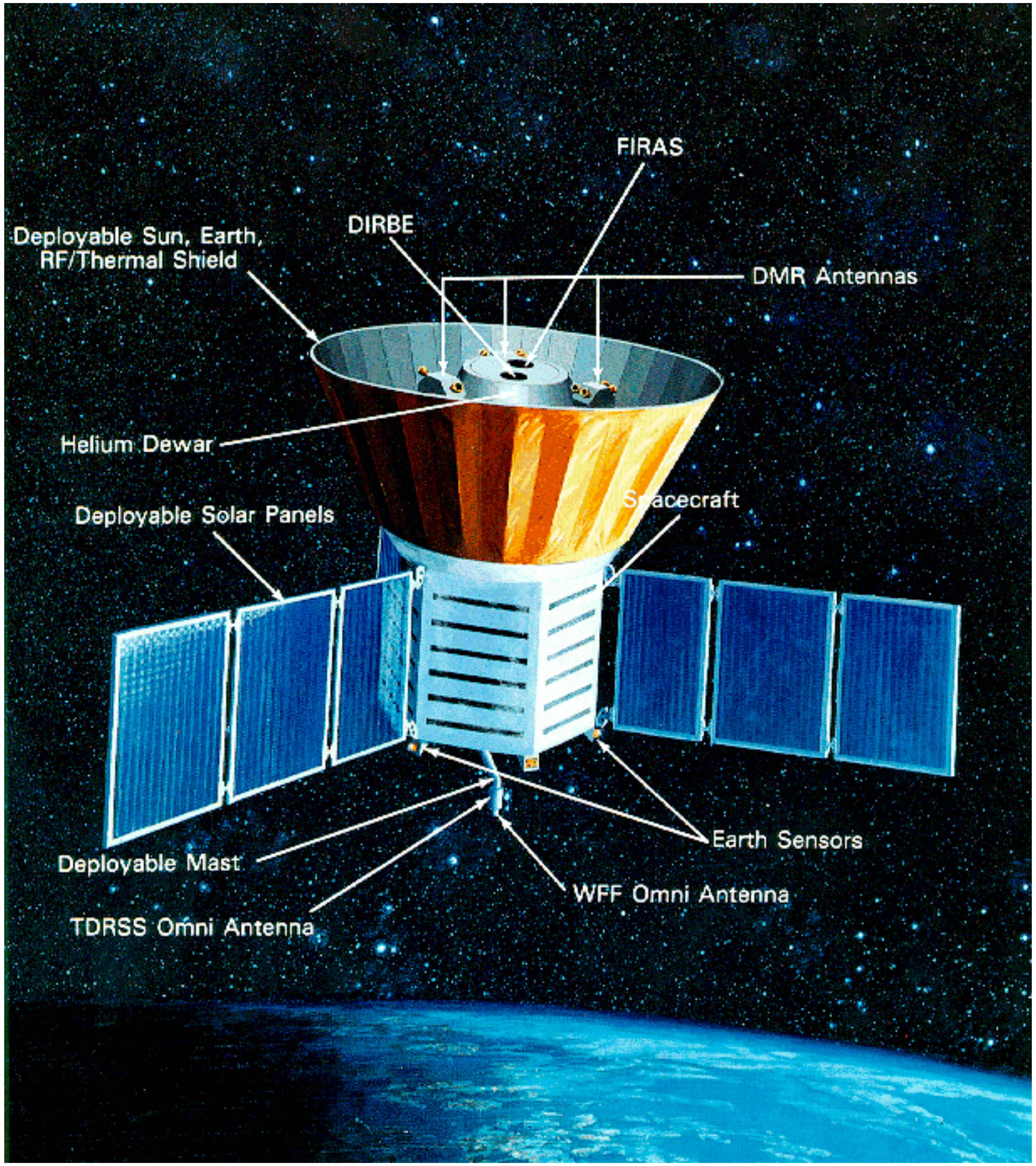

Credit: NASA

Launched on Nov. 1989 on a Delta rocket.

DIRBE: Measured the absolute sky brightness in the 1–240 μm wavelength range, to search for the Infrared Background

FIRAS: Measured the spectrum of the CMB, finding it to be an almost perfect blackbody with $T_0 = 2.725 \pm 0.002$ K

DMR: Found "anisotropies" in the CMB for the first time, at a level of 1 part in 10^5

2006 Nobel prize in physics

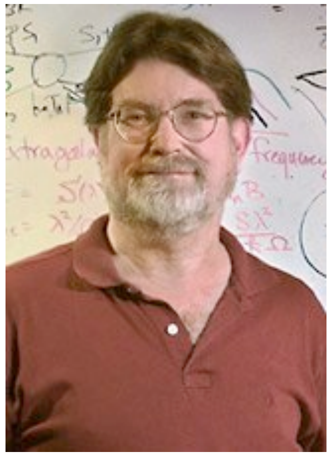

BOOMERanG and MAXIMA

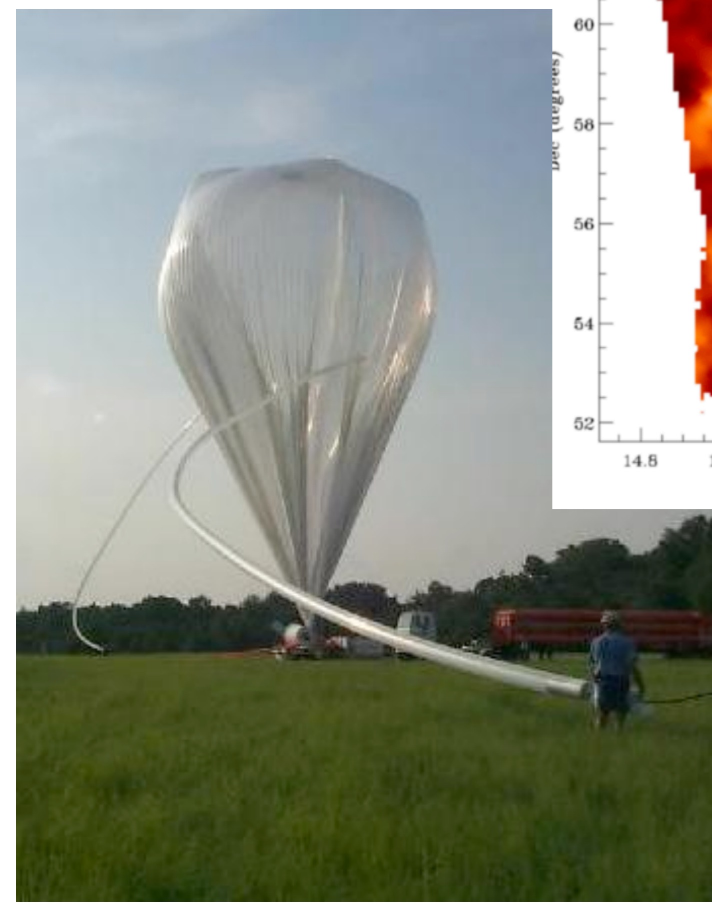

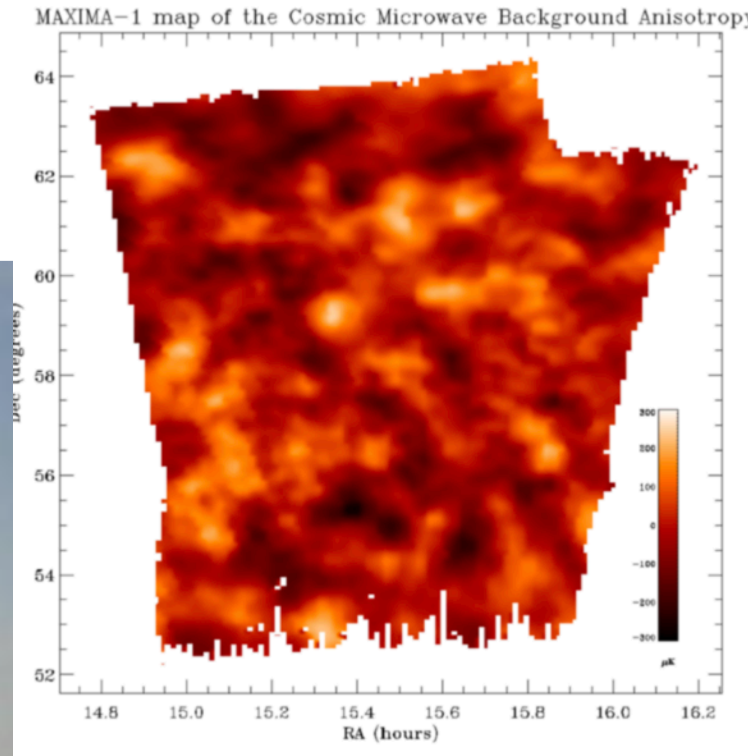

Boomerang launch Dec 1998

(Balloon Observations Of Millimetric Extragalactic Radiation ANd Geophysics)

Maxima launch Aug 98, Jun 99

Launched from Texas

DASI from South Pole

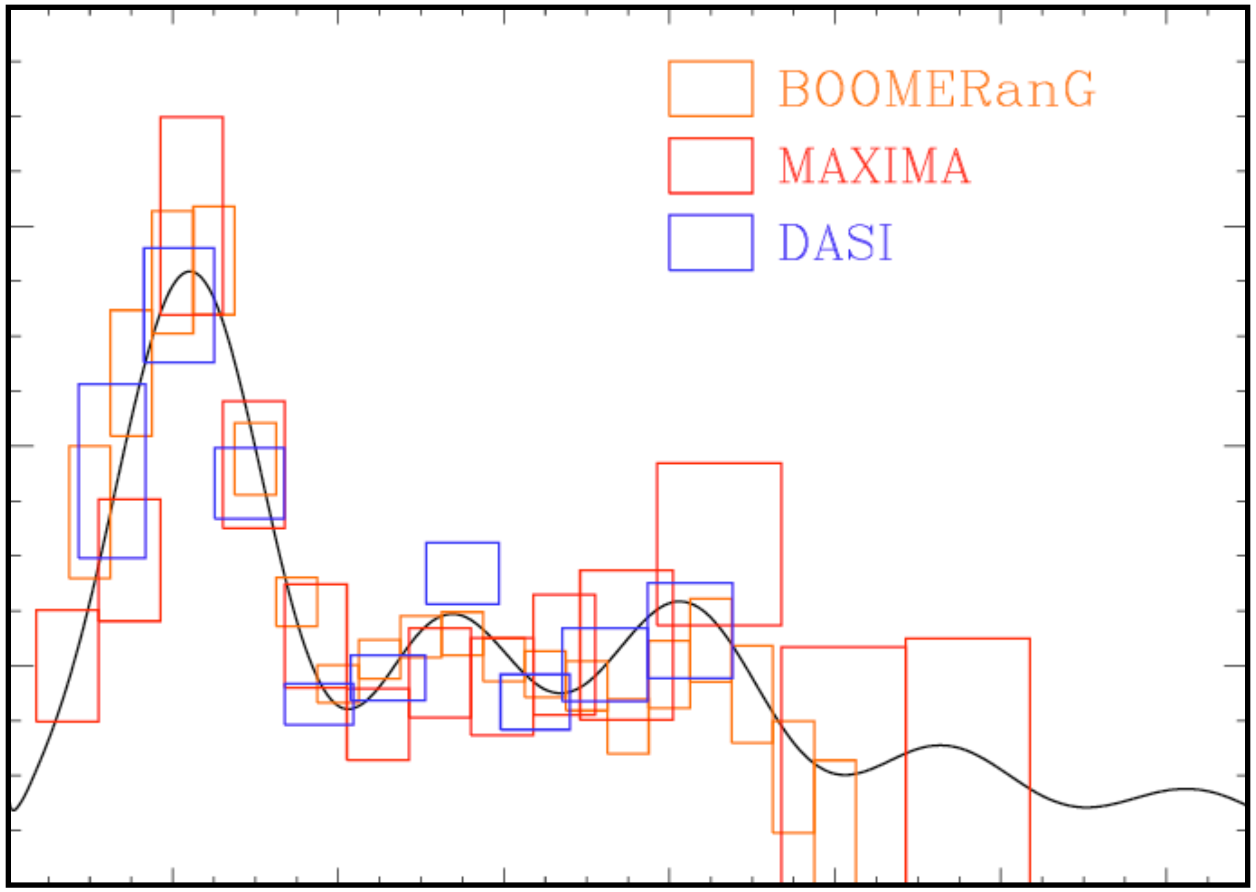

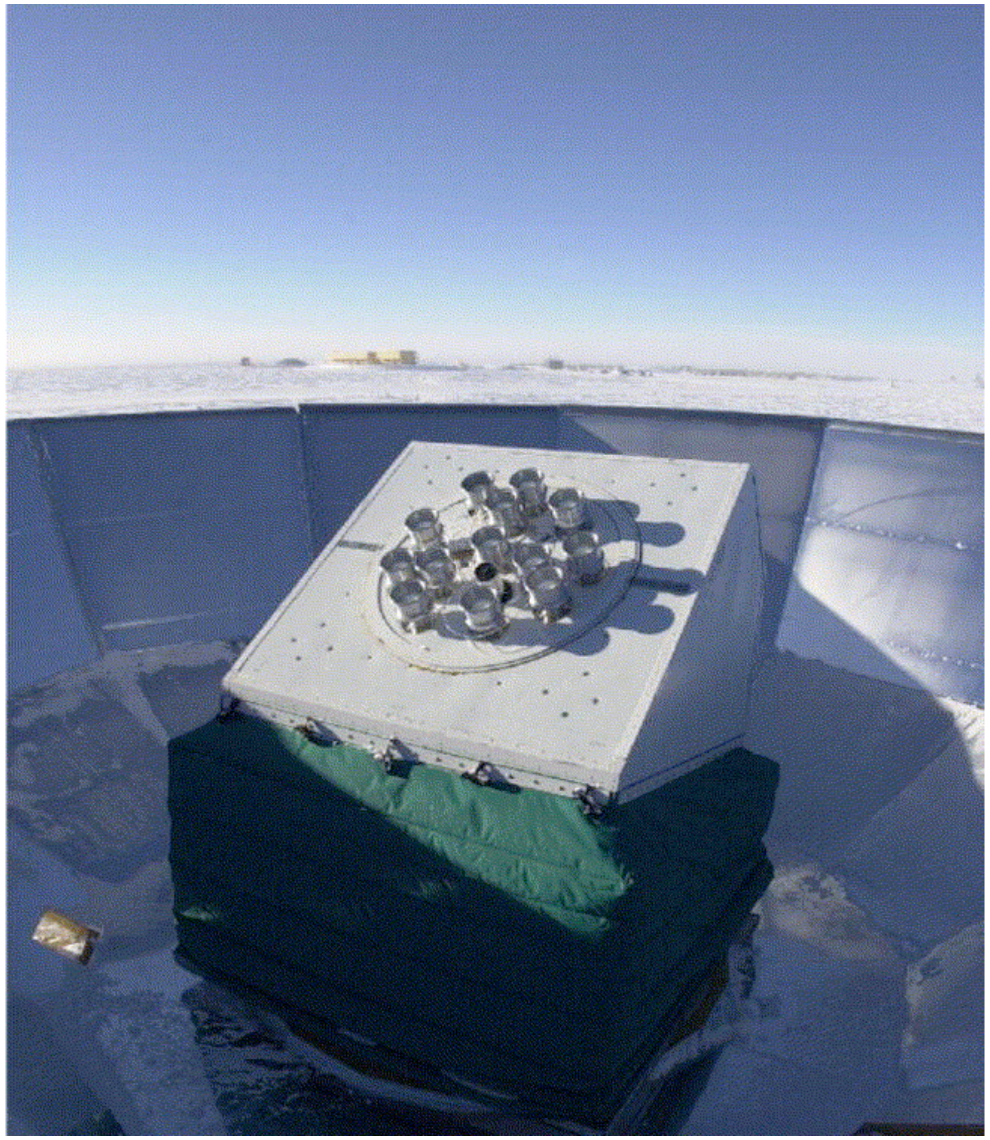

DASI (Degree Angular Scale Interferometer) was a 13-element **interferometer** operating from South Pole, and in 2002 reported the first detection of polarization anisotropies (E-mode).

DASI was replaced by the QUaD and then Keck Array, both bolometer instruments.

Planck satellite (2009–2013)

Credit: ESA

PLANCK launch: May 2009

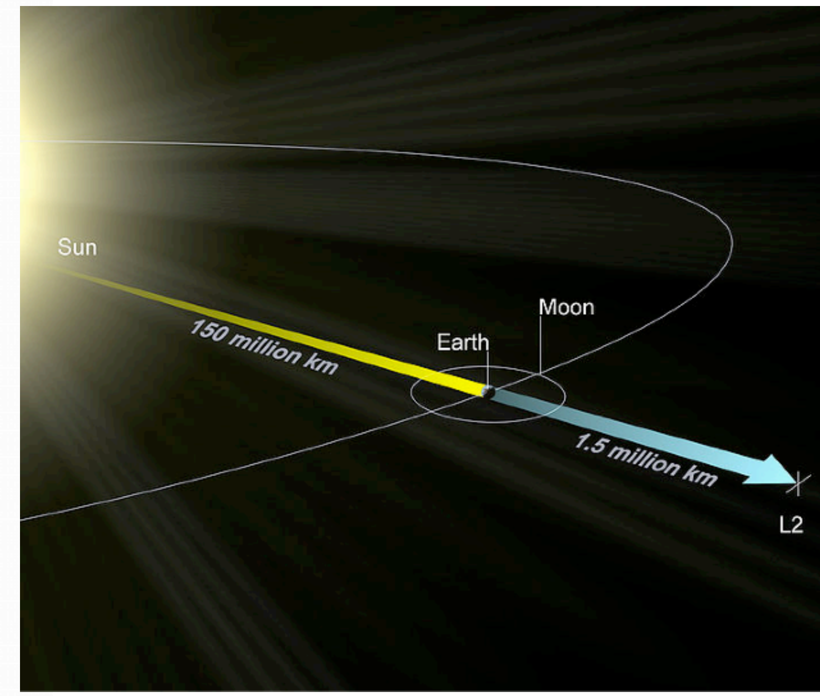

Destination L2: the second Lagrangian point

(getting crowded there!)

Credit: ESA

Planck transforming the CMB science

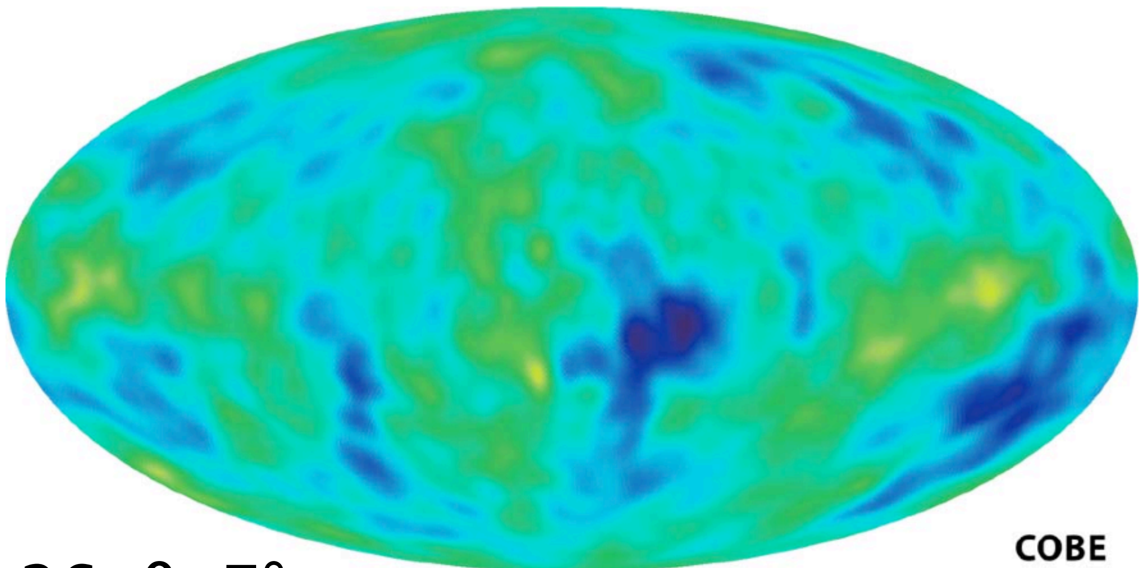

$l<26,\ \theta\sim7^\circ$

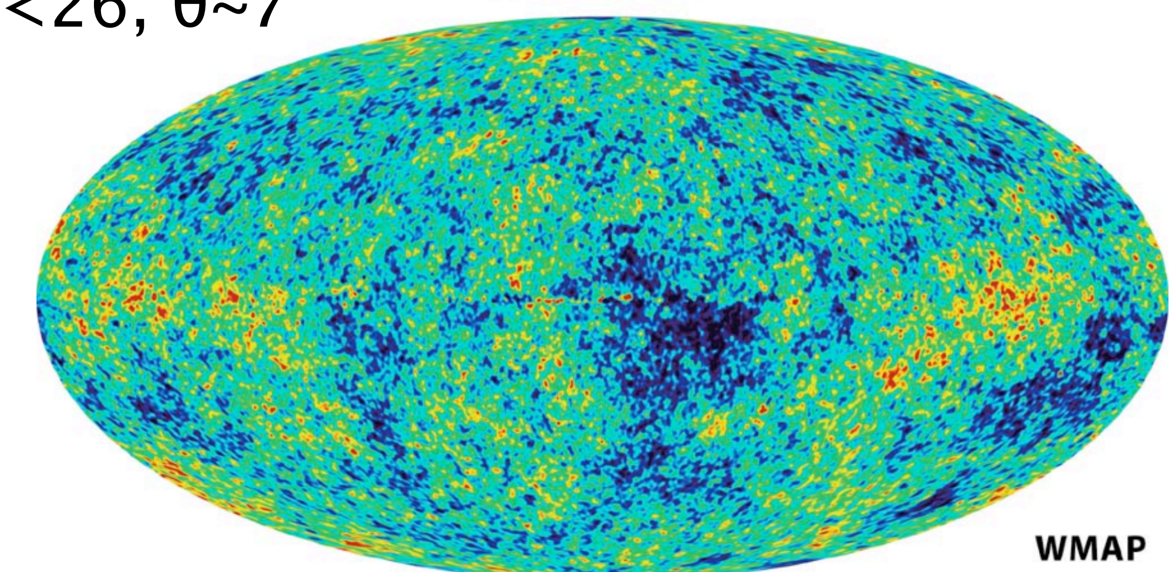

$l<780,\ \theta\sim0.2^\circ$

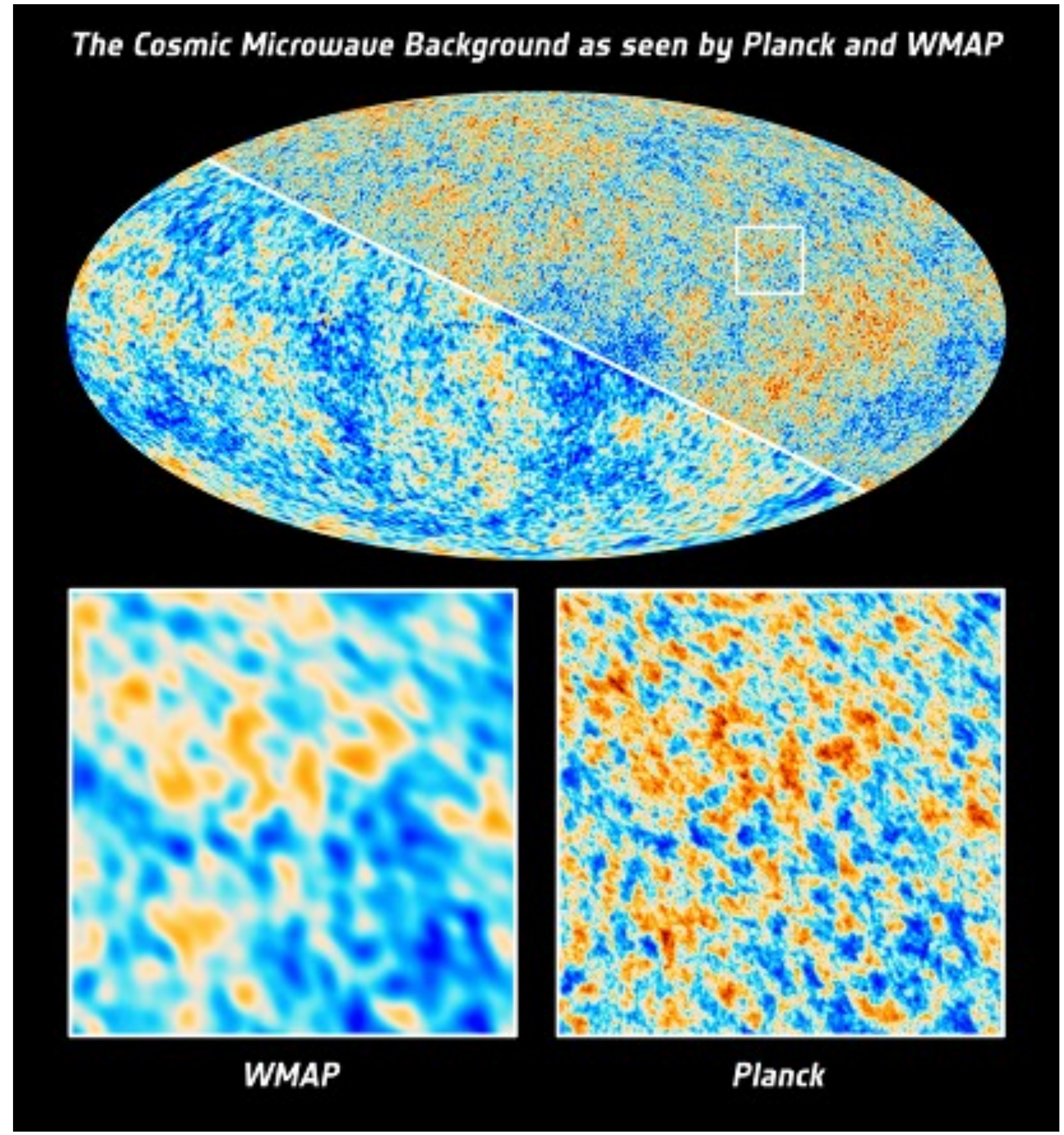

$l<2160,\ \theta\sim0.1^\circ$

Slide courtesy Yutaro Sekimoto (ISAS/JAXA)

LiteBIRD Spacecraft

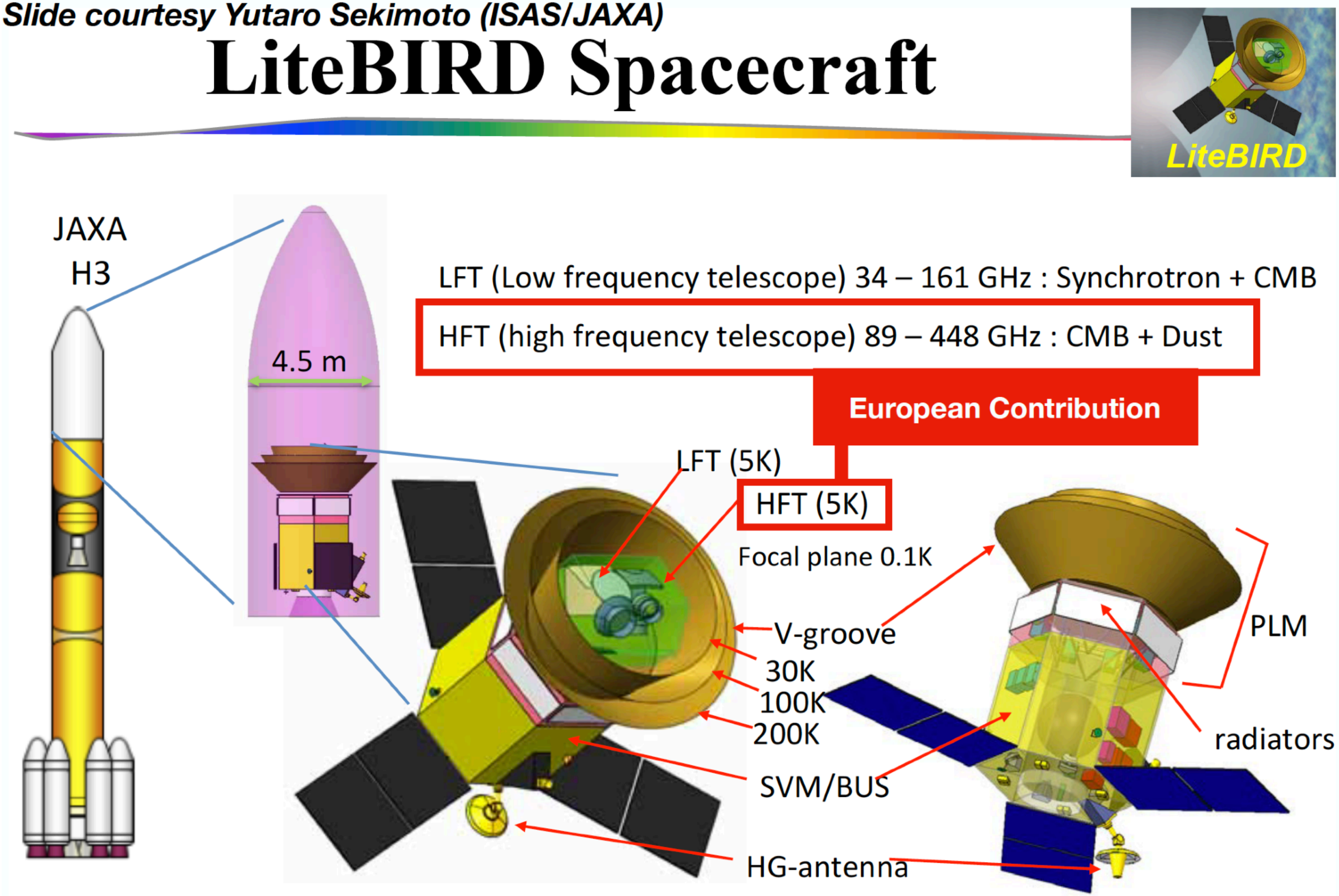

Possible launch 2027+

Planck satellite detector array

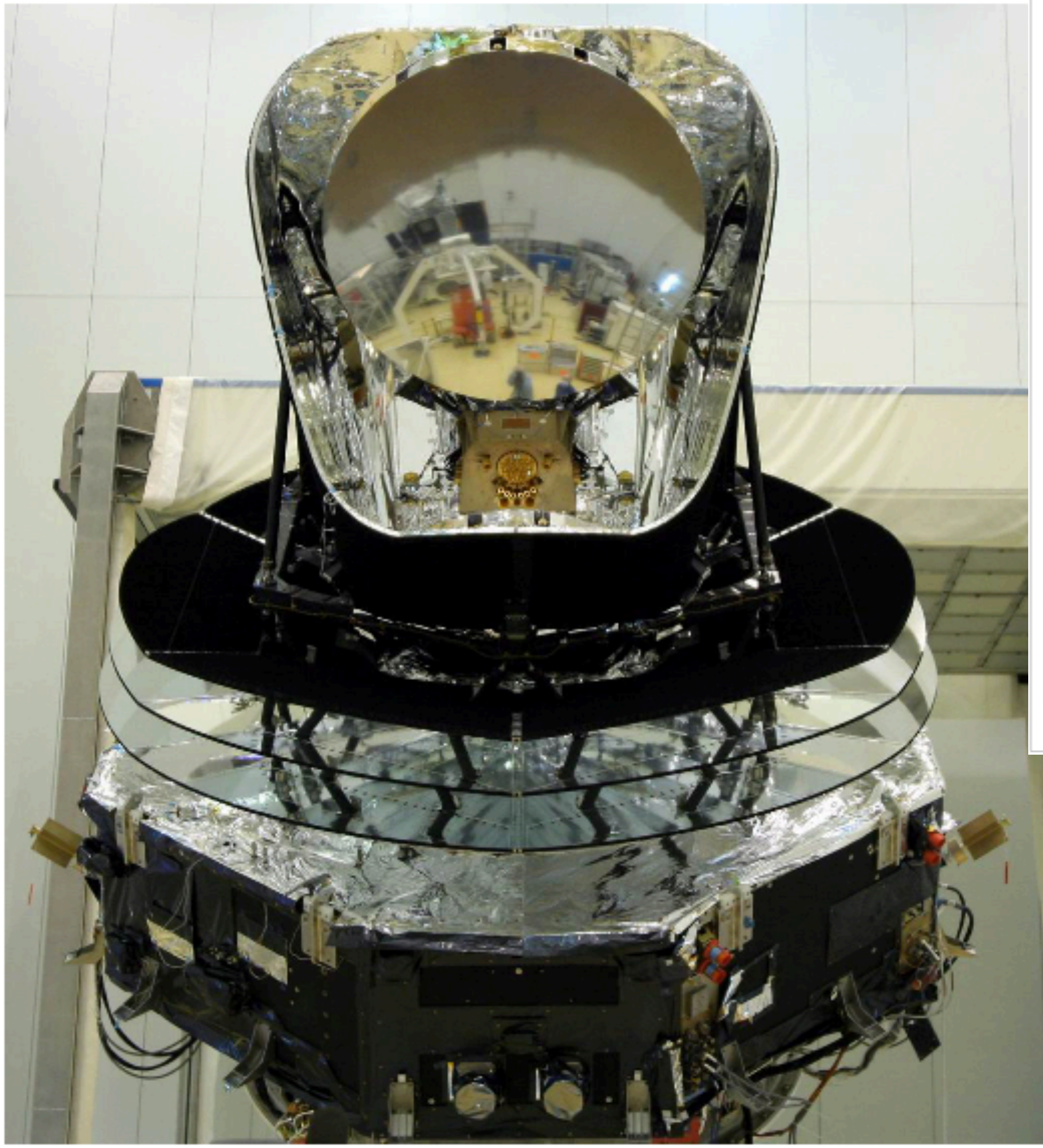

The fully assembled Planck satellite a few days before integration into the Ariane 5 rocket. Herschel is visible by reflection on the primary reflector.

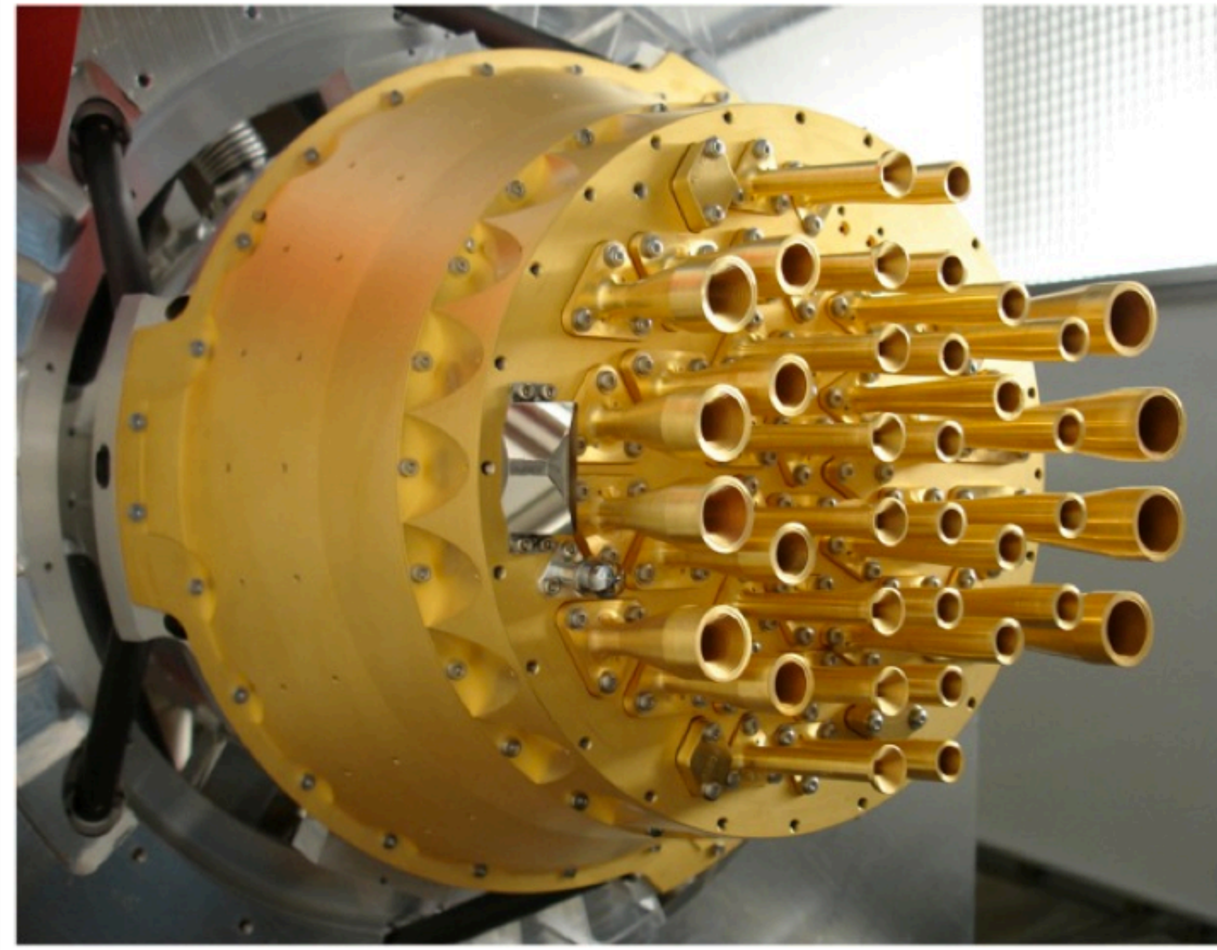

The HFI focal plane optics and 4K thermo-mechanical stage

Planck

- 20K HEMT amplifiers at 30, 45, 70 GHz
  - ~ 20 amplifiers
- 100 mK bolometers at 100 -> 850 GHz
  - ~ 50 bolometers

Planck detectors

Instrument Characteristic	LFI			HFI					
Detector Technology	HEMT arrays			Bolometer arrays					
Center Frequency [GHz]	30	44	70	100	143	217	353	545	857
Bandwidth ($\Delta\nu/\nu$)	0.2	0.2	0.2	0.33	0.33	0.33	0.33	0.33	0.33
Angular Resolution (arcmin)	33	24	14	10	7.1	5.0	5.0	5.0	5.0
$\Delta T/T$ per pixel (Stokes I)[a]	2.0	2.7	4.7	2.5	2.2	4.8	14.7	147	6700
$\Delta T/T$ per pixel (Stokes Q &U)[a]	2.8	3.9	6.7	4.0	4.2	9.8	29.8	...	...

[a] Goal (μK/K, 1σ), 14 months integration, square pixels whose sides are given in the row "Angular Resolution".

Planck Bluebook

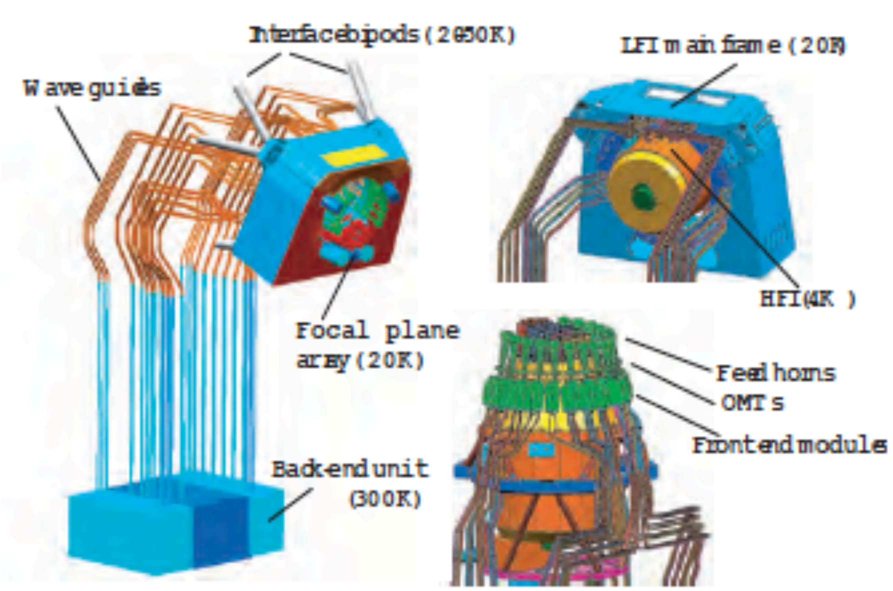

Planck Bluebook

Thales/Alenia Space+ESA

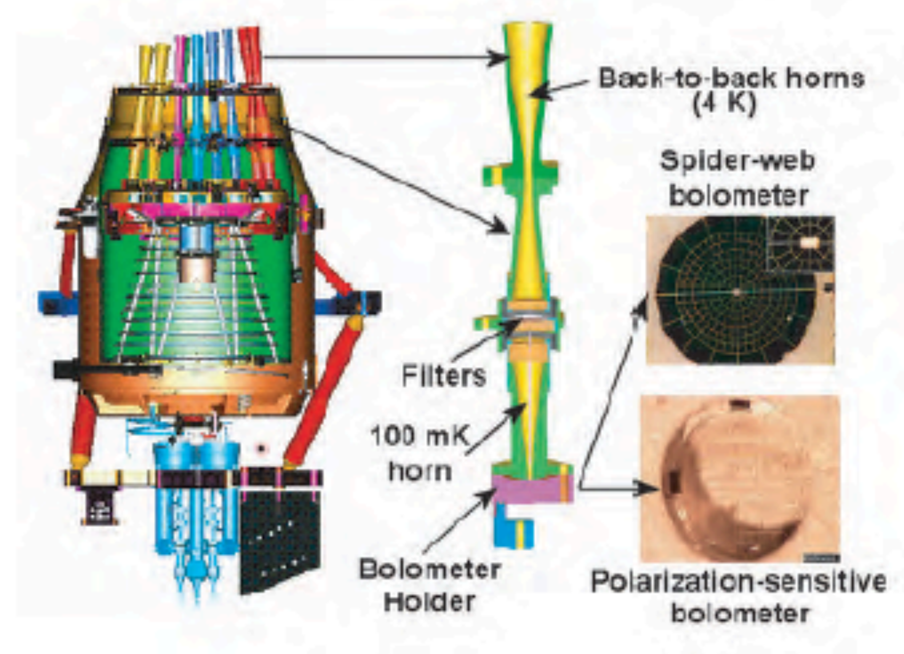

Planck Bluebook

Planck HFI

Center Frequency (GHz)	100	143	217	353	545	857
N Detectors	8	11	12	12	3	4
Resolution (arcmin)	9.5	7.1	4.7	4.5	4.7	4.4
Noise in maps μK_{CMB} deg	1.6	0.9	1.4	5.0	70	1180
Array NET (μK s)	22.6	14.5	20.6	77.3	4.9 (RJ)	2.1 (RJ)

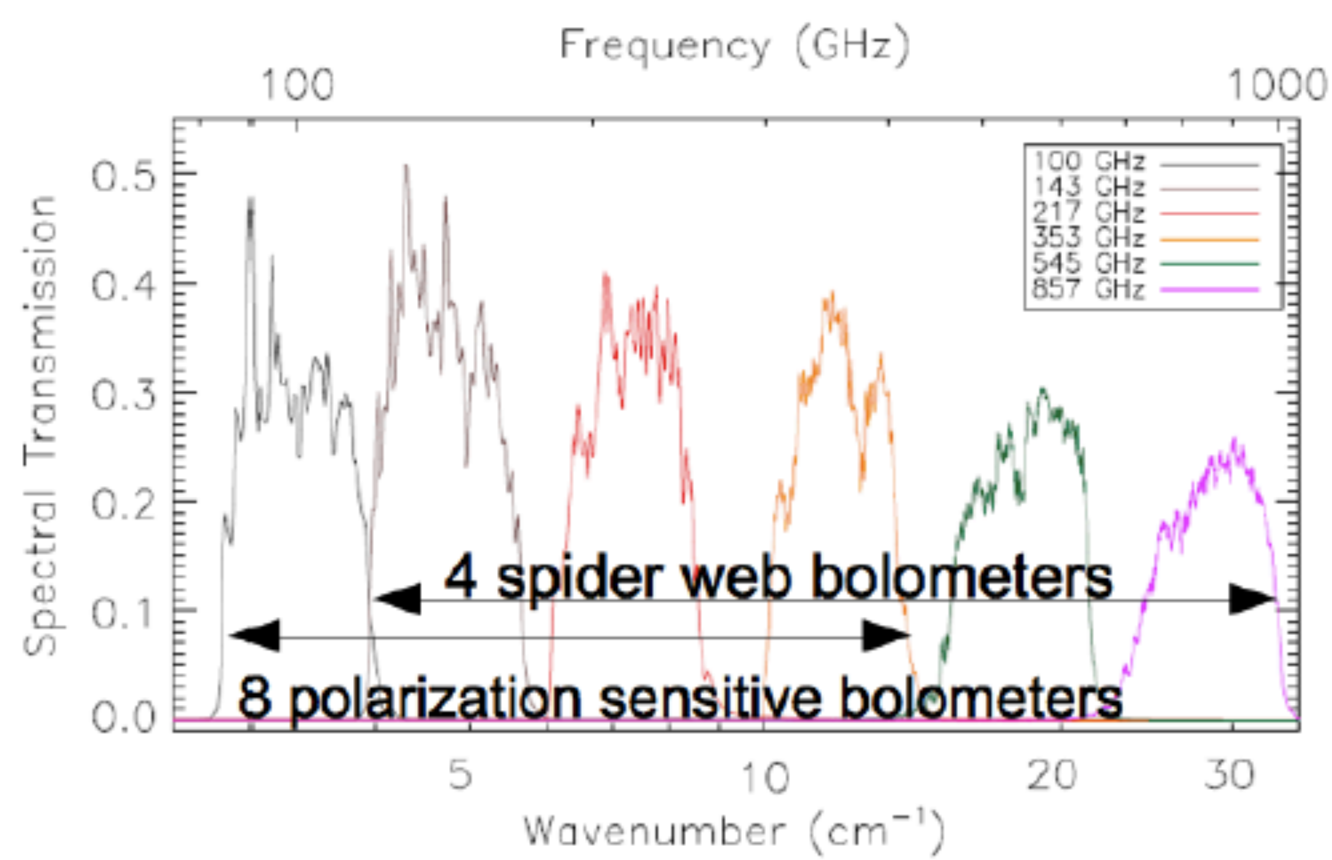

Planck: polarization sensitivity

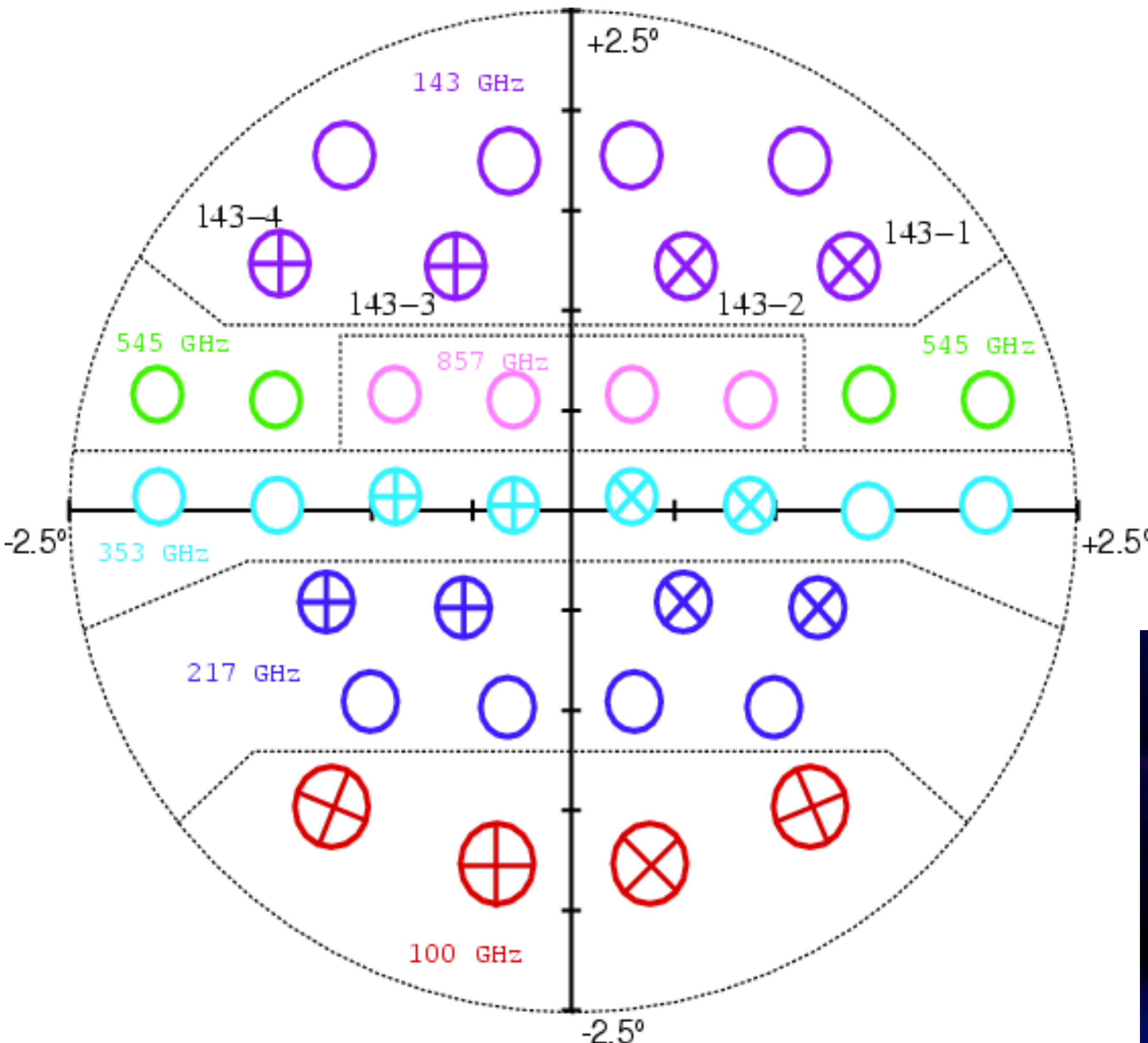

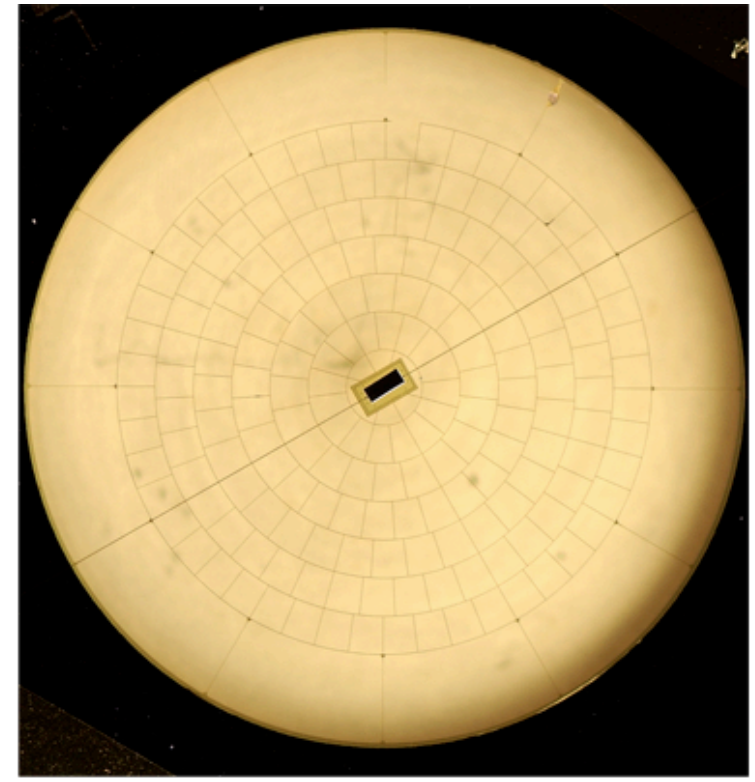

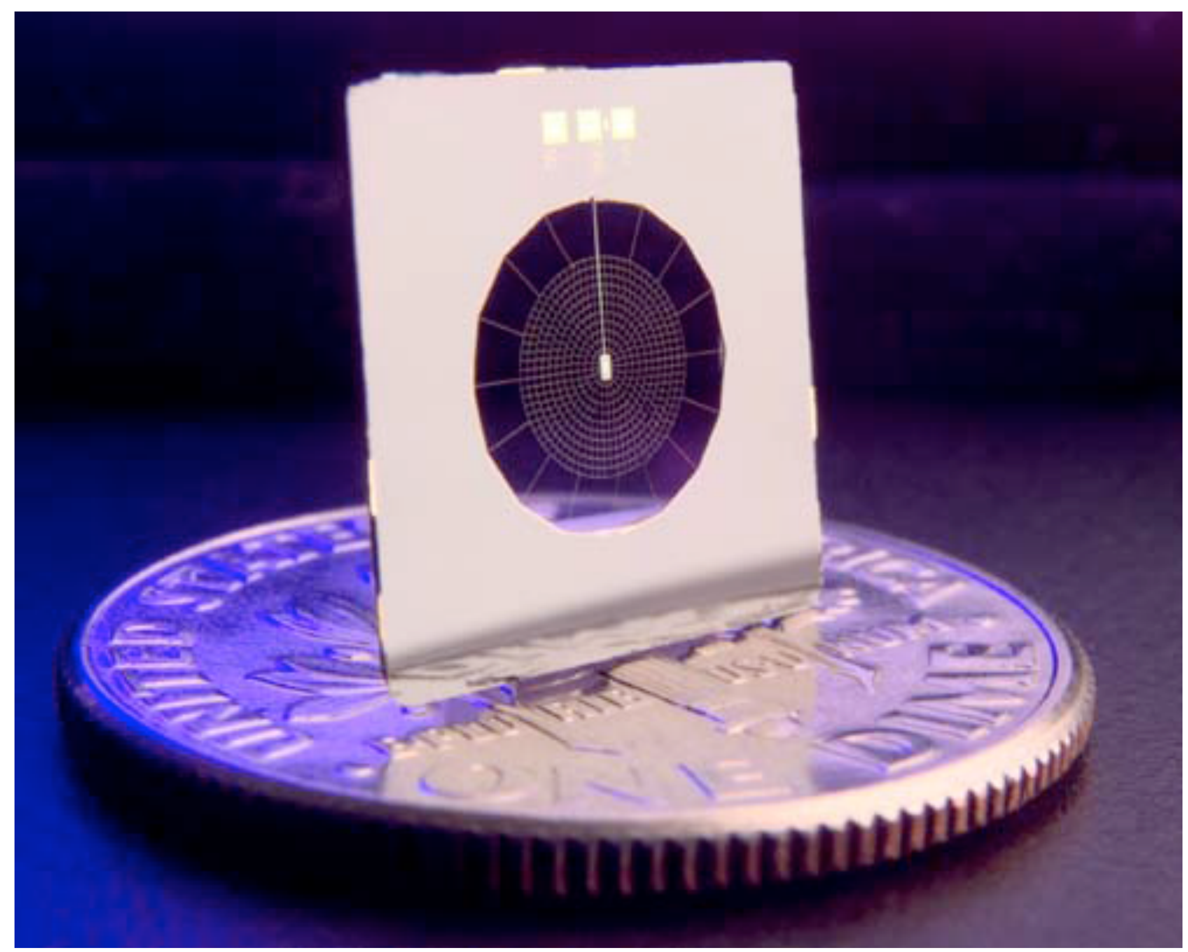

Planck Focal Plane Unit with polarization sensitive bolometers (spiderweb bolometers). Here one has two bolometers back-to-back with orthogonal grids.

CMB receiver types

Coherent receivers:

Phase-preserving amplification
Correlation of different polarization

- Correlation/Pseudocorrelation receiver (e.g. WMAP, CAPMAP)
- Interferometer (e.g. DASI, CBI)

Incoherent receivers (bolometers):

Direct detection of radiation,
No phase information kept
Large arrays!

- Bolometers (e.g. ACBAR, Boomerang, BICEP, Clover, Planck)

Coherent receivers: Interferometers for CMB

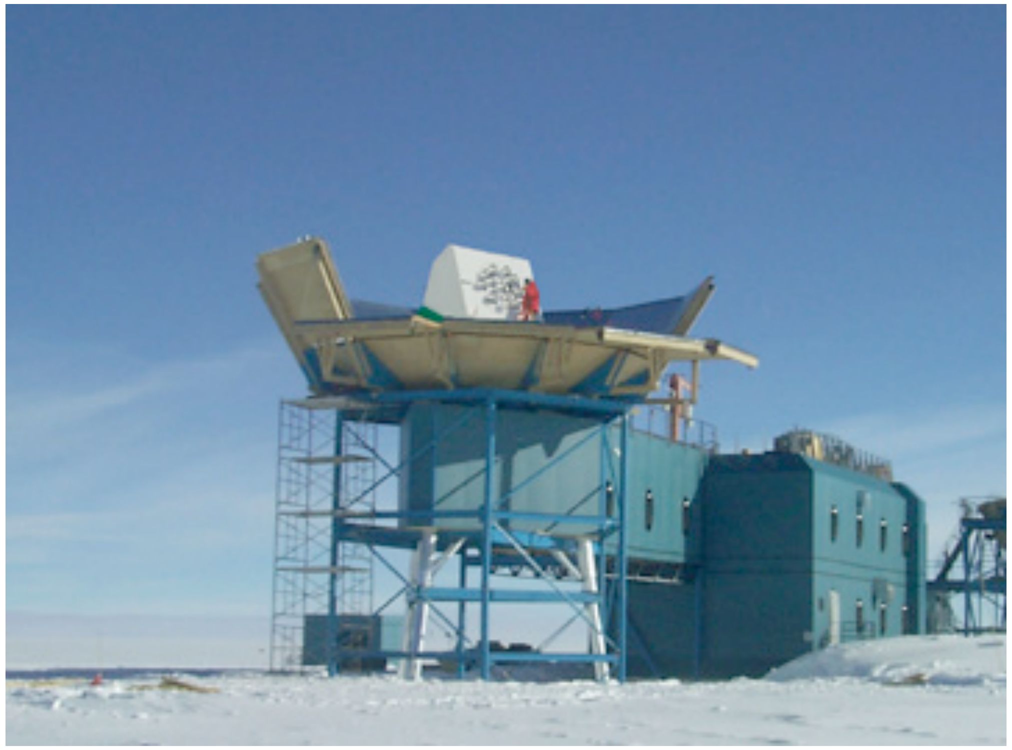

DASI in South Pole

CBI in Atacama desert

Coherent receivers: Can be configured so that the output is the correlation of two input signals.
HEMT (High Electron Mobility Transistor) allow coherent amplification with low noise and high gain.

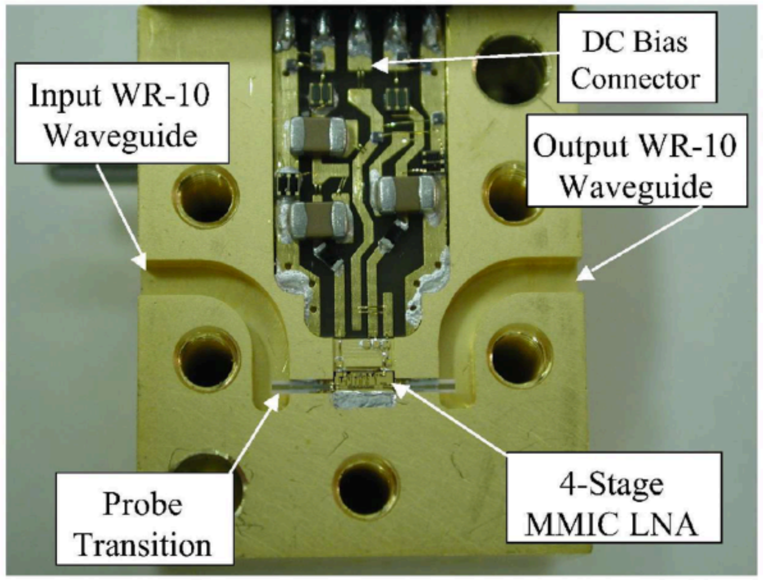

Interferometric measurement

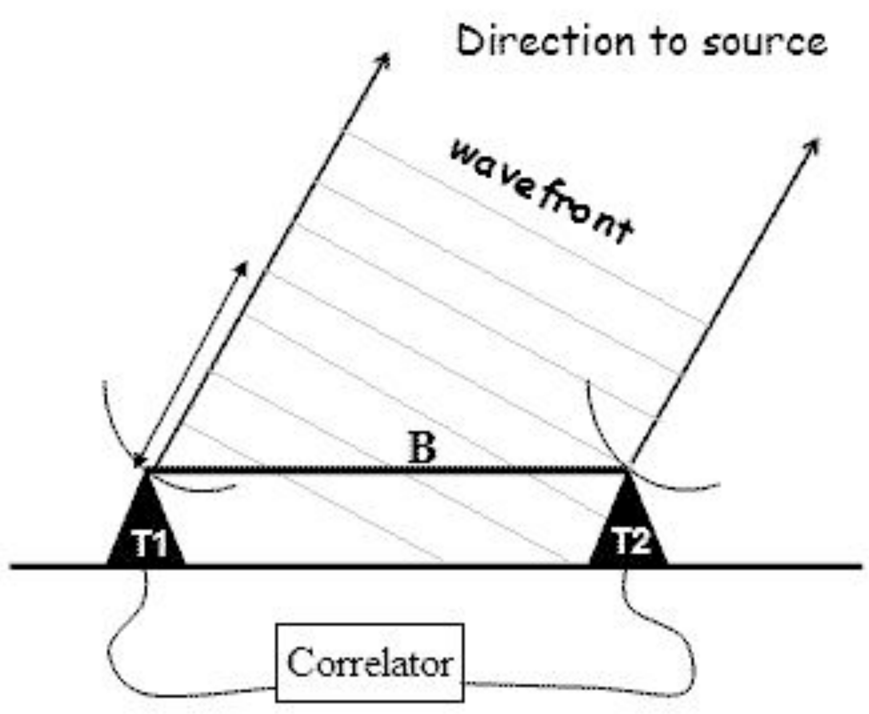

Properties of interferometers that make them ideally suited for CMB observation:

- Automatic subtraction of the mean signal
- Intrinsically stable (no skynoise)
- Beamshape is easy to obtain (and is not as important as in single dish observations)
- Direct measurement of visibilities (which are very nearly the Fourier transform of sky brightness distribution)
- Precision radiometry and polarimetry
- Repeated baselines allow variety of instrumental checks

Bolometers (heat detectors): Workhorse of all CMB experiments

ACBAR

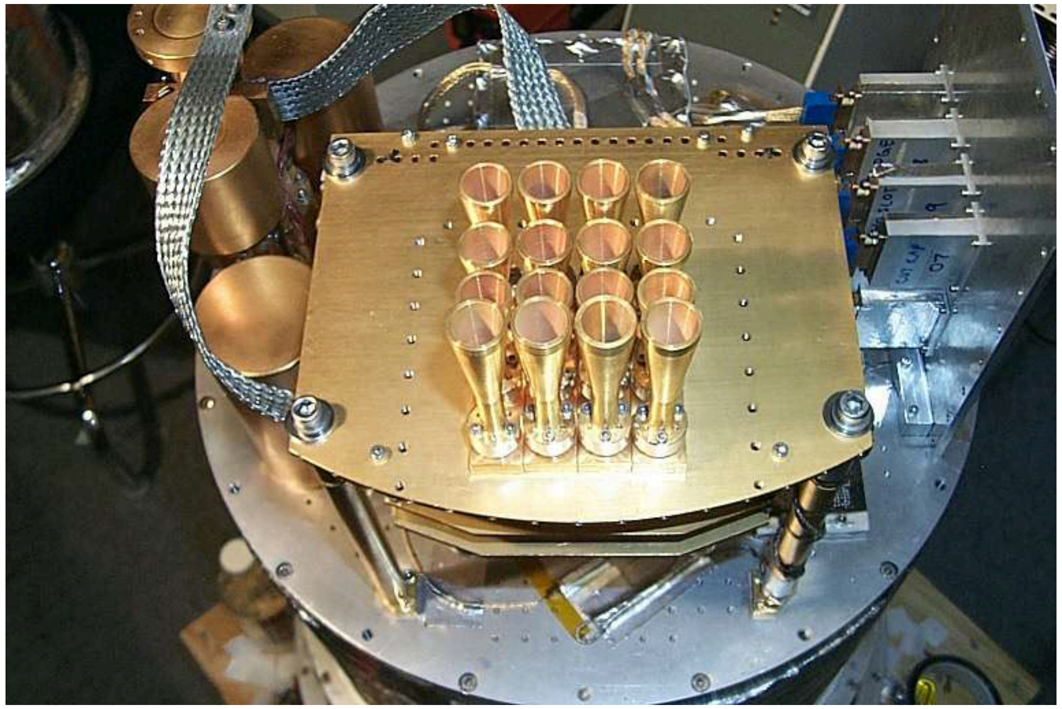

Boomerang

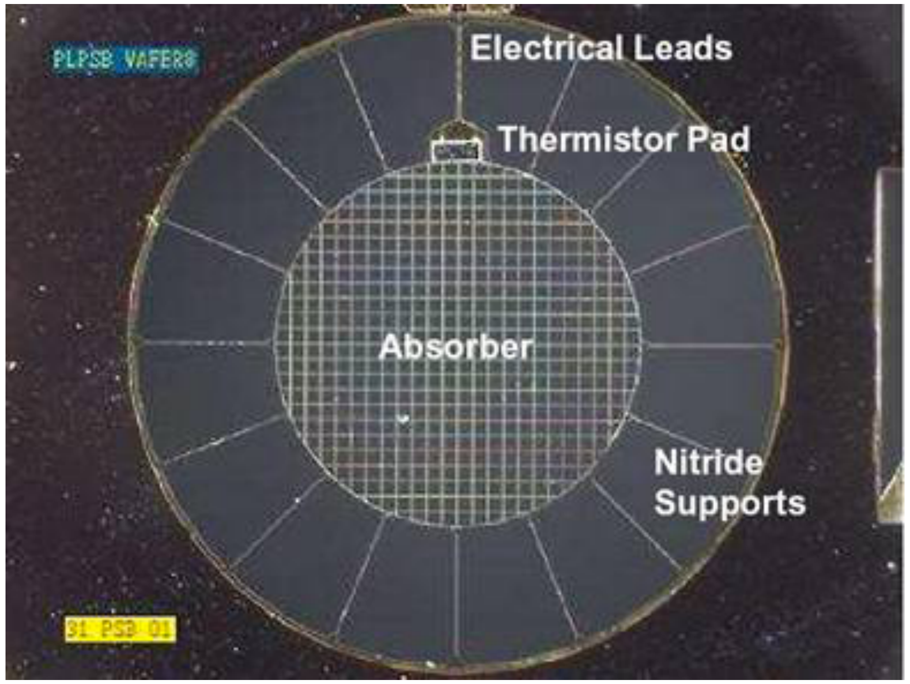

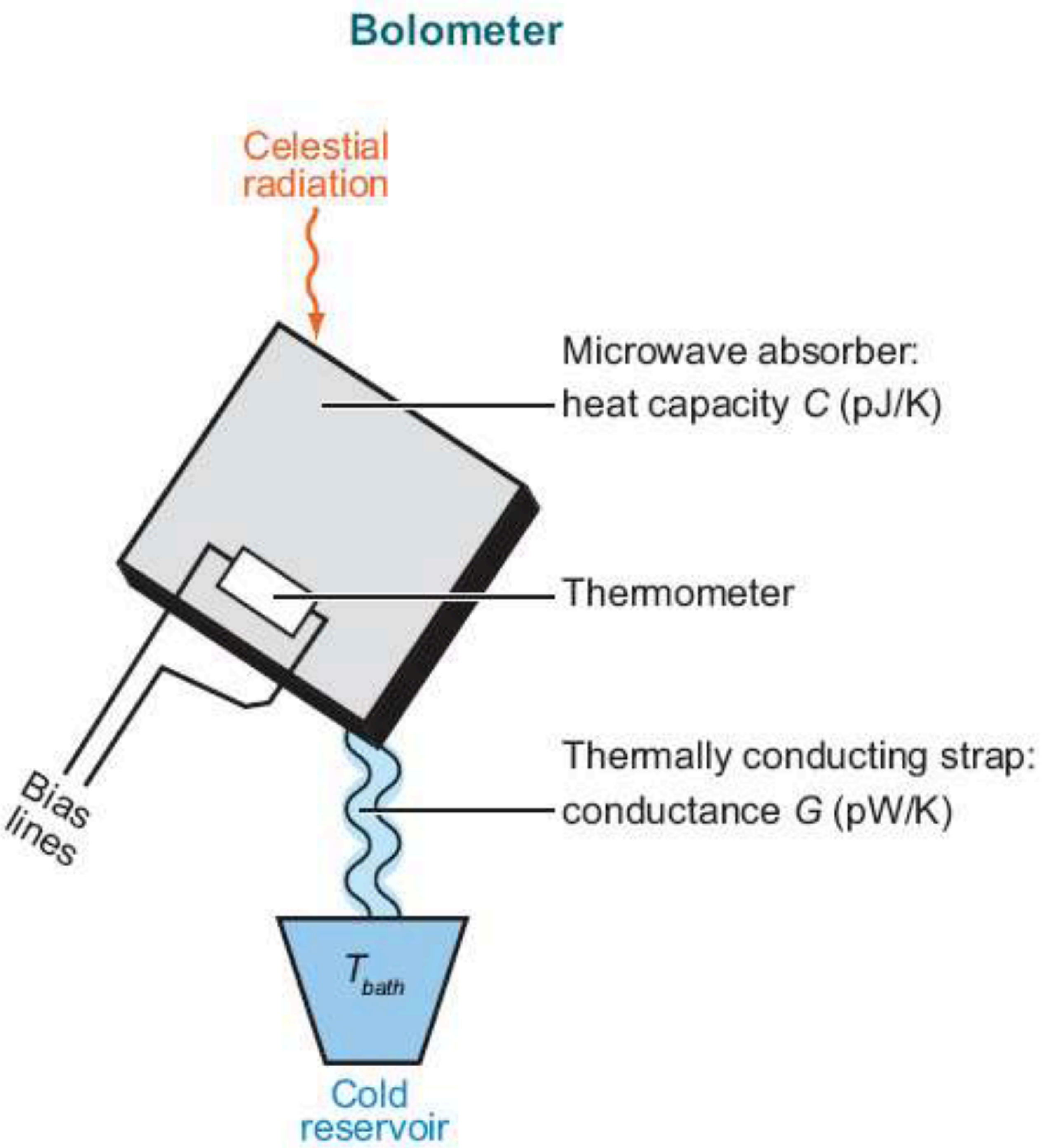

Bolometer and HEMT sensitivities

Fluctuations in the arrival rate of CMB photons impose a fundamental limit of ~30 μK√(sec) for detection of a single mode of radiation in a fractional bandwidth of 25% from ~30 to 220 GHz. This is called the **photon noise limit**.

Modern bolometers are essentially photon noise limited.

	2005[b]		2010[c]	
Freq.	Bolometer	HEMT $/\sqrt{2}$	Bolometer	HEMT $/\sqrt{2}$
[GHz]	[$\mu K_{cmb}\sqrt{s}$]	[$\mu K_{cmb}\sqrt{s}$]	[$\mu K_{cmb}\sqrt{s}$]	[$\mu K_{cmb}\sqrt{s}$]
30	–	93	57	48
40	–	115	51	51
60	–	175	44	60
90	67	224	40	75
120	–	–	40	93
150	48	–	43	–
220	68	–	64	–
350	224	–	220	–

(Already a decade ago)

(CMB Task Force Report)

Bolometer and HEMT sensitivities

	Bolometers	MMIC HEMTs
• Sensitivity	great	good @ < 100 GHz
• Response time	~ msec -> sub-msec	fast
• Frequency Coverage	comprehensive	limited
• Cooling Requirements	little P at low T	large P at higher T
• Linearity	adequate	excellent
• Gain Stability	excellent	poor
• Offset Stability	excellent	good
• Focal Plane Density	better	feedhorn limited
• Polarization Sensitivity	good	good
• EMI / RFI / B-field / microphonic susceptibility	adequate	better
• Array Uniformity	good	???

(Slide from Andrew Lange)

A modern bolometer feedhorn array

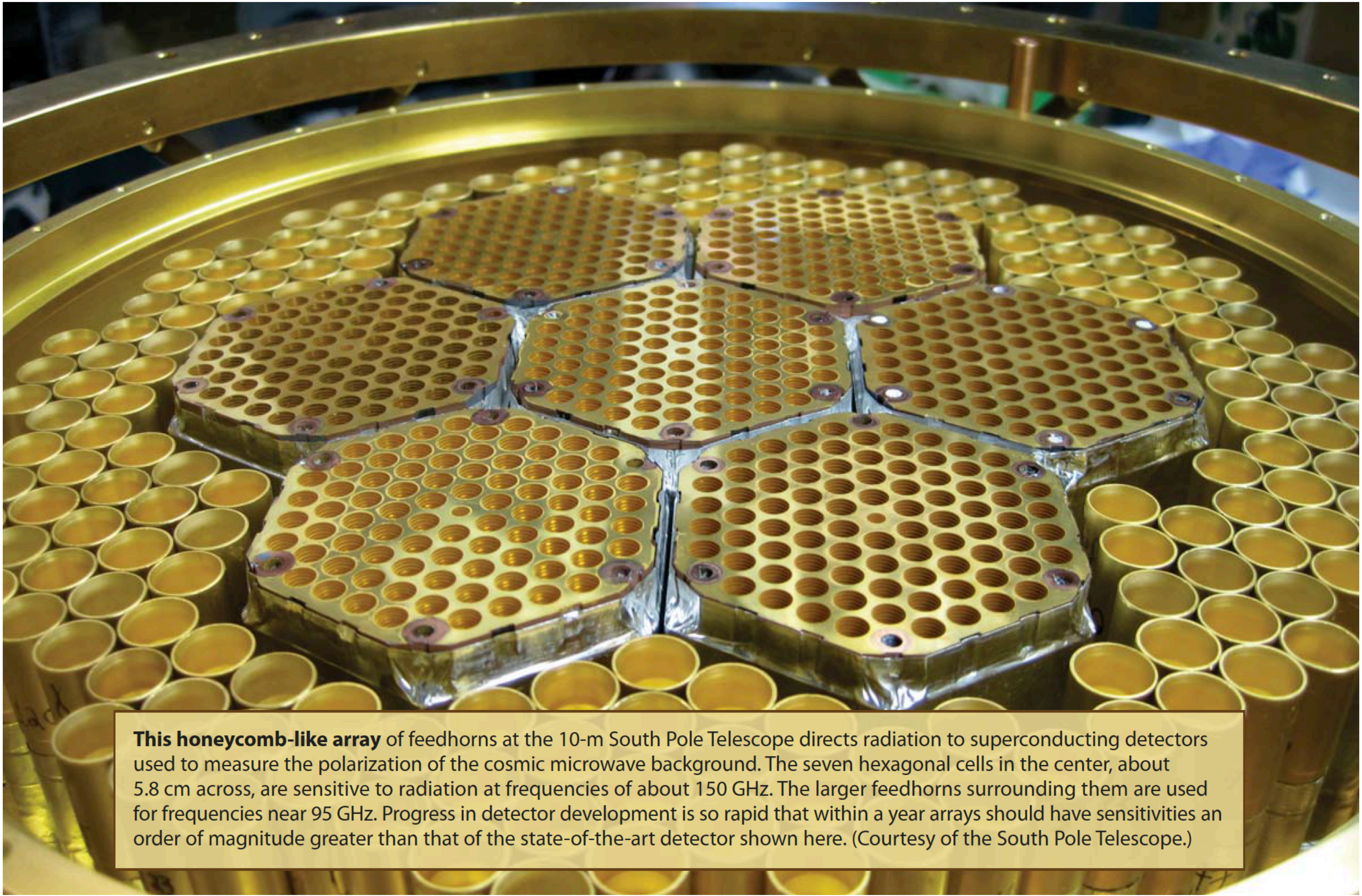

This honeycomb-like array of feedhorns at the 10-m South Pole Telescope directs radiation to superconducting detectors used to measure the polarization of the cosmic microwave background. The seven hexagonal cells in the center, about 5.8 cm across, are sensitive to radiation at frequencies of about 150 GHz. The larger feedhorns surrounding them are used for frequencies near 95 GHz. Progress in detector development is so rapid that within a year arrays should have sensitivities an order of magnitude greater than that of the state-of-the-art detector shown here. (Courtesy of the South Pole Telescope.)

More bolometer array examples

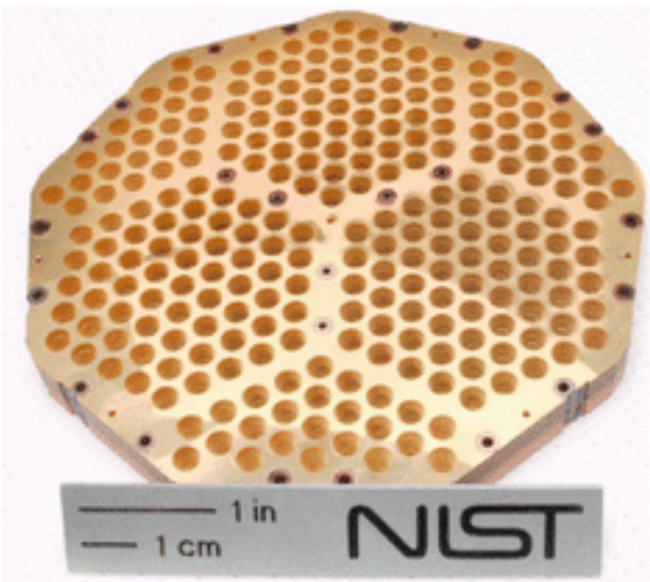

Platelet Feedhorn Array

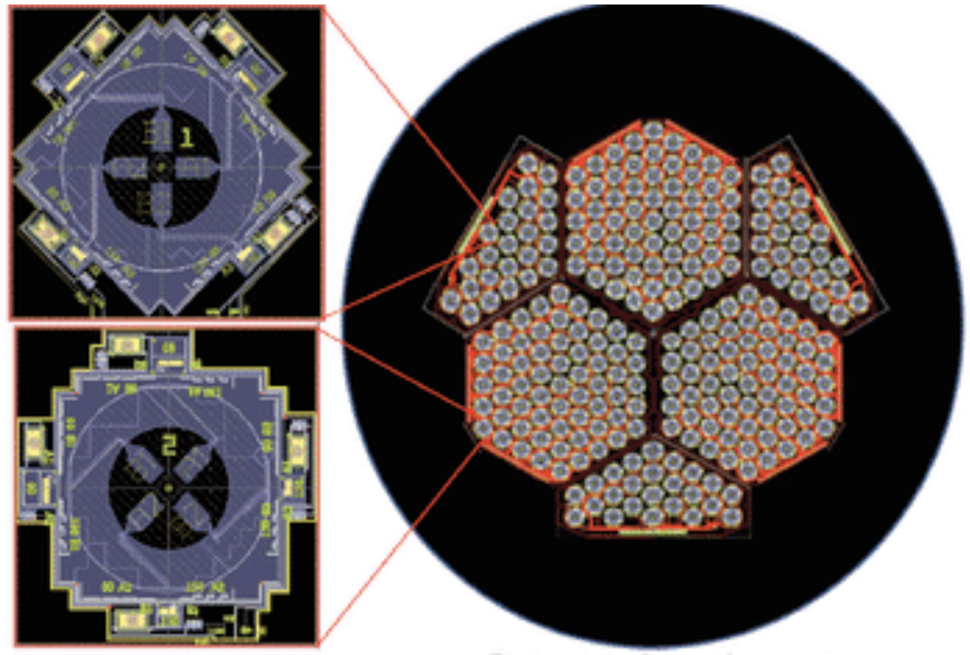

Detector Array Layout

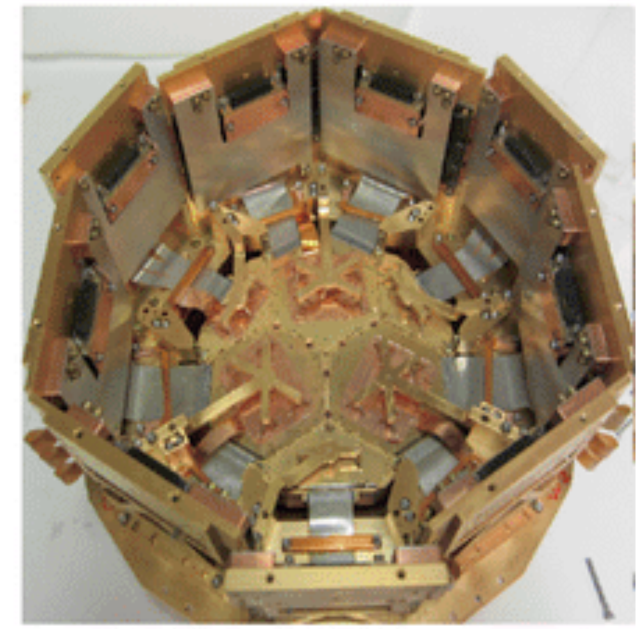

Assembled Detector Array Package

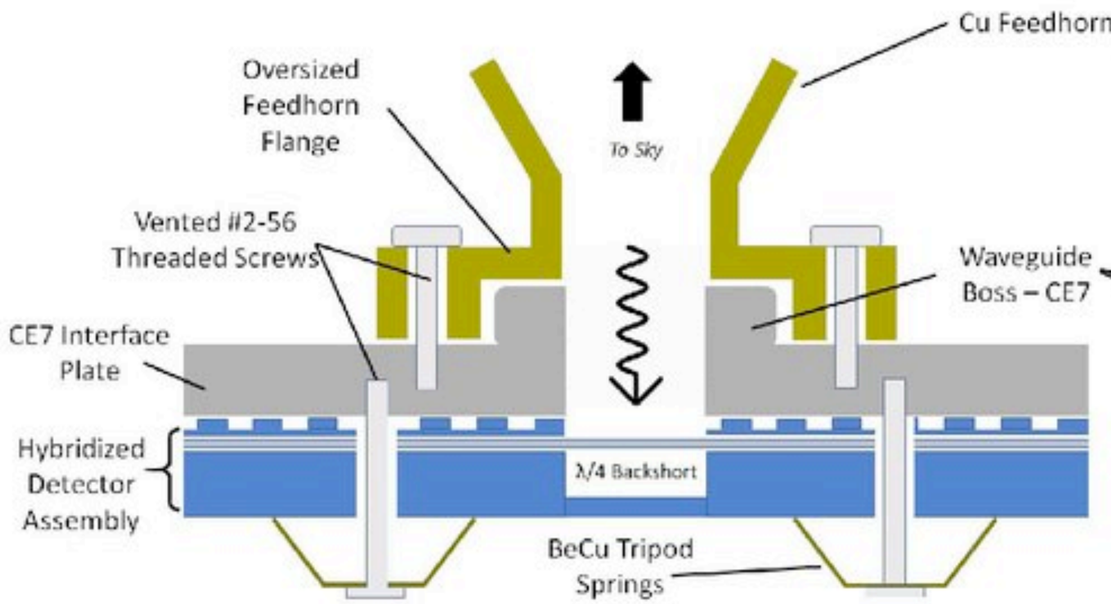

Bolometer cryostat for the ACT

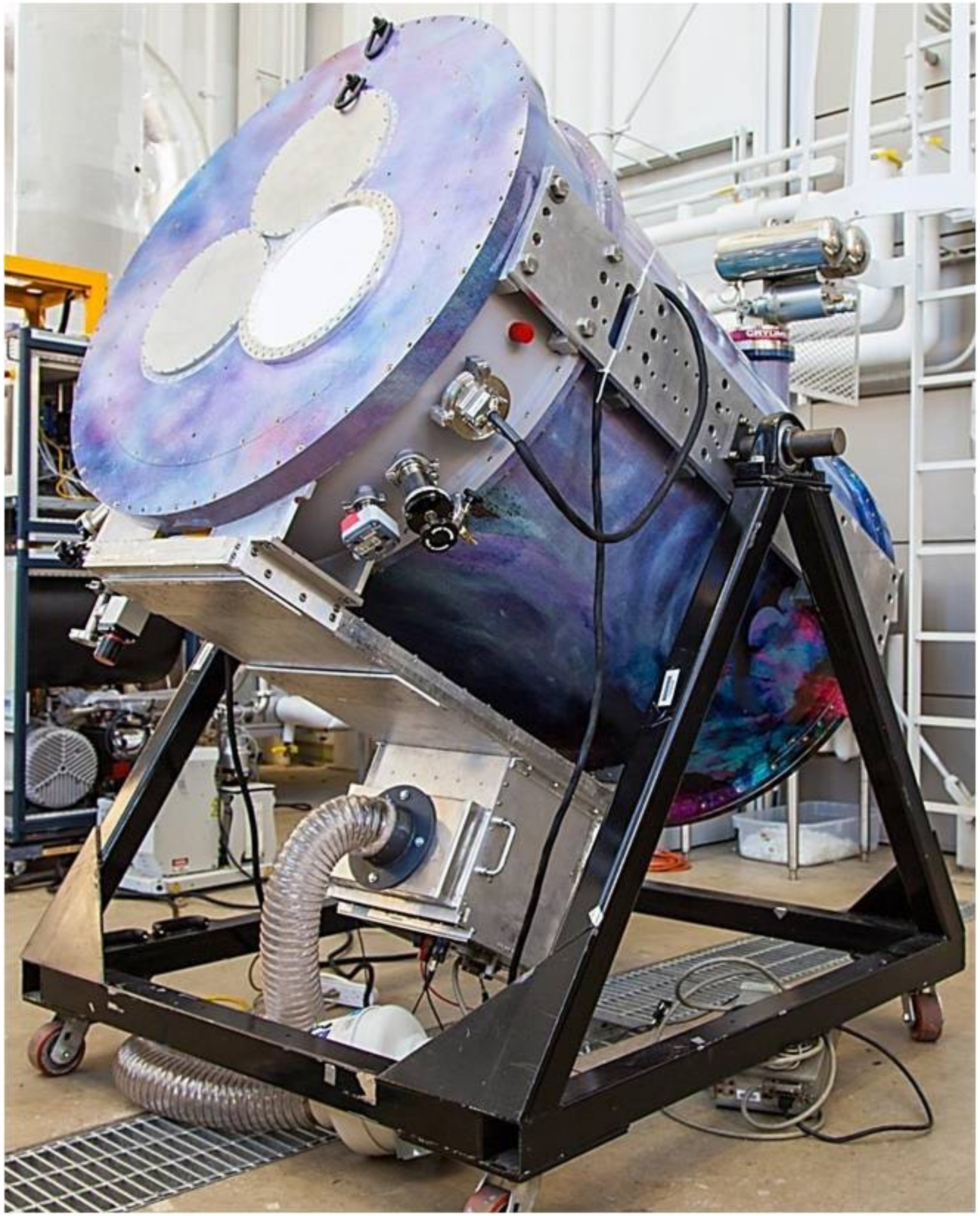

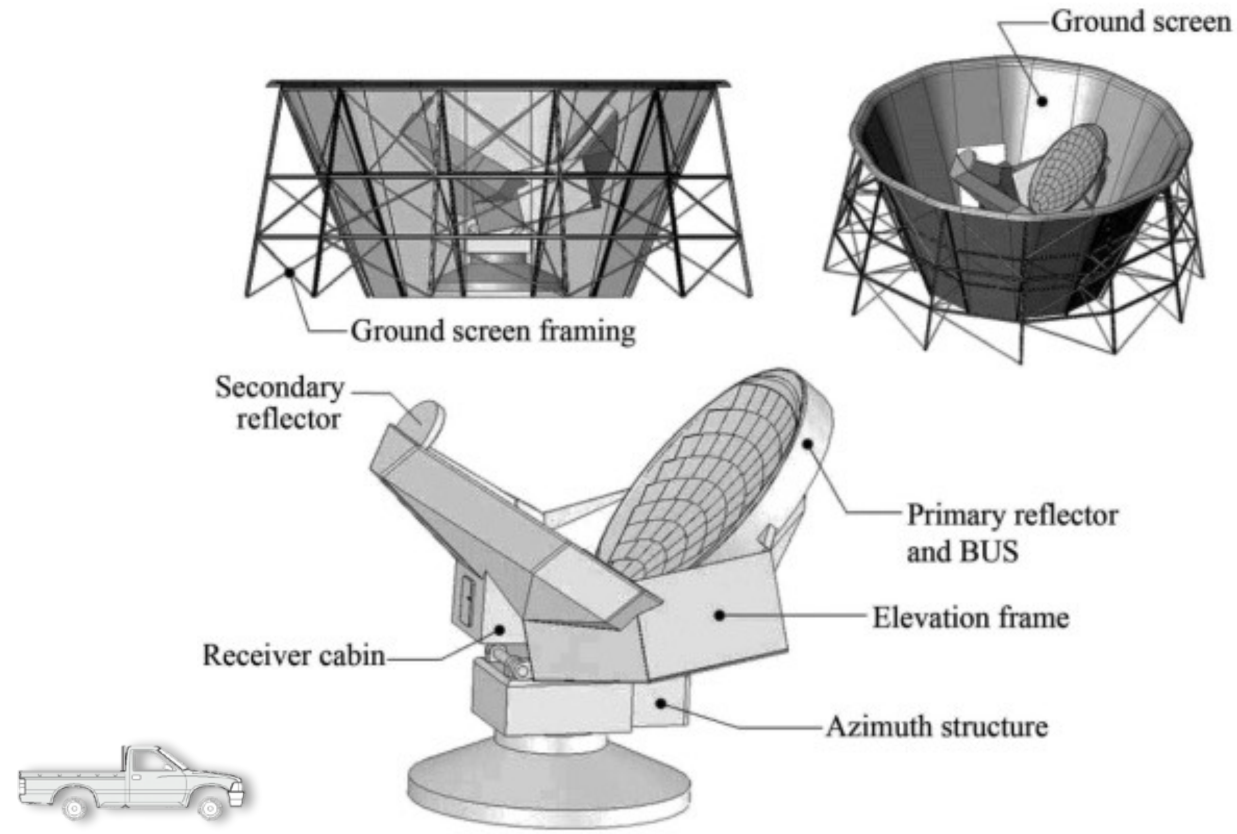

Ground- and space-based Bolometer detector arrays

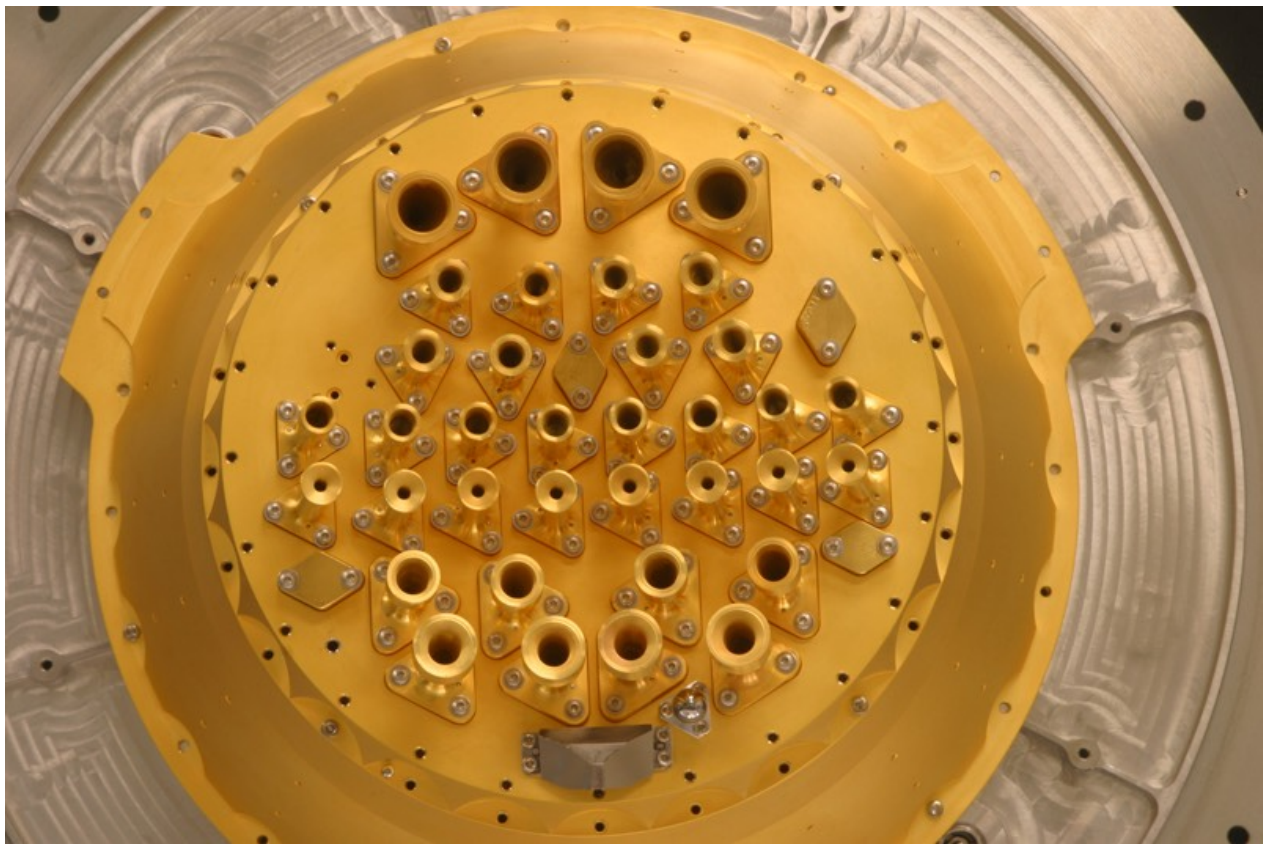

Planck HFI focal plane, showing the feed horns for 32 bolometer detectors

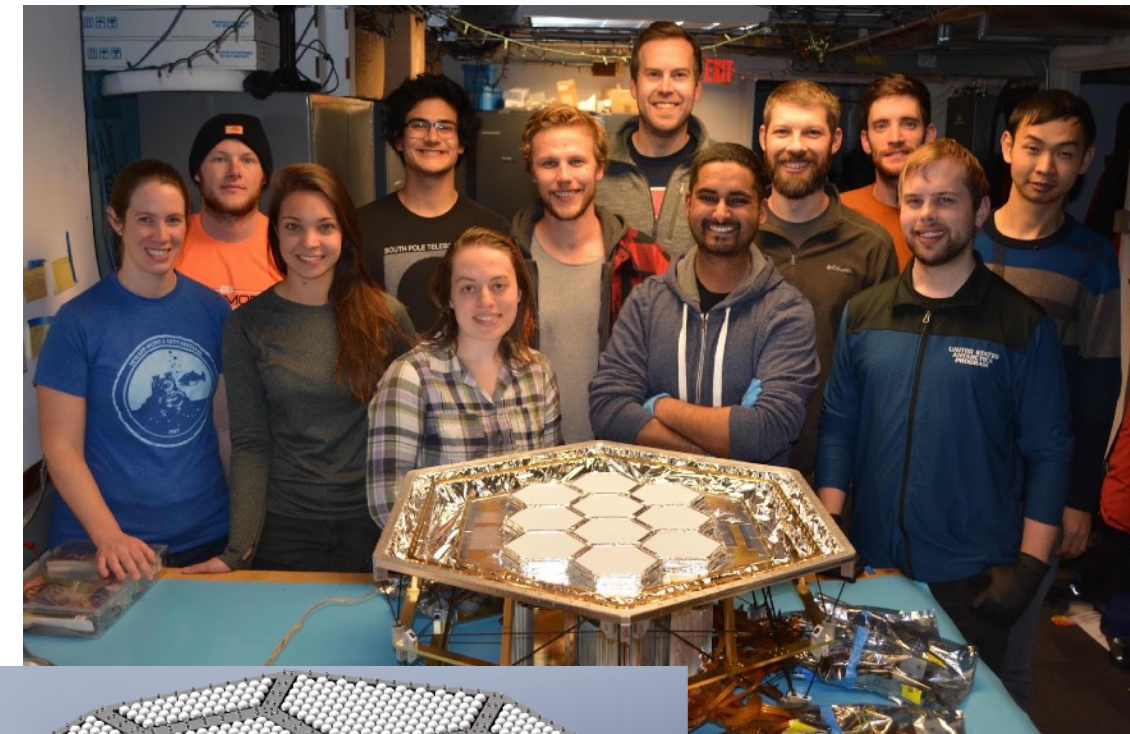

SPT-3G collaboration
Dec 2017

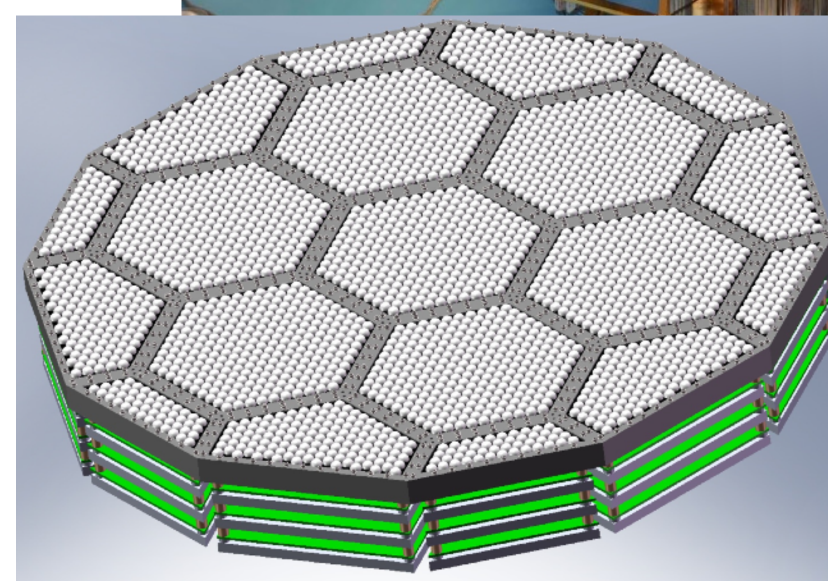

SPT-3G focal plane, with over 15 000 detectors (0.5 m diameter)

Why space? Ground- and space-based detector load comparison

From Delabrouille et al., CORE mission paper

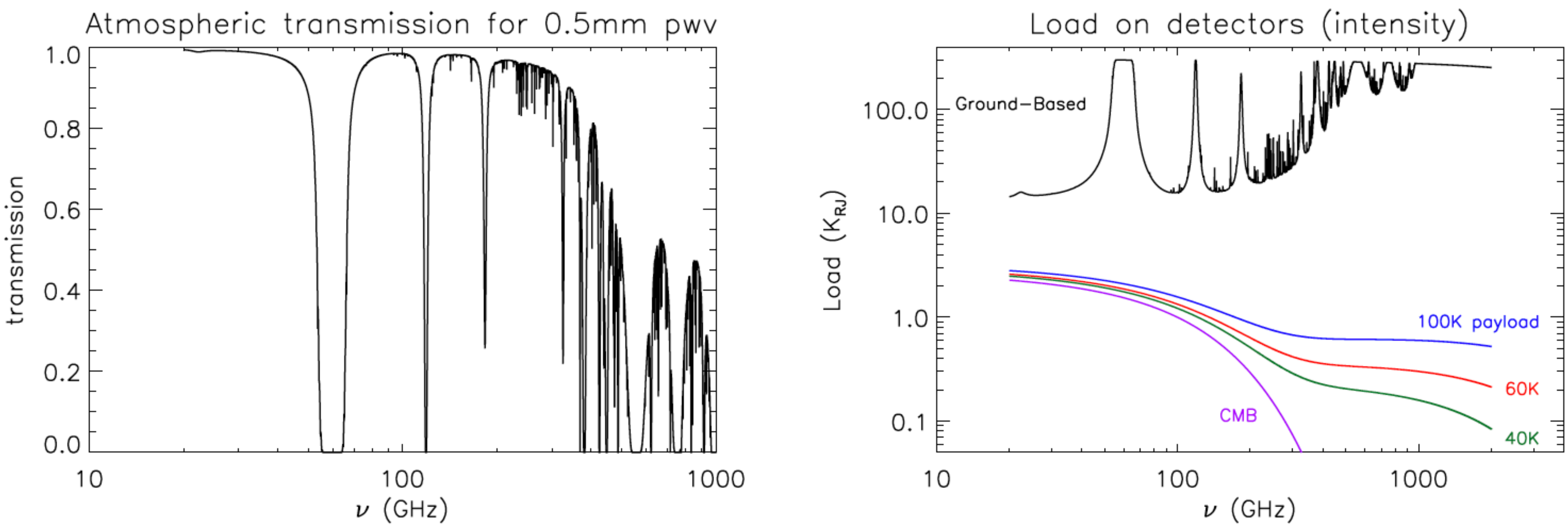

Figure 11. *Top left*: Typical atmospheric transmission from the Atacama plateau at 60° elevation, for an average of half a millimetre of integrated precipitable water vapour. *Top right*: Load on a detector for a ground-based instrument (black) and for a space-borne instrument with various payload temperatures.

A single space-borne detector can reach a sensitivity equivalent to 100-1000 ground-based detectors (depending on frequency).

Noise from atmosphere and ground

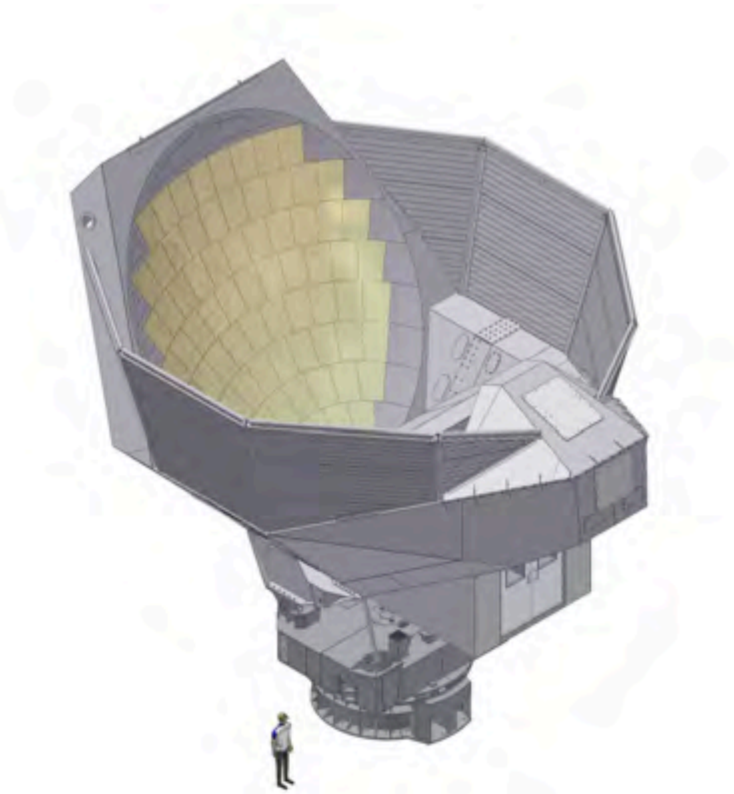

Atacama Cosmology Telescope

Since 3 K << 300 K, CMB measurements are sensitive to thermal emission from their environments.

CMB telescopes are specially designed to be very directional, but ~300 K in the sidelobes is always a worry. **Hence most telescopes use ground shields.**

The atmospheric noise totally dominates scales larger than ~few tens of arcminutes, making low multipole CMB measurements from the ground extremely challenging.

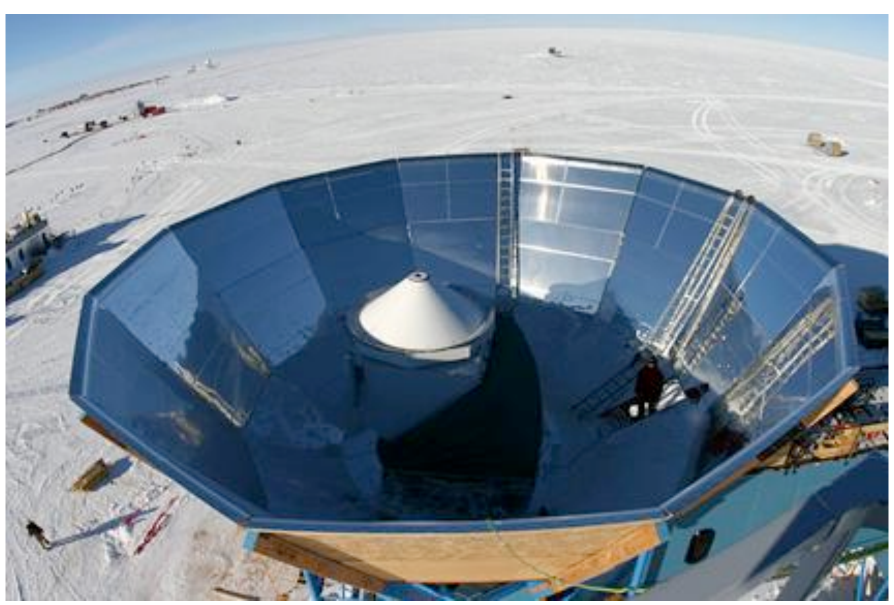

QUaD at south pole

A receiver measures system temperatre, T_{sys}

$$T_{sys} = T_{detector} + T_{CMB} + T_{atmosphere} + T_{ground} + \ldots$$

The radiometer equation is: $$\delta T = \frac{bT_{sys}}{\sqrt{\Delta\nu\,\tau}}$$

antenna efficiency (b); bandwidth ($\Delta\nu$); time (τ)

Atmospheric noise in polarization

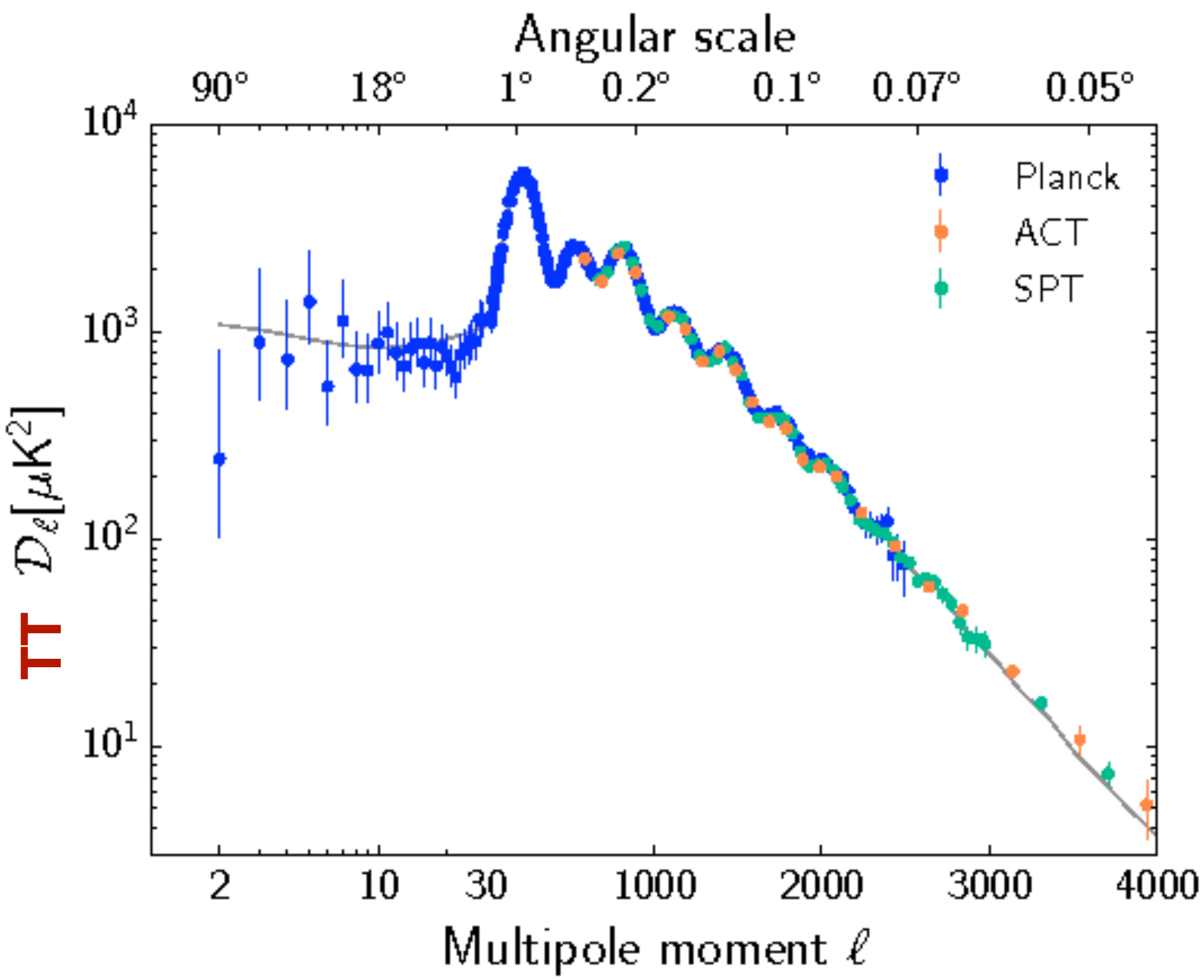

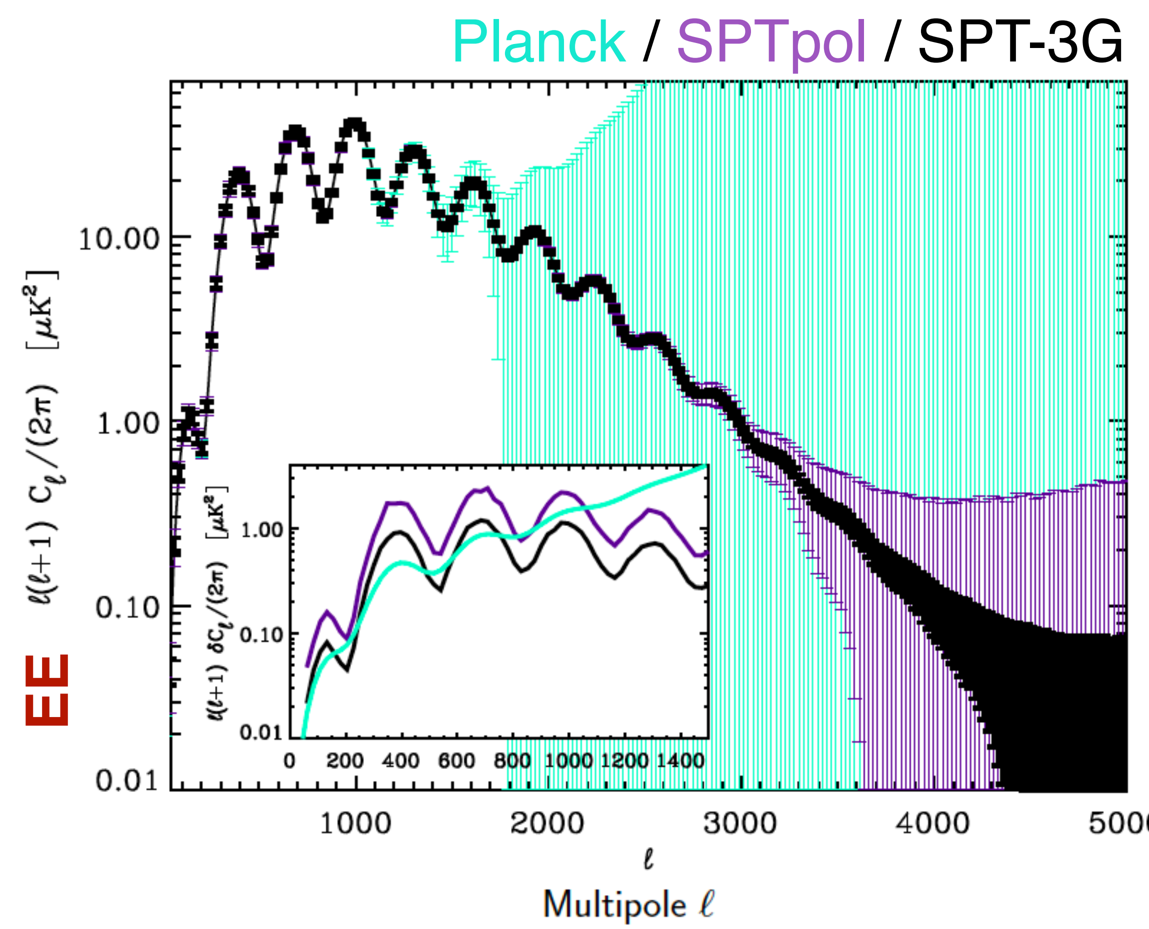

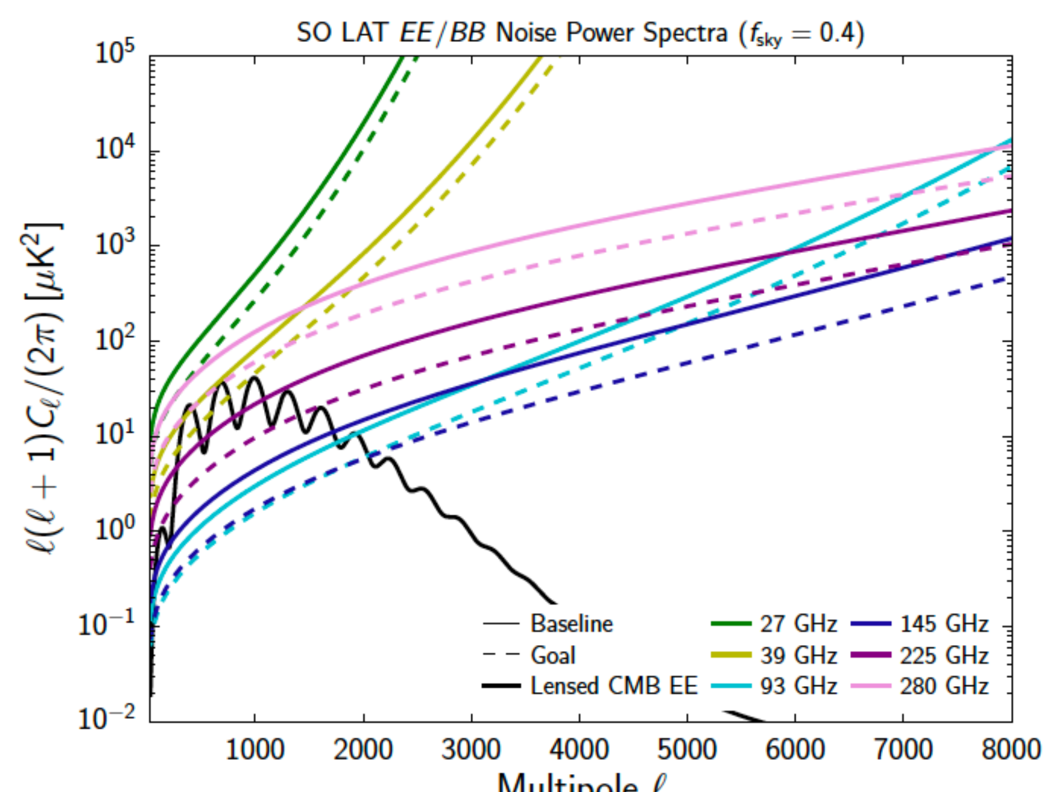

The atmospheric emission is unpolarized, so it is easier to make low-multiple EE/BB power measurements. The main concern is the Galactic foregrounds (polarized dust emission and synchrotron emission).

Detectors for the ground-based telescopes

(Credit: SPT collaboration)

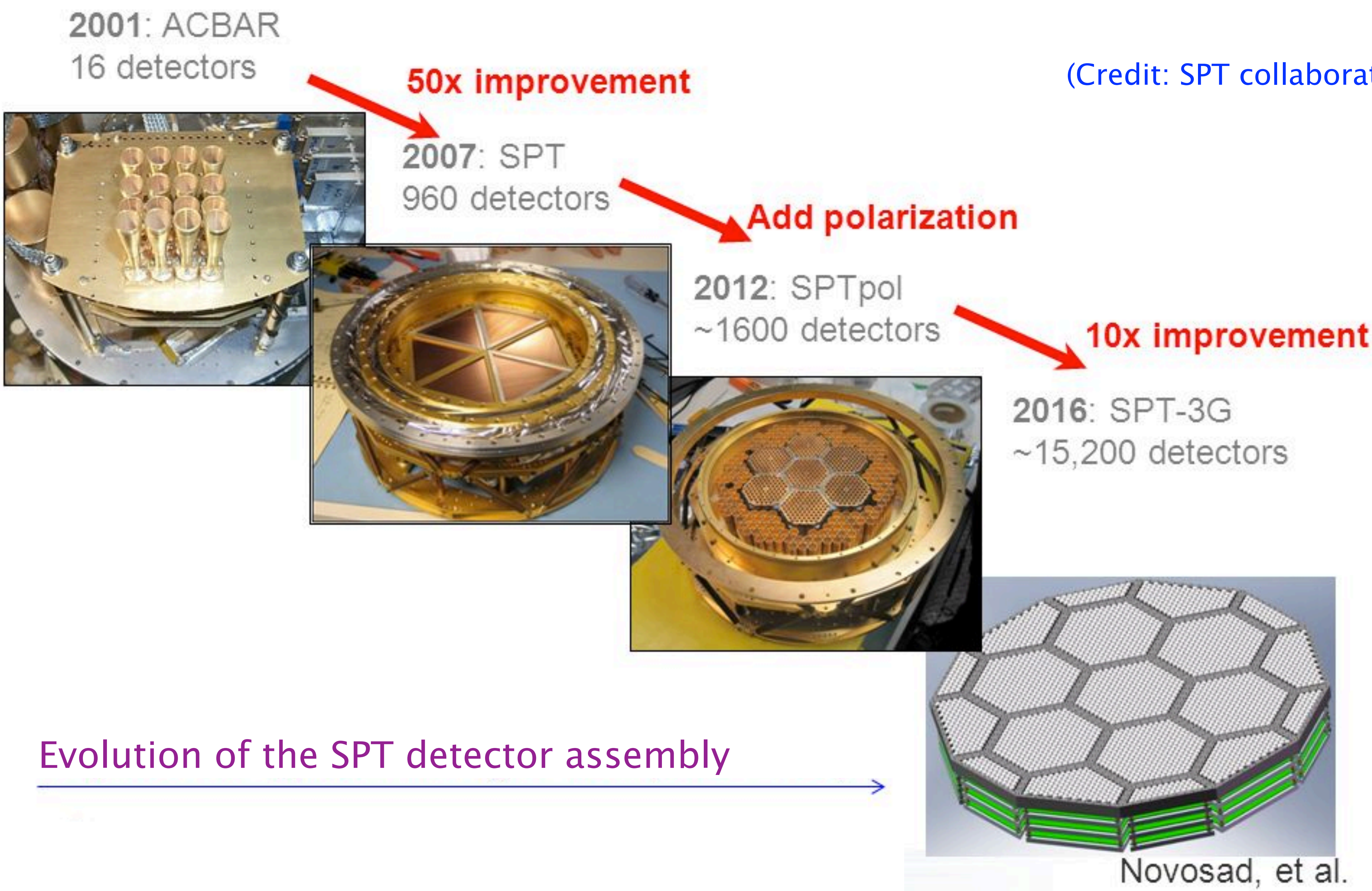

Evolution of the SPT detector assembly →

Moore's law for CMB detectors

CMB-S4
Next Generation CMB Experiment

CMB Stages

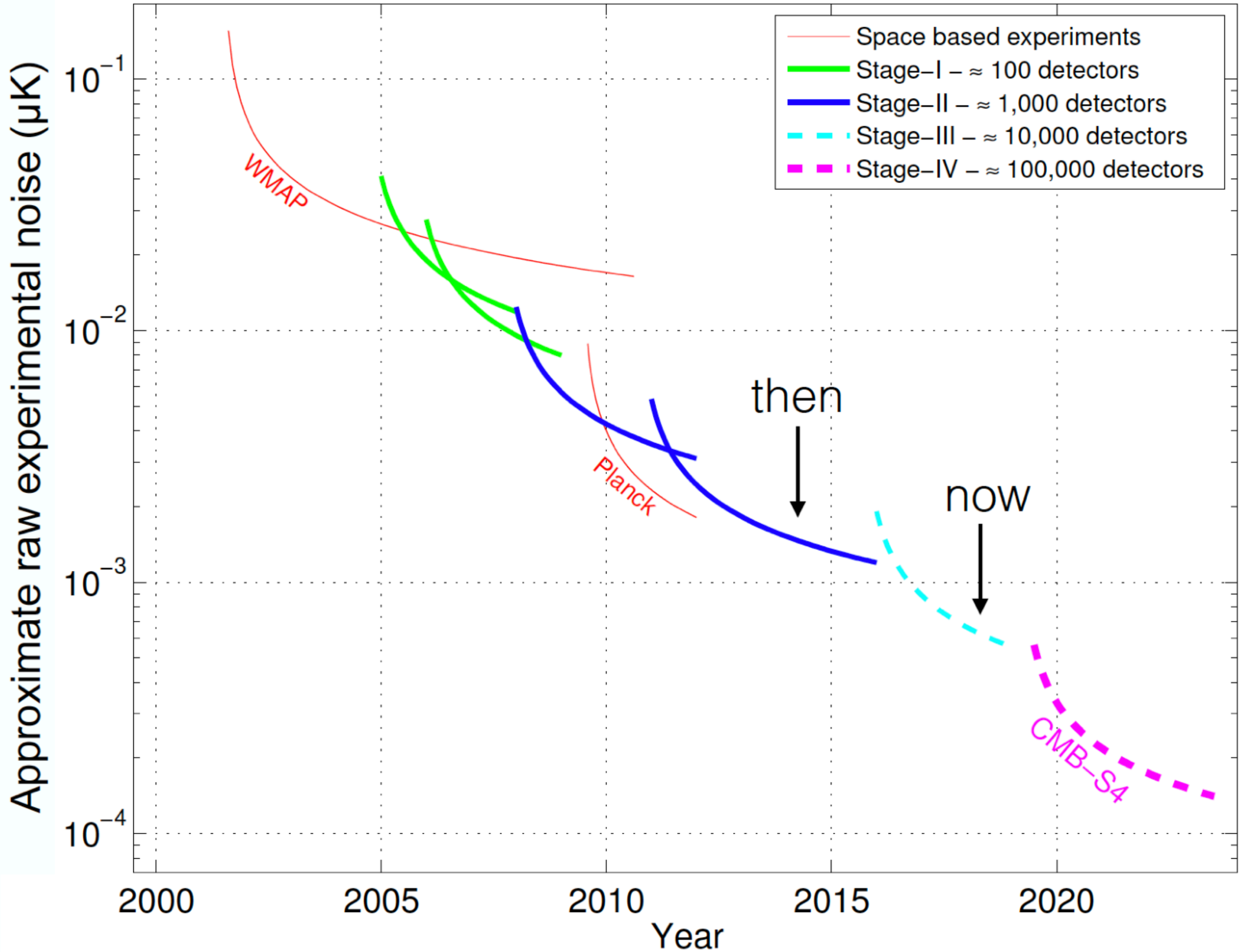

Detector development for Simons Observatory

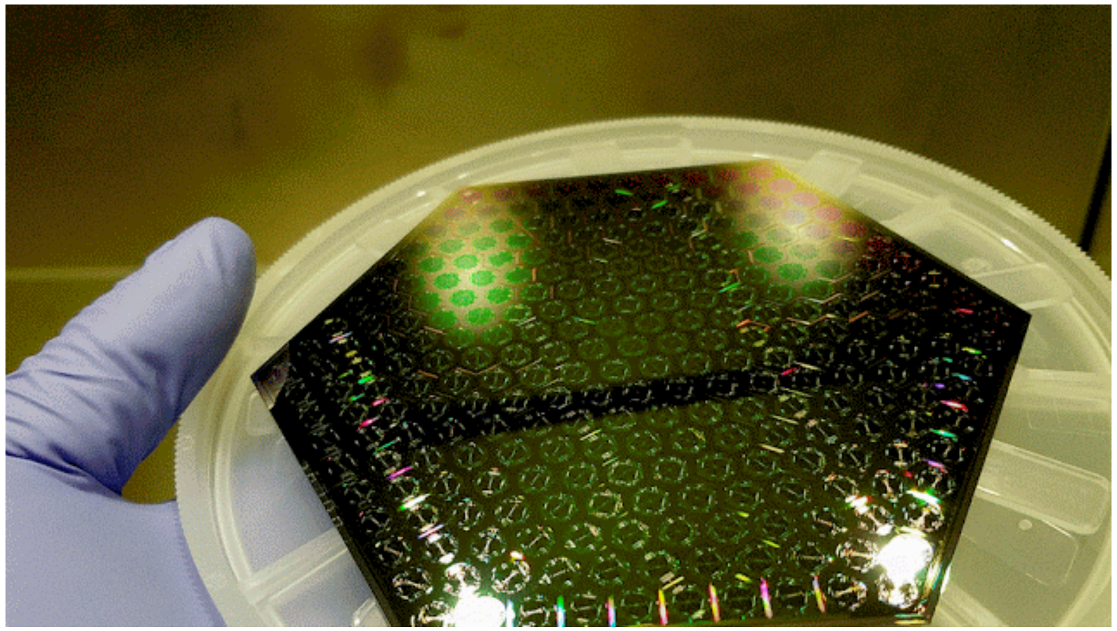

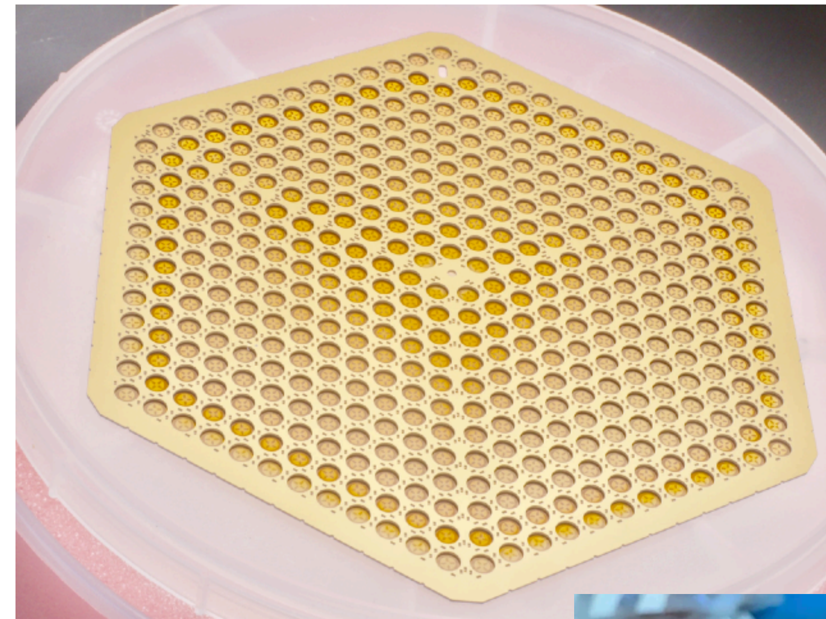

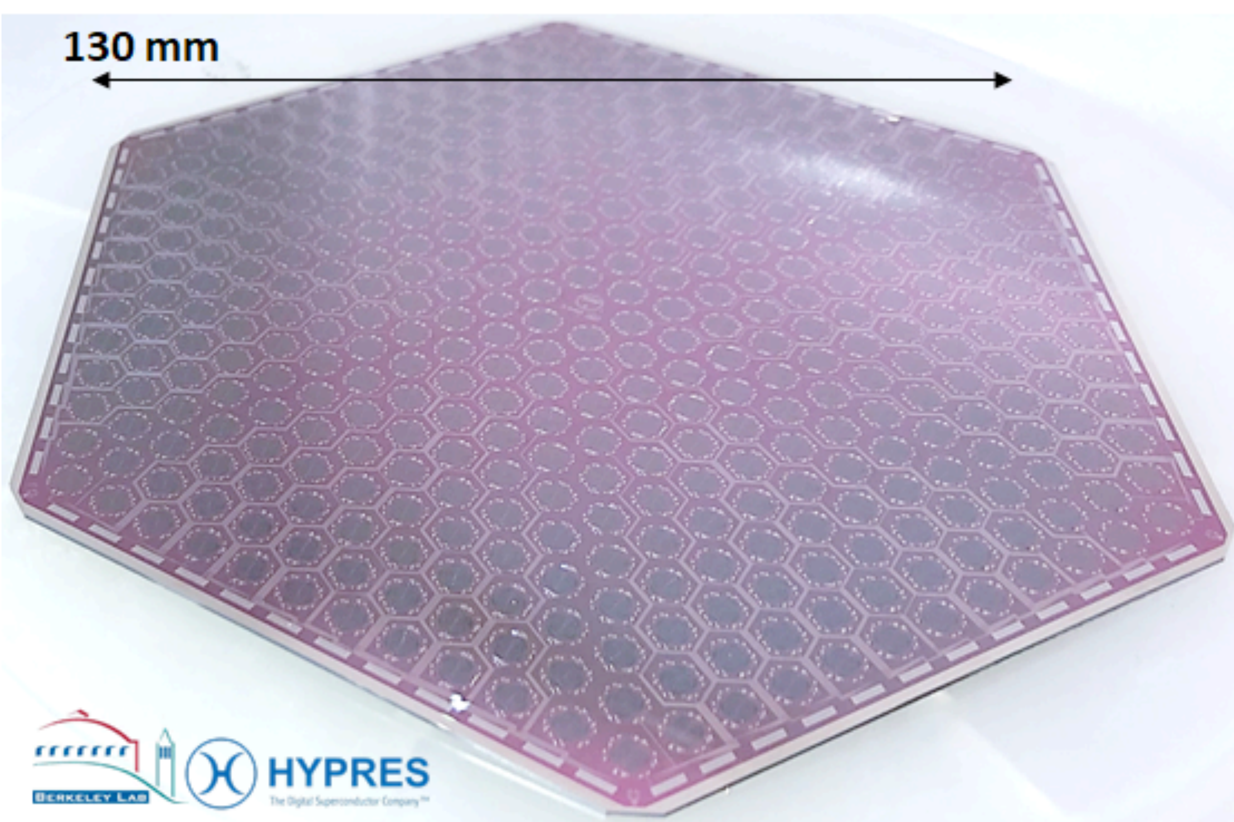

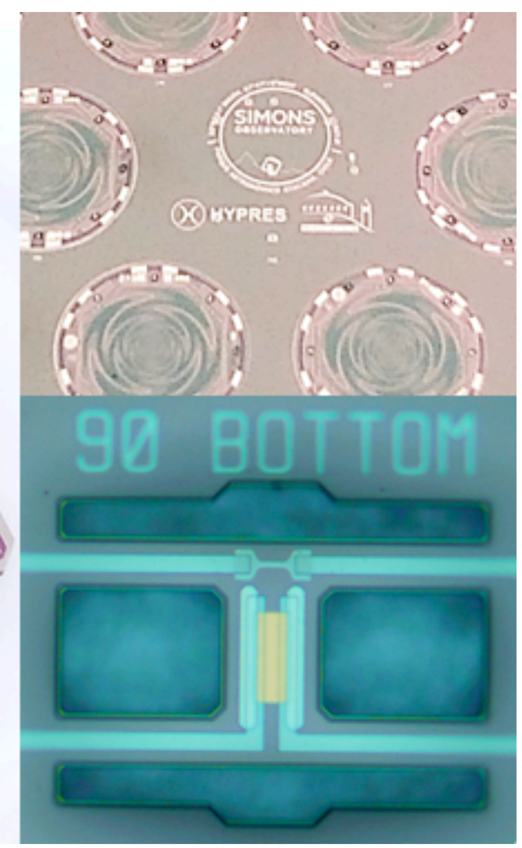

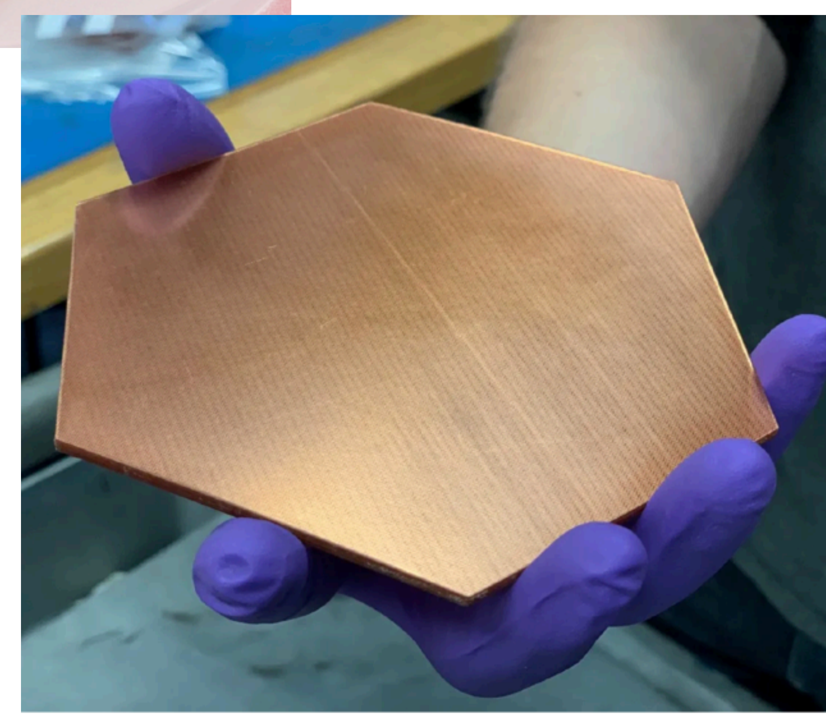

Detector development for Simons Observatory

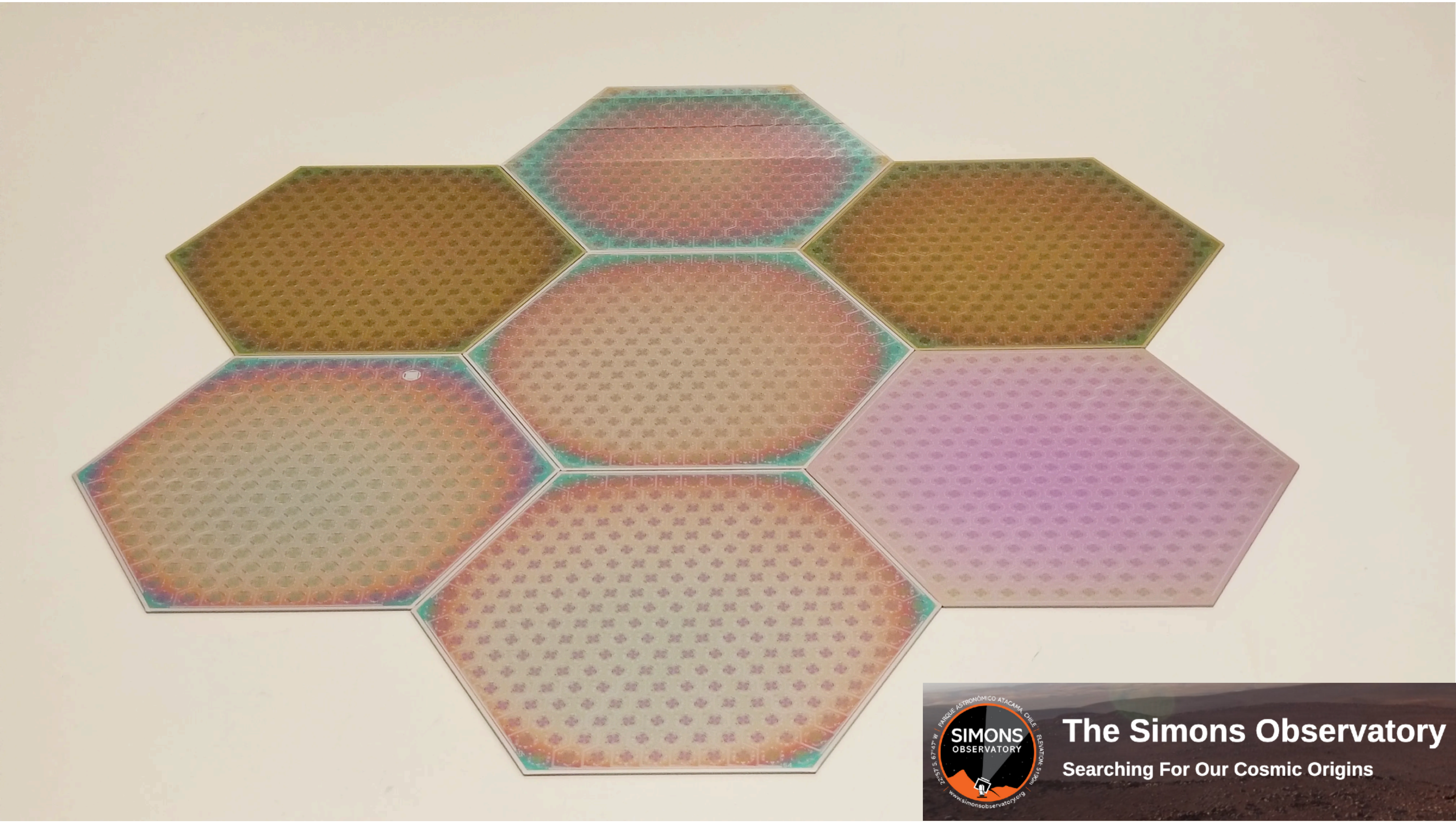

CMB–S4 plans

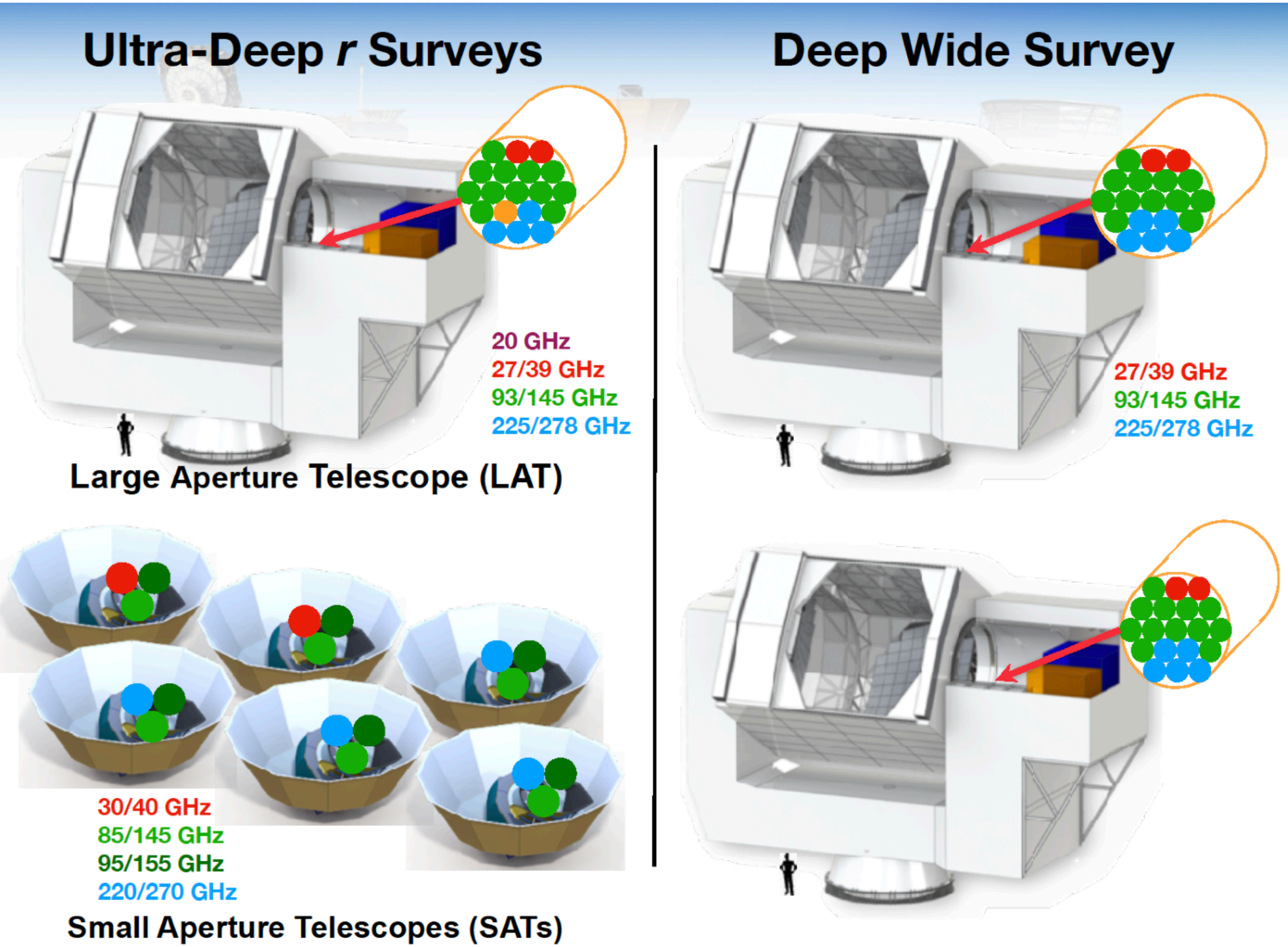

- Uses field proven technology, including multiplexed TES detectors
- CMB-S4 requires 500 science-grade 150 mm detector wafers
- CMB-S4 has 57 LAT optics tubes and 18 SAT tubes, **500,000** detectors
- SPO has 1 LAT and 5 SAT tubes, 52,000 detectors (CMB-S4 compatible LAT proposed)
- SO nominal has 7 LAT optics tubes plus 3 SAT tubes, 60,000 detectors (CMB-S4 compatible LAT)

Credit: CMB-S4 collaboration

Fred Young Submillimeter Telescope (FYST)

Project originally called CCAT-prime

6 meter aperture and *extremely large* field-of-view sub-millimeter telescope on the Cerro Chajnantor (at 5600m) Chile

Partners: Cornell, **Bonn**-Cologne-Munich, Canadian universities

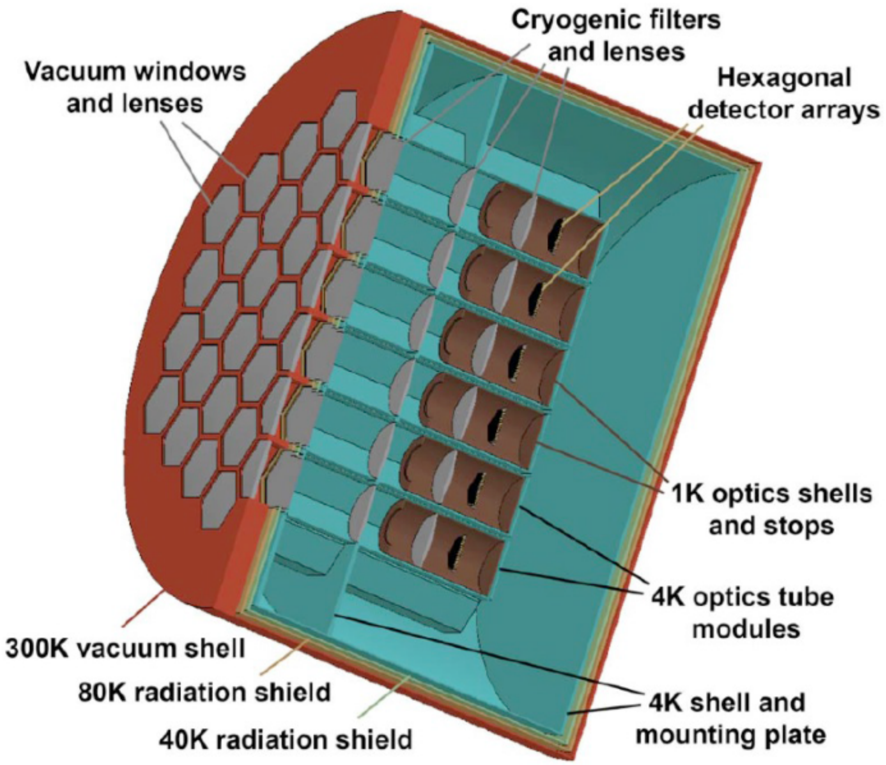

2.5 m diameter bolometer receiver

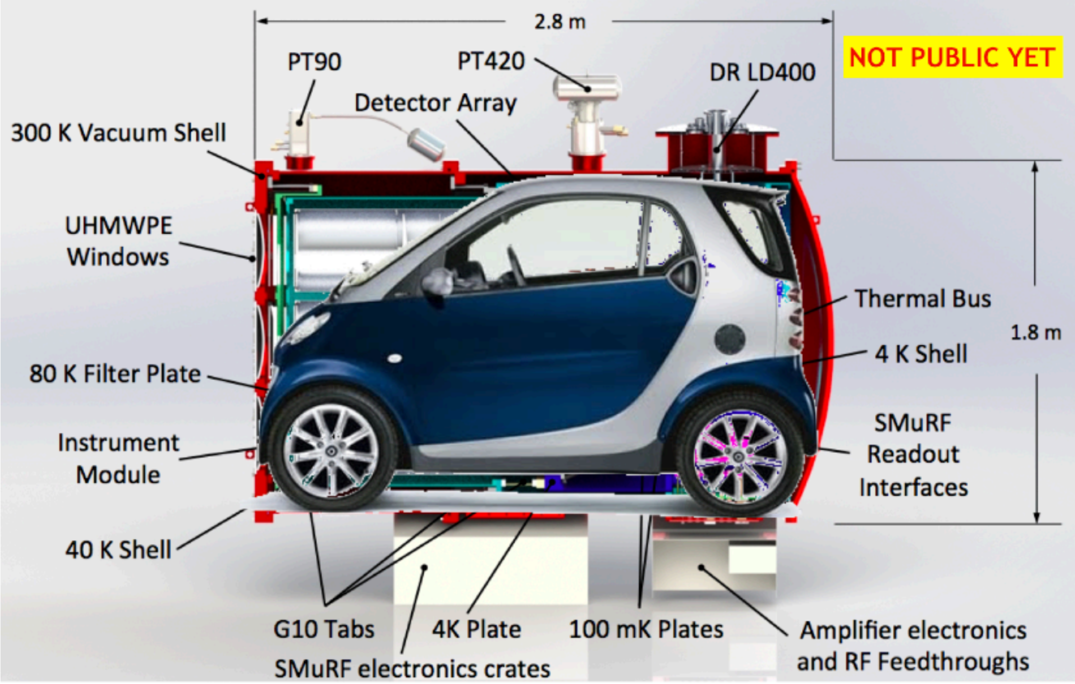

More on FYST/CCAT-prime

Partnership with Uni Bonn and Uni Köln

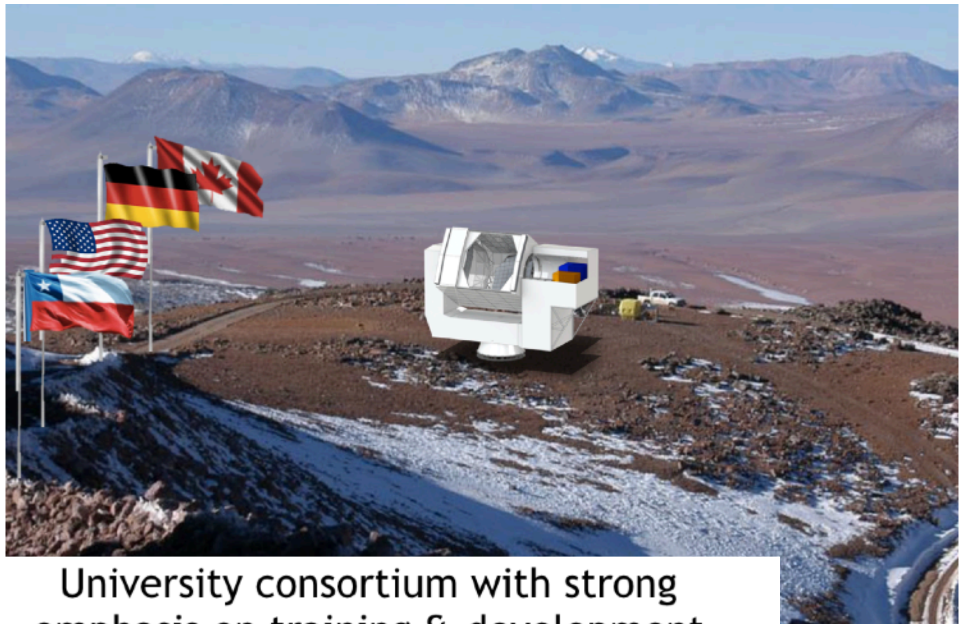

University consortium with strong emphasis on training & development

- Cornell University, Director 70%
- Univ. Cologne & Univ. Bonn 25%
  - joining: LMU (Mohr), MPA (Komatsu)
- **Canadian University consortium 5%**

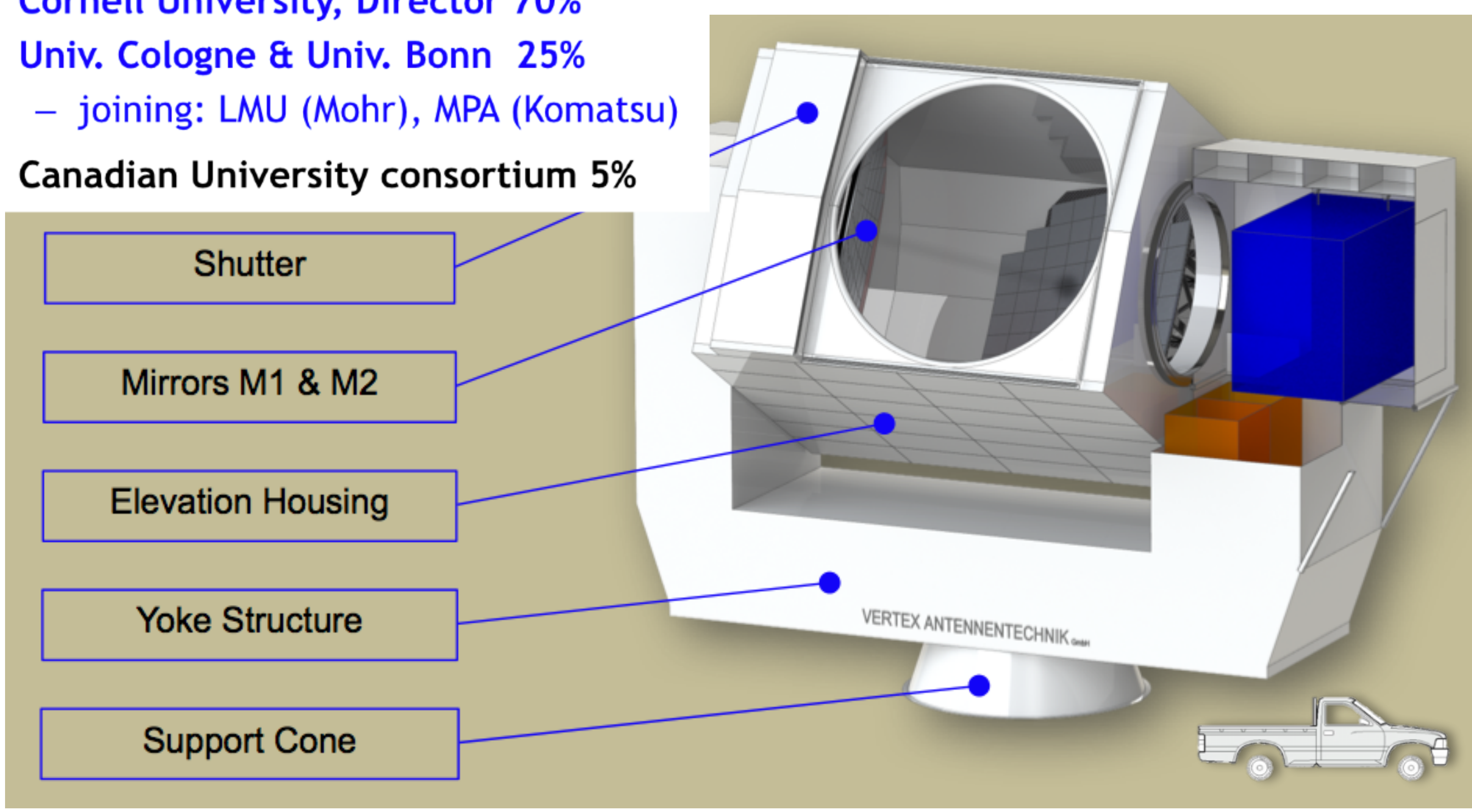

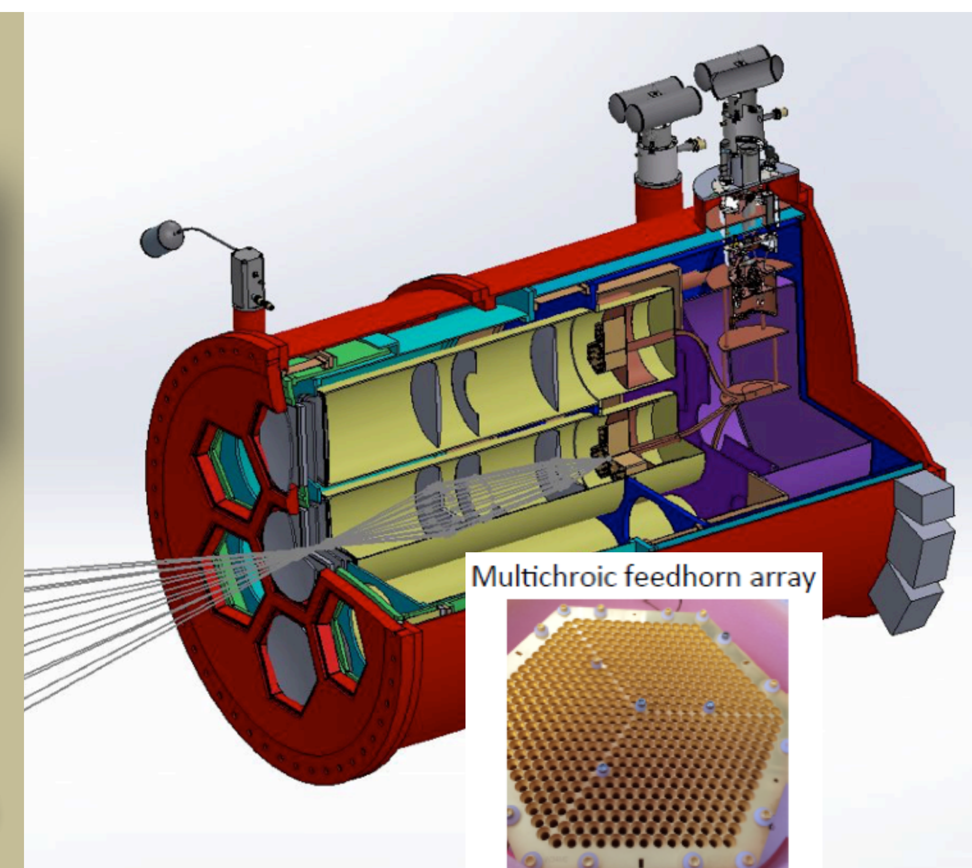

More on FYST/CCAT-prime

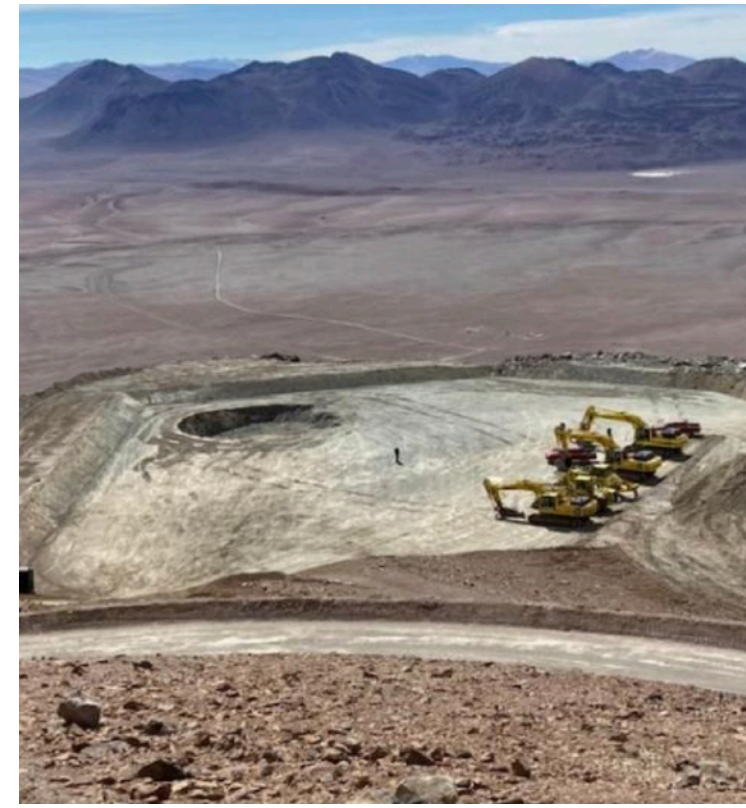

Preparation of the site at Chile and test-assembly in Germany, 2021

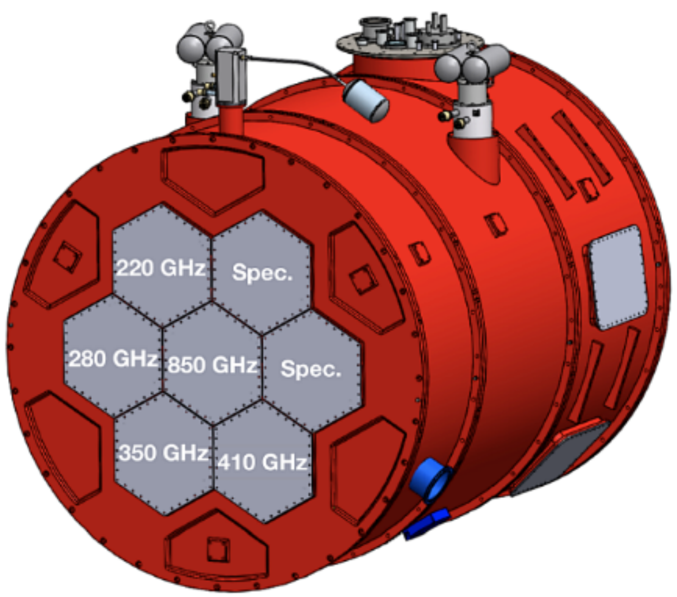

Will these fly to space?

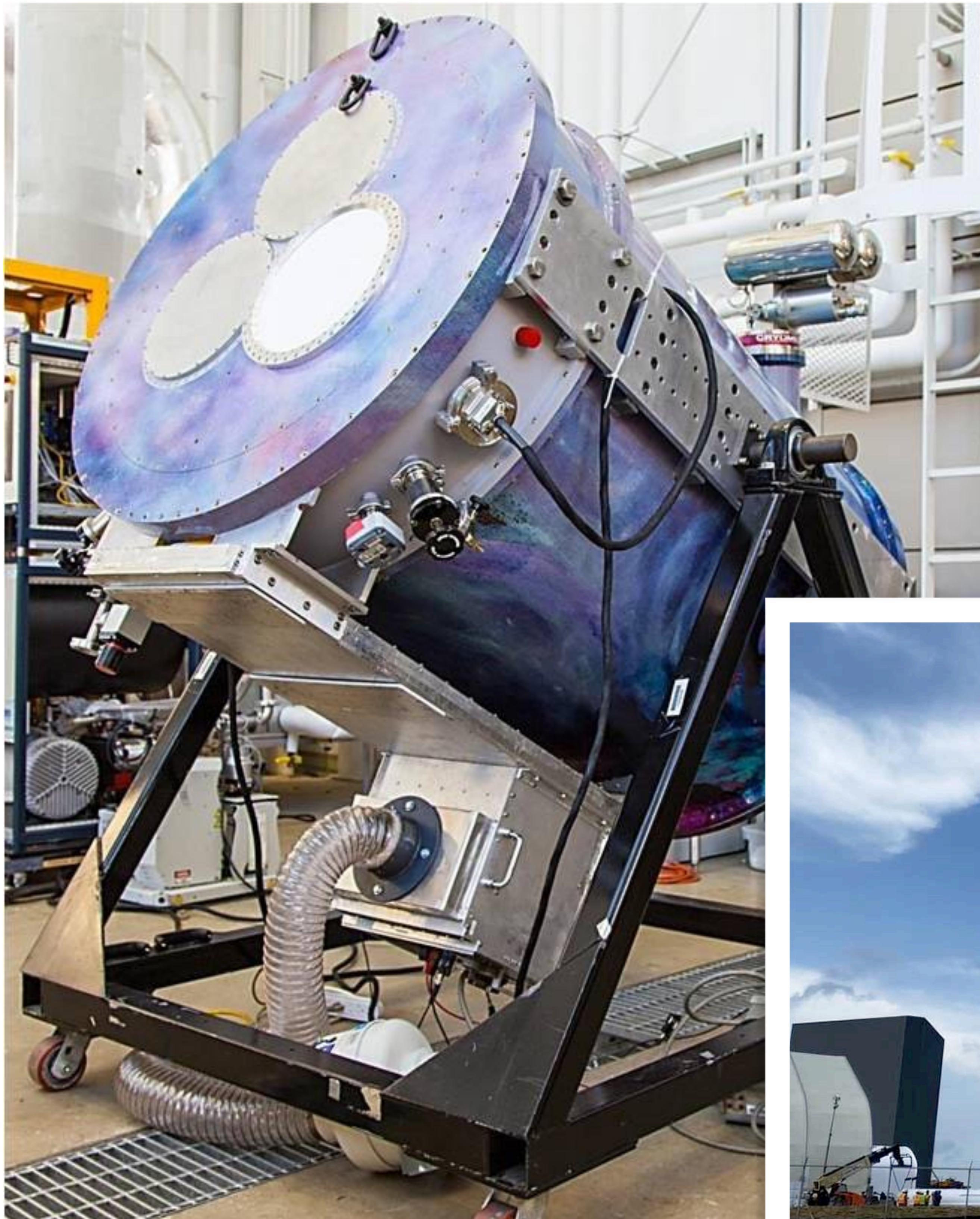

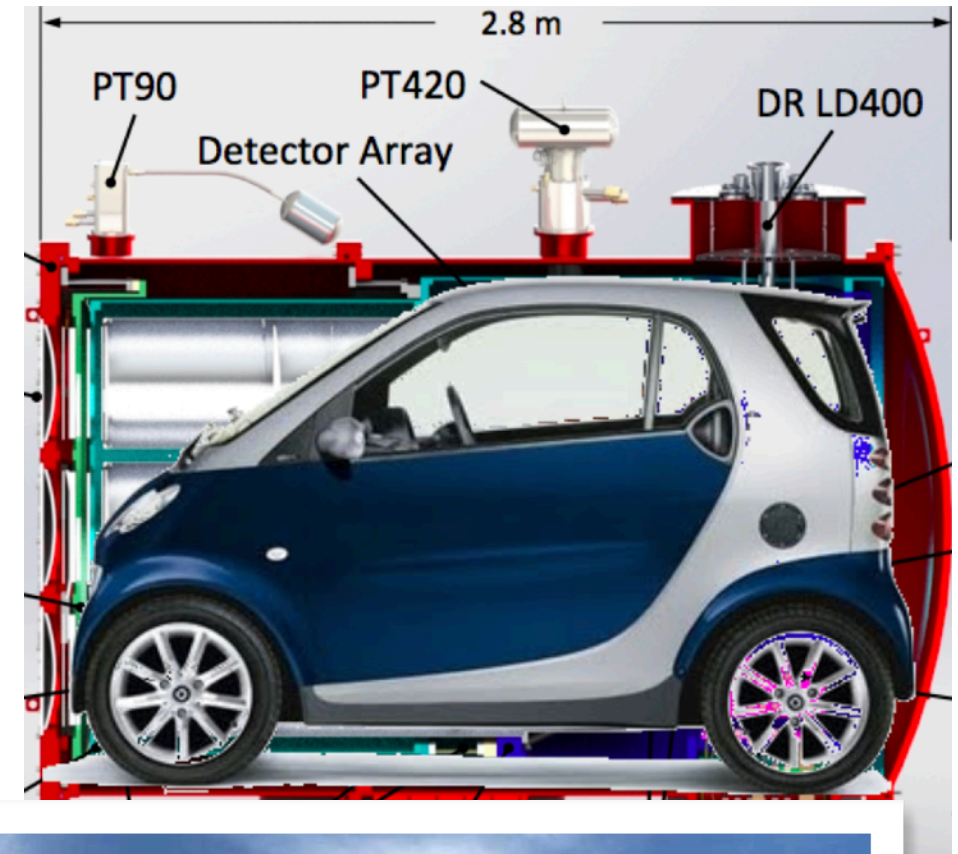

Questions?

Feel free to email me or ask questions in our eCampus Forum